ESPOO 2005 VTT WORKING PAPERS 41

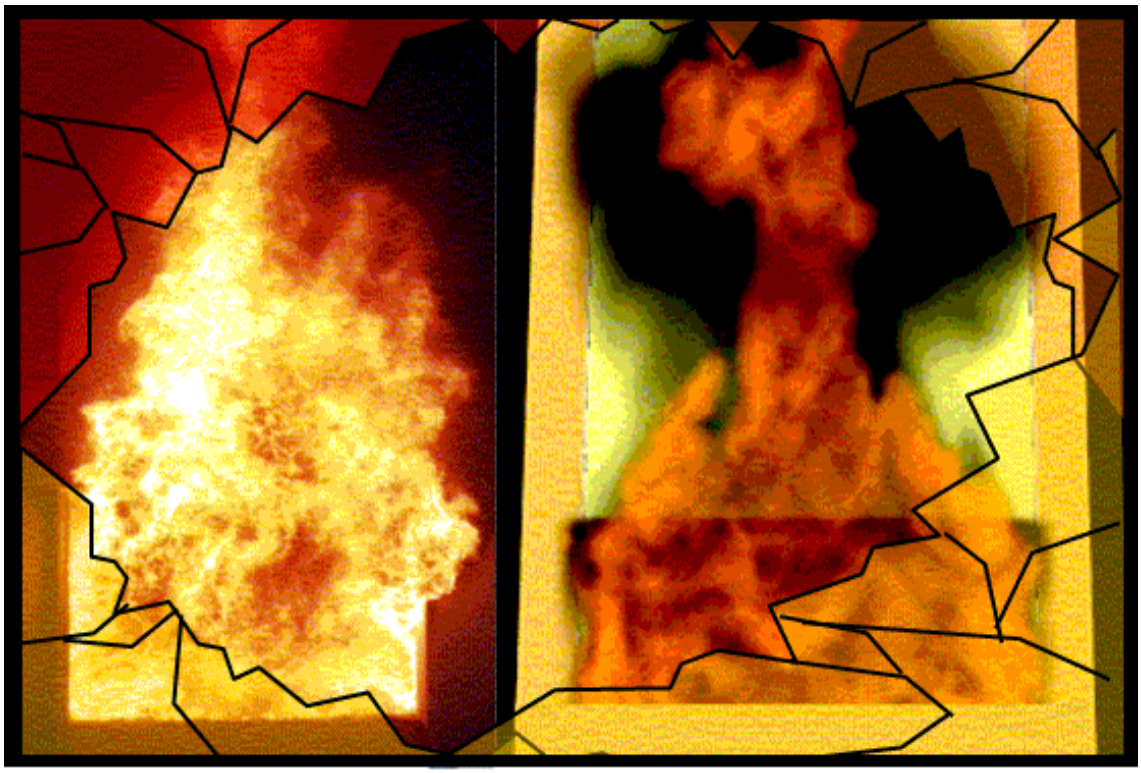

Probabilistic simulation of glass fracture and fallout in fire

Jukka Hietaniemi

VTT Building and Transport

ISBN 951–38–6593–2 (URL: http://www.vtt.fi/inf/pdf/)
ISSN 1459–7683 (URL: http://www.vtt.fi/inf/pdf/)

JULKAISIJA – UTGIVARE – PUBLISHER

VTT, Vuorimiehentie 5, PL 2000, 02044 VTT
puh. vaihde 020 722 111, faksi 020 722 4374

VTT, Bergsmansvägen 5, PB 2000, 02044 VTT
tel. växel 020 722 111, fax 020 722 4374

VTT Technical Research Centre of Finland, Vuorimiehentie 5, P.O.Box 2000, FI–02044 VTT, Finland
phone internat. +358 20 722 111, fax +358 20 722 4374

VTT Rakennus- ja yhdyskuntatekniikka, Kivimiehentie 4, PL 1803, 02044 VTT
puh. vaihde 020 722 111, faksi 020 722 4815

VTT Bygg och transport, Stenkarlsvägen 4, PB 1803, 02044 VTT
tel. växel 020 722 111, fax 020 722 4815

VTT Building and Transport, Kivimiehentie 4, P.O.Box 1803, FI–02044 VTT, Finland
phone internat. +358 20 722 111, fax +358 20 722 4815

Technical editing Anni Kääriäinen

Published by

Series title, number and
report code of publication

VTT Working Papers 41
VTT–WORK–41

Author(s)
Hietaniemi, Jukka

Title

Probabilistic simulation of glass fracture and fallout in fire

Abstract

Window openings act as ventilation openings for the fire after the glass closing the window opening has been broken and fallen out. Because ventilation is one of most important factors influencing the fire severity, the question that when a window breaks during a fire to such extent that it forms a ventilation opening is one the most important problems of fire sciences. Due to the importance of the understanding of the performance of window glass in fire, it has been addressed in many outstanding theoretical and experimental studies. The models and programs developed predict the occurrence of the first cracking of the window pane exposed to fire and often a very good agreement with experiments can be obtained. The models do not, however, answer the question of when a window turns into a ventilation opening. They can give a very conservative lower bound estimate on the opening formation time, but experiments show that catastrophic window failure leading to glass fallout and creation of ventilation openings takes place at much higher temperatures and later times than the occurrence of the first crack in the window pane. Keski-Rahkonen was the first author to emphasise the variabilities involved in the problem of evaluation of response of window glass to fire: both the fires we have to consider in fire safety engineering and the glass response properties vary within a broad range.

This report presents a probabilistic approach to evaluate the conditions when a window pane exposed to fire heating fails in such extent that it forms a ventilation opening. The variability in the glass response in included explicitly. The variability in the fire characteristics is not addressed directly, but in an indirect manner so that the output of the probabilistic glass failure model, i.e., is used as an input to the Probabilistic Fire Simulator (PFS) of VTT. The decoupling of the variability in the response of glass and the fire description reflects the pragmatic approach taken in this study: the objective of the work has been to establish well-founded guidelines and tools to fire safety engineers to treat glass breaking in fire, not to provide an all-inclusive calculation theory of the problem. In brief, the approach comprises two parts: the first one is calculation of the time and gas and glass temperature at the first occurrence of a crack in the window pane by using Monte Carlo simulation with the BREAK1 program. The second part involves assessment of subsequent crackings by using a more simple thermal response model of the glass, the isothermal lumped-heat capacity model. With this heating model we determine the glass fallout following the suggestion of Pagni that glass fallout results from multiple crackings. Thus, in our model, the glass is deemed fall out and form a ventilation opening when sufficiently many calculated crackings have taken place. The key factor, i.e., how many calculated cracking events constitute sufficiently many for the glass to fallout is obtained from experimental data found in the literature.

Keywords
fire simulation, fire modelling, glass breaking, glass fallout, probabilistic simulation, Monte Carlo

Activity unit
VTT Building and Transport, Kivimiehentie 4, P.O.Box 1803, FI–02044 VTT, Finland

ISBN		Project number
951–38–6593–2 (URL: http://www.vtt.fi/inf/pdf/)		R4SU00232
Date November 2005	Language English	Pages 88 p. + app. 33 p.
Name of project New simulation methods for fire safety analysis	Commissioned by National Technology Agency of Finland Tekes, VTT Technical Research Centre of Finland	
Series title and ISSN VTT Working Papers 1459–7683 (URL: http://www.vtt.fi/inf/pdf/)	Publisher VTT Information Service P.O.Box 2000, FI–02044 VTT, Finland Phone internat. +358 20 722 4404 Fax +358 20 722 4374	

Preface

This report presents a probabilistic approach to evaluate the conditions when a window pane exposed to fire heating fails in such extent that it forms a ventilation opening. The objective of the work has been to establish well-founded guidelines and tools for fire safety engineers to treat glass breaking in fire.

The work has been out in the Fire Research group of VTT Building and Transport, Finland. It forms a part of a larger research project launched to develop new tools for fire simulation with the aim set at producing generally acceptable and valid science-based tools to meet the needs of fire safety design and risk assessment within the industry and other stakeholders.

The project is funded by the National Technology Agency of Finland (Tekes) and VTT Building and Transport.

Contents

1. Introduction

Ventilation is one of most important factors that influence the fire safety in buildings. Fire ventilation can take place via open doors, building leakages, air-conditioning and via window openings provided that the glass closing the window opening has been broken. While windows constitute the largest openings in buildings, especially in many modern buildings with virtually fully glazed facades, the question that when a window breaks during a fire to such extent that it forms a ventilation opening is among the most important problems of fire sciences (Emmons 1986).

Due to the importance of the understanding of the performance of window glass in fire, this issue has been addressed in many outstanding research endeavours, including theoretical studies (e.g. Keski-Rahkonen 1988, Keski-Rahkonen 1991, Joshi & Pagni 1990, Pagni & Joshi 1991, Joshi & Pagni 1994a, Cuzzillo & Pagni 1998) and experimental studies (Richardson & Oleszkiewicz 1987, Skelly et al. 1991, Joshi & Pagni 1994a, Hassani et al. 1994/1995, Hassani et al. 1995/1996, Shields et al. 1997/1998a, Shields et al. 1997/1998b, Mowrer 1998, Anon. 1999, Harada et al. 2000, Shields et al. 2001, Shields et al. 2002).

The studies carried out by Joshi and Pagni have been implemented as a computer program BREAK1 (Joshi & Pagni 1991) which is a Fortran program enabling to calculate the occurrence of the first fire-induced fracture in the glass pane. BREAK1 is freely available at the NIST Internet site[1]. The results calculated with BREAK1 have been found to agree well with experimental data (see, e.g. Pagni 2003 and refs. ibid.). Cuzzillo and Pagni (1998) modified BREAK1 to include fracture calculation of double-pane windows (program McBreak). Another widespread glass-fracture model is the computer code for implementation in fire zone models (the FIRST model [Mitler & Rockett 1987]) by Sincaglia and Barnett (1997) who adapted the numerical one-dimensional heat-transfer model of Gardon (1958) to assess the influence of fire on the window glass. A combination model using the heat transfer model of Sincaglia and Barnett (1997) and the fracture criterion of BREAK1 (Joshi & Pagni 1991) have been implemented to a glass-fracture routine in the BRANZFIRE zone model (Parry et al. 2003).

All the models and programs developed thus far predict the occurrence of the first cracking of the window pane exposed to fire heating and usually the predictions agree well with experiments. These models do not, however, answer to the primary question

[1] http://www.bfrl.nist.gov/866/fmabbs.html#BREAK1

of when a closed window turns into a ventilation opening in a fire. They can give a very conservative lower bound estimate on the formation time of the opening, but experiments (see the refs. quoted above) show that catastrophic window failure leading to glass fallout and creation of ventilation openings takes place at much higher temperatures and later times than the occurrence of the first crack in the window pane.

Keski-Rahkonen was the first author to emphasise the variabilities involved in the problem of evaluation of response of window glass to fire: both the fires we have to consider in fire safety engineering and the glass response properties vary within a broad range (Keski-Rahkonen 1988).

This report presents a probabilistic approach to evaluate the conditions when a window pane exposed to fire heating fails in such extent that it forms a ventilation opening in which the variability in the glass response in included explicitly. The variability in the characteristic of the fire are not addressed directly, but in an indirect manner so that the output of the probabilistic glass failure model, i.e., the distribution of the gas temperature at glass failure is used as an input to the Probabilistic Fire Simulator (PFS). The PFS tool and its use is described in details in reports and articles by Hostikka et al. (2003), Hostikka and Keski-Rahkonen (2003) and Hietaniemi et al. (2004). The decoupling of the variability in the response of glass and the fire description reflects the pragmatic approach taken in this study: the objective of the work has been to establish well-founded guidelines and tools to fire safety engineers to treat glass breaking in fire, not to provide an all-inclusive calculation theory of the problem. In brief, the approach comprises two parts: the first one is calculation of the time and gas and glass temperature at the first occurrence of a crack in the window pane by using Monte Carlo simulation with the BREAK1 program. The second part involves assessment of subsequent crackings by using a more simple thermal response model of the glass, the isothermal lumped-heat capacity model. With this heating model we determine the glass fallout following the suggestion of Pagni (2003) that glass fallout results from multiple crackings. Thus, in our model, the glass is deemed fall out and form a ventilation opening when sufficiently many calculated crackings have taken place. The key factor, i.e., how many calculated cracking events constitute sufficiently many for the glass to fallout is assessed on the basis of experimental data found in the literature.

This study deals with ordinary soda-lime float glass, tempered, laminated and other special glasses fall beyond the scope of this report.

This report is organised as follows: the above quoted conceptual model is described in more details in Chapter 2. Chapter 3 describes how the BREAK1 program is executed in the Monte Carlo mode with special emphasis on the characterisation of the input parameters as stochastic entities. The model for the glass heating after the time of the

first cracking and the eventual creation of a ventilation opening is described in Chapter 4: section 4.1 presents a simplified glass heating model and the key question of how many crackings are required to turn a closed window into a vent is elucidated in section 4.3 through comparison of the calculated results with experimental observations obtained from the literature. An example of the use of the model in combination of the PFS probabilistic fire simulator is given in Chapter 5. There are three Appendices in the report with the first one, Appendix A, was addressing the importance of the value that is assigned to the enclosure gas temperature leading to glass fallout and vent creation and the second one, Appendix B, presents a parametric study using the BREAK1 program on the influence of the several influential factors on the glass fracture. The third Appendix, Appendix C, presents listing of the main program *MCB.for* as well as the BREAK1 converted into a Fortran function (*Breakf.for*). This Appendix gives also practical guidance on the evaluation of the random numbers needed in the execution of the program MCB.for. It also shows the format and contents of the input and output files of the *MCB.for* program. The input comprises two files: 1) the file with fixed name *MCB.config* from which the program needs some input data and 2) the data file from which the *MCB.for* reads the time series data characterising the fire (specifically the time, upper layer temperature and the heat release rate that is used in the calculation of the direct radiation exposure from the fire). The most important output file is a file BreakingConditions.cvs with comma-separated format: as its name indicates, this file gives the results concerning the conditions corresponding to the first fracture formation in the glass pane. Other outfiles are there mainly for checking purposes.

2. Description of the conceptual model

Following the suggestion by Pagni (2003), we model the glass fallout as an event which takes place after a certain number of glass crackings have occurred (Figure 1). The sequence of the glass cracings is determined so that the next cracking is deemed to take place when the glass temperature has risen on an average by an amount of ΔT_g.

The average glass temperature rise ΔT_g forms the basis of the modelling of the glass crackings following the first crack: it is assumed that there will be a cracking of the glass pane always when the average glass temperature has increased by an amount of ΔT_g after the preceding cracking. Due to its importance, ΔT_g is calculated using the BREAK1 program which has been shown to predict well the occurrence of the first cracking of glass exposed to fire (see Pagni [2003] and refs. ibid.); Figure 2. In our model we take into account the uncertainties and variabilities in the glass properties and its response to heating by running the BREAK1 program in the Monte Carlo mode as explained in the next Chapter (Chapter 3).

When the glass pane has shattered for the first time, its response to heating changes is much less predictable due to the influence on the first cracking on the system. One implication of this greatly increased uncertainty is that for practical purposes it seems quite unnecessary to model the system response to heating at the high level of sophistication afforded by the BREAK1 code, but a less rigorous but computationally simpler approach suffices. Hence we *assess* the occurrence of the 2nd cracking and the following crackings on the basis of the glass temperature rise evaluated using a simple lumped-heat capacity model described in Chapter 4 (see Figure 3).

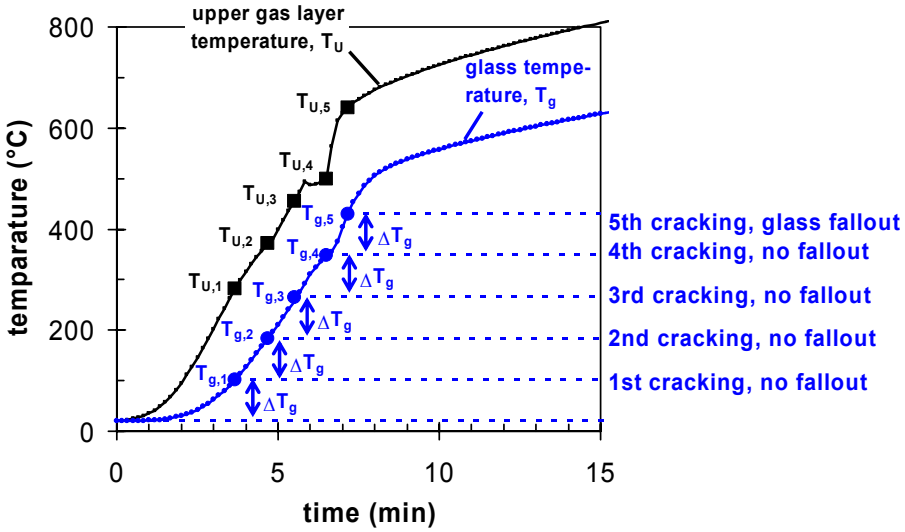

Figure 1. Conceptual model of the glass fracture and eventual fallout as a series of crackings taking place when glass temperature rises by an amount of ΔT_g: an example of glass fallout at the 5th cracking.

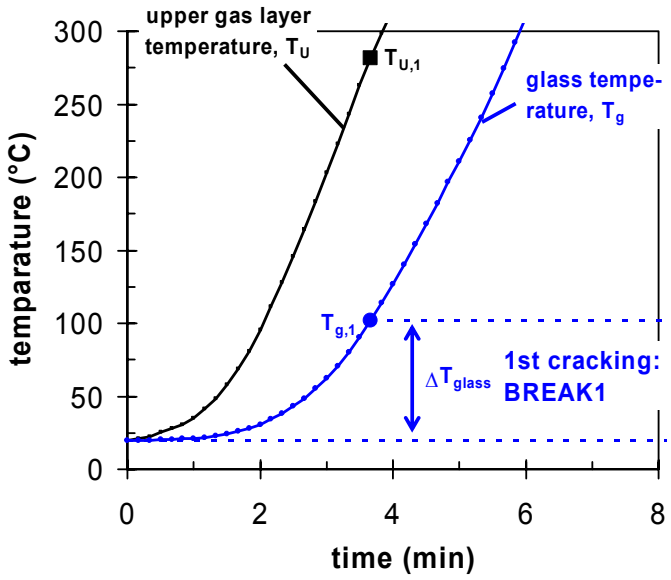

Figure 2. Calculation of the first cracking with the BREAK1 program, which gives the value for the quantity ΔT_g. To take into account the variabilities in the glass properties and response to heating, BREAK1 is run in the Monte Carlo mode (see Chapter 3).

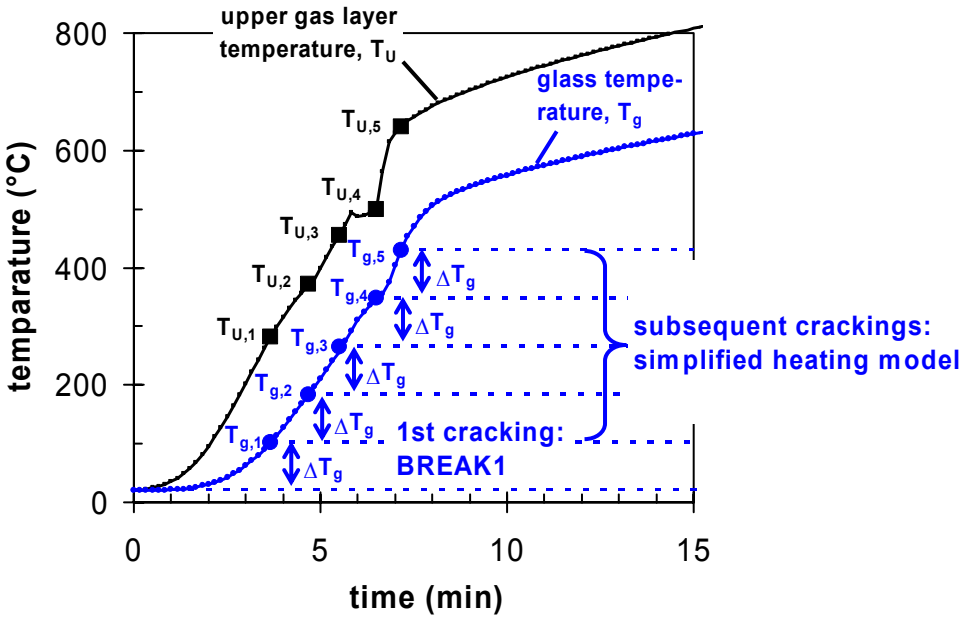

Figure 3. Calculation of the following crackings after the first crack using a simplified lumped-heat capacity model (see Chapter 4). The number of crackings needed for glass pane fallout is determined from experimental findings in section 4.3.

3. Evaluation of the occurrence of the first fracture: using the BREAK1 program in the Monte Carlo mode

We consider the window as slab of soda-lime float glass (Pagni 2003). Below we first describe the relevant thermal and mechanical properties as well as the heat transfer characteristics with their variability characterised by suitable statistical distribution. The Chapter ends with examples of use of the Monte Carlo BREAK1 (MCB) model.

3.1 Stochastic characterisation of the BREAK1 input parameters

3.1.1 Thermal properties of glass

The density of the glass, ρ, is modelled according to the data given by Pagni (2003): $\rho = (2500 \pm 100)$ kgm^{-3}. We model the uncertainty in the density by the triangular distribution shown in Figure 4a: the minimum value equals 2400 kgm^{-3} and maximum value 2600 kgm^{-3} and the distribution is peaked at 2500 kgm^{-3}. At 50 °C, the specific heat c_p equals 820 JK^{-1}kg^{-1} and the thermal conductivity k equals 0,95 WK^{-1}m^{-1} (Pagni 2003). The ranges of variability of these quantities are the following: c_p varies between 750 JK^{-1}kg^{-1} and 950 JK^{-1}kg^{-1} and k varies between 0,7 WK^{-1}m^{-1} and 1,4 WK^{-1}m^{-1} (Pagni 2003). We characterise also the variability of c_p and k using the triangular distributions, see Figure 4b and Figure 4c. For c_p the minimum, maximum and peak values are 750 JK^{-1}kg^{-1}, 950 JK^{-1}kg^{-1} and 820 JK^{-1}kg^{-1}, respectively and for k they are 0,7 WK^{-1}m^{-1} and 1,4 WK^{-1}m^{-1} and 0,95 WK^{-1}m^{-1}, respectively.

Thermal diffusivity α is determined by the three above mentioned quantities via the relation $\alpha = k/(\rho \cdot c_p)$. Thus, in the calculations there is no need to know the distribution of α. However, out of interest we have analysed the distribution of α using the Monte Carlo method. The resulting distribution, shown in Figure 4d, has a somewhat distorted triangular shape with the minimum value equal to 3,67·10^{-7} m^{2}s^{-1} and the maximum value equal to 5,65·10^{-7} m^{2}s^{-1}, respectively. The distribution is peaked at 4,8·10^{-7} m^{2}s^{-1}.

In the temperature range 0...300 °C, the thermal coefficient of linear expansion β has a value $\beta = (9{,}0 \pm 0{,}5) \cdot 10^{-6}$ K^{-1} (Pagni 2003). The triangular distribution used to model the variability in the β value is shown in Figure 4e: the minimum, maximum and peak values are 0,85·10^{-6} K^{-1}, 0,95·10^{-6} K^{-1} and 0,90·10^{-6} K^{-1}, respectively.

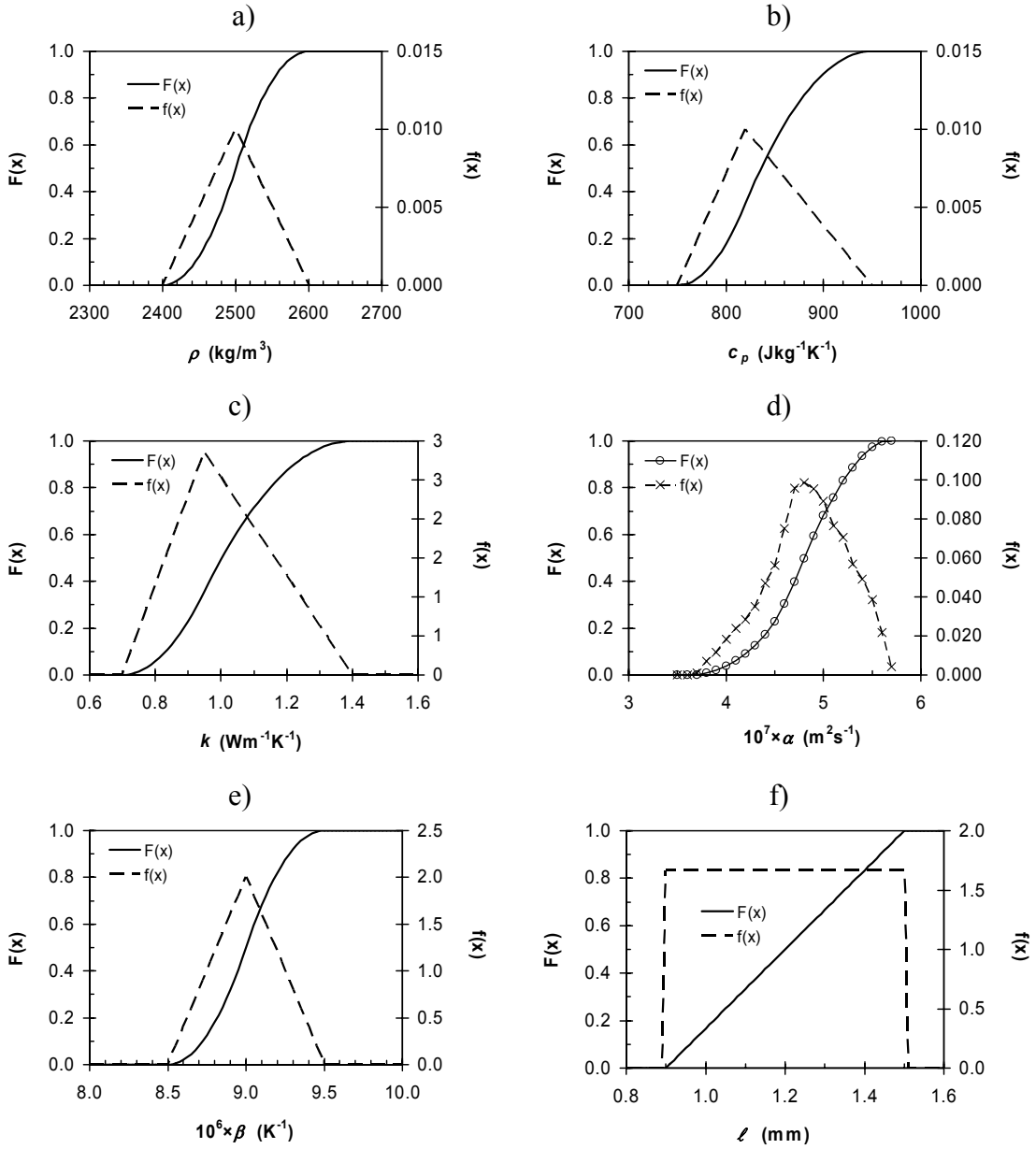

Figure 4. Characterisation of variability in the thermal properties of soda-lime glass: a) density, b) specific heat, c) thermal conductivity, d) thermal diffusivity and e) thermal coefficient of linear expansion. The curves shown depict the cumulative frequency function F(x) and the probability density function f(x) with the argument x standing for the relevant quantity.

3.1.2 Parameters governing the heat transfer onto and from the glass surfaces

The source term in the governing equation of glass heating in BREAK1 includes a source term of the form $I \cdot \exp(-x/\ell)/\ell$ where I is the incident intensity and ℓ is the absorption length (Cuzzillo & Pagni 1998, Pagni 2003). According to the User Information file included in the BREAK1 downloadable package this quantity varies between 0.9...1,5 mm. We describe its variability by the uniform distribution, see Figure 5a.

The emissivity of glass at the wavelength range corresponding to heat radiation is about 0,9 Pagni (2003). We take into account the variability in the glass emission by treating it as a random variable with uniform distribution with lower bound equal to 0,85 and upper bound equal to 0,95 (Figure 5b). Emissivity of the boundary to the ambient is taken to be equal to unity.

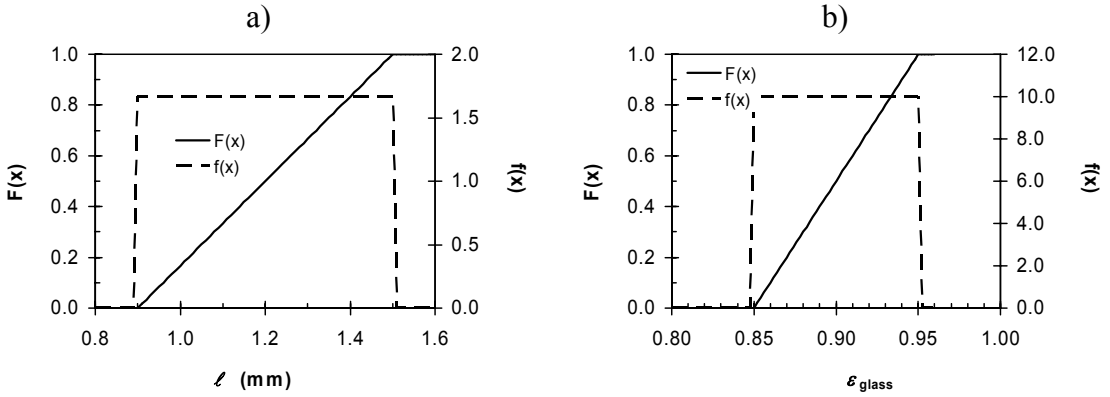

Figure 5. Characterisation of the parameters influencing the glass response to heat radiation: a) absorption length and b) emissivity. The curves shown depict the cumulative frequency function F(x) and the probability density function f(x) with the argument x standing for the relevant quantity.

The convective heat transfer coefficient on the fire-exposed side of the glass h_{hot} depends on several factors and, thus, it is not an easy task to assign values to it. We consider here two separate cases:

1. the hot side heat transfer coefficient suitable to describe heat transfer from the hot gas layer in a compartment fire

2. the hot side heat transfer coefficient suitable to describe heat transfer in a fire-resistance furnace.

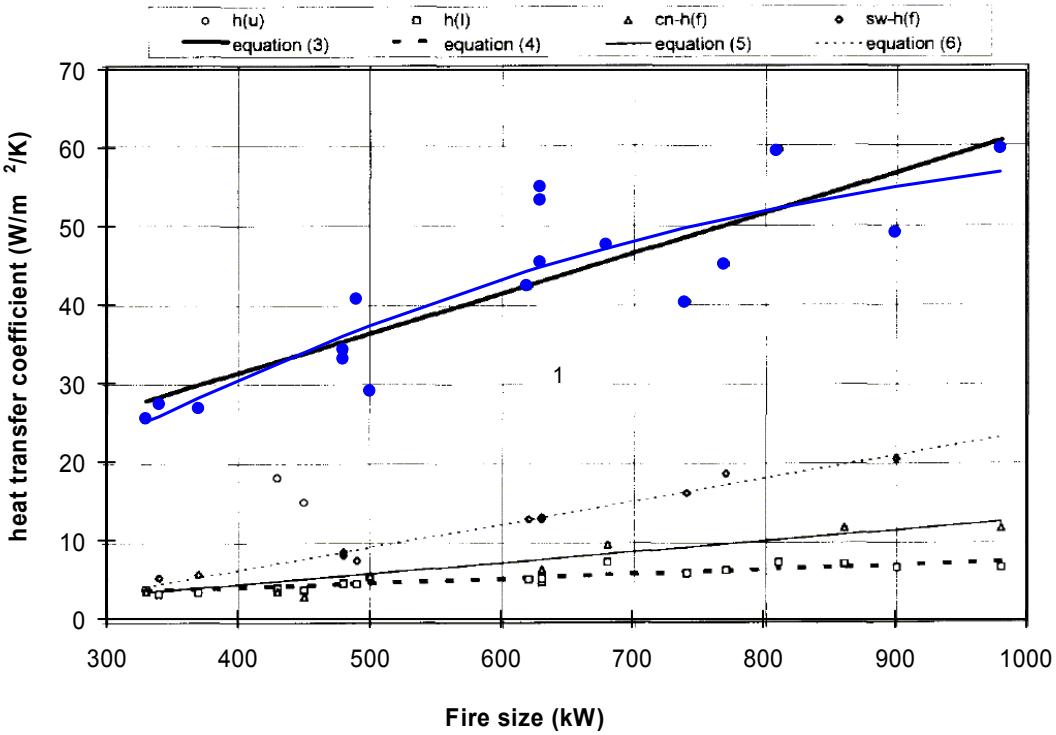

Figure 6. Relationship between the hot layer heat transfer coefficient in a compartment fire and the fire heat release rate: reproduction of Fig. 8 in the article of Dempsey et al. (1996) with the relevant data points emphasised (large blue dots) and the fitting curve describing Eq. (1) shown with the blue solid curve.

Case 1: We base our estimate of the hot side heat transfer coefficient related to the hot gas layer in a compartment fire to the experimental data of Dempsey et al. (1996). Figure 6 shows a reproduction of their result on the dependence of the hot layer heat transfer coefficient on the heat release rate $\dot{Q}$ of the fire. Dempsey et al. fitted the data using an expression $h_{hot}/\left(\mathrm{W/K/m^2}\right) = 0{,}051 \cdot \left(\dot{Q}/\mathrm{kW}\right) + 11$. We carried out an analysis of the data using a saturating functional shape as an automatic device to put an upper limit to the h_{hot} values. In addition to this, we modelled the scatter in the data points. This analysis yields the random function

$$\frac{h_{hot}}{\mathrm{kW}} = 60 \cdot \frac{\left(\dot{Q}/\mathrm{kW}\right)^{2{,}193}}{\left(\dot{Q}/\mathrm{kW}\right)^{2{,}193} + 995{,}5^2} + \eta \qquad (1)$$

where η is a random parameter following the Gamma distribution[2] with parameters $\alpha = 4.116$ and $\beta = 2.536$ W/m^2/K (see Figure 7).

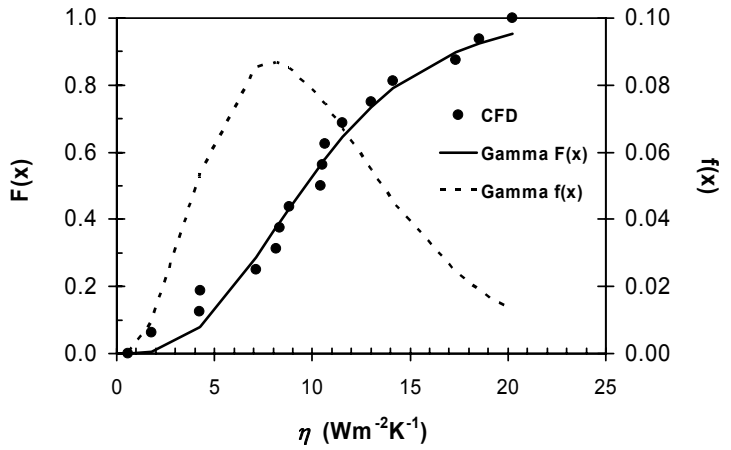

Figure 7. Distribution of random quantity η in the function describing the hot layer heat transfer coefficient (the compartment fire case).

Case 2: Our estimate of the hot side heat transfer coefficient related to heat exposure in a fire-resistance furnace is based on data provided by Hostikka (2004) on the basis of CFD simulation of the model furnace of VTT. The least-squares fitting results of these data using a 3-parameter Weibull distribution[3] are shown in Figure 8a and the outcome of the analysis is summarised in Figure 8b: h_{hot} in this case is described by a the Weibull distribution with parameters $\alpha = 1.254$, $\beta = 5.465$ W/m^2/K and $x_{\min} = 9.64$ W/m^2/K.

---

[2] The density function of gamma distribution is given by

$$f(x) = \frac{1}{\Gamma(\alpha)\beta^{\alpha}} x^{\alpha-1} e^{-\frac{x}{\beta}}$$

where $\Gamma(\alpha)$ is a gamma function.

[3] The probability density of the Weibull distribution is

$$f(x) = \left(\frac{\alpha}{\beta^{\alpha}}\right) \cdot \left(x - x_{\min}\right)^{\alpha-1} \cdot \exp\left(-\left(\frac{x - x_{\min}}{\beta}\right)^{\alpha}\right)$$

and cumulative distribution function

$$F(x) = 1 - \exp\left(-\left(\frac{x - x_{\min}}{\beta}\right)^{\alpha}\right).$$

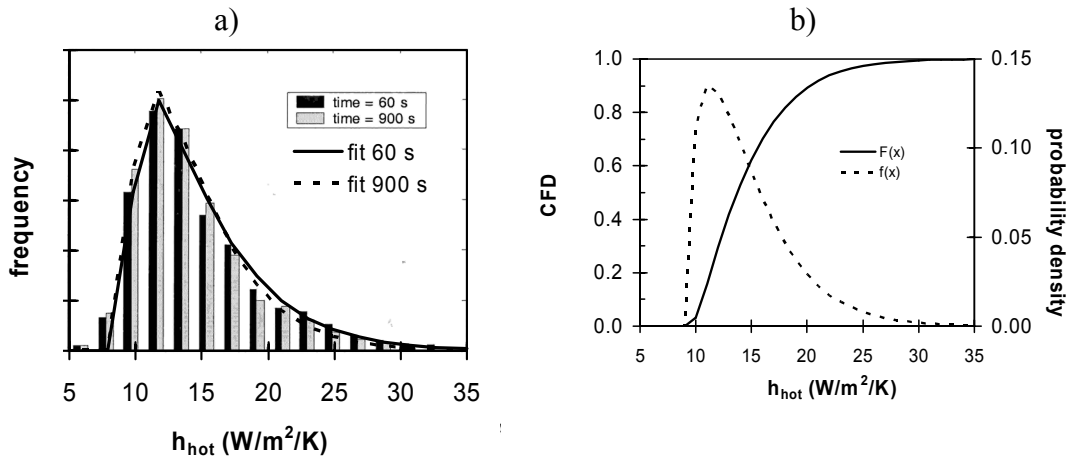

Figure 8. Distribution of the heat transfer coefficient in a fire-resistance furnace and 3-parameter Weibull random quantity η in the function describing the hot layer heat transfer coefficient.

The cold side heat transfer coefficient h_{cold} can be modelled as (Pagni 2003):

$$\frac{h_{cold}}{\mathrm{W/m2/K}} = \begin{cases} 1{,}24 \cdot \left(\dfrac{\Delta T/\mathrm{K}}{H_w/\mathrm{m}} \right)^{1/4}, & \text{when } \left(\dfrac{H_w}{\mathrm{m}} \right)^3 \cdot \left(\dfrac{\Delta T}{\mathrm{K}} \right) < 15; \\ 1{,}27 \cdot \left(\Delta T/\mathrm{K} \right)^{1/3}, & \text{when } \left(\dfrac{H_w}{\mathrm{m}} \right)^3 \cdot \left(\dfrac{\Delta T}{\mathrm{K}} \right) \geq 15; \end{cases} \tag{2}$$

where H_w is window height and ΔT is the temperature difference. Figure 9a shows results of Monte Carlo analysis of the above expression where H_w has been varied between 20 cm and 2 m (uniform distribution) and ΔT between 20 °C and 200 °C (uniform distribution). The resulting distribution for h_{cold} can be approximated by a triangular distribution as shown in Figure 9b. The parameters of the triangular distribution are: minimum value 2.82 W/m^2/K, maximum value 7.479 W/m^2/K and peak value 7.405 W/m^2/K.

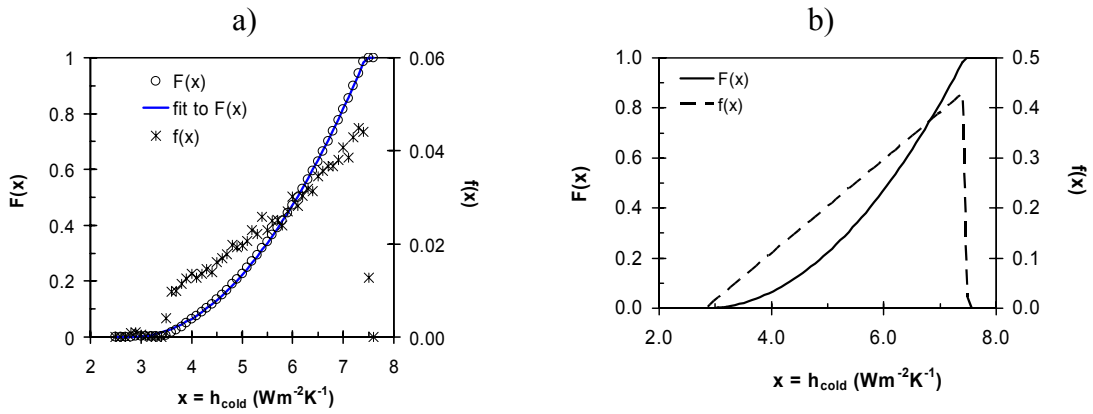

Figure 9. Heat transfer coefficient on the cold side: a) outcome of Monte Carlo analysis of Eq. (2) and b) the resulting model for h_{cold} utilising the triangular distribution.

3.1.3 Mechanical properties of glass

Joshi and Pagni (1994b) carried out 59 tests to evaluate the breaking stress of glass specimens with dimensions 178 mm × 25,4 mm × 2,5 mm. This breaking stress which we denote by σ_t was found to be distributed according to the 3-parameter Weibull distribution with the cumulative frequency distribution given by

$$F(\sigma_t) = 1 - \exp\left[\left(\frac{\sigma_t - \sigma_u}{\sigma_0}\right)^m\right] \tag{3}$$

with $\sigma_u = 35{,}8$ MPa, $\sigma_0 = 33$ MPa and $m = 1{,}21$ (see Figure 11a). Further experiments by Prime (Pagni 2003) with different glass thicknesses enabled to assess the dependence of these parameters on the glass thickness L. The equations characterising this dependence written in a non-dimensional form[4] read:

$$\frac{\sigma_u}{\text{MPa}} = 0{,}5016 \cdot \left(\frac{L}{\text{mm}}\right) + 34{,}59 \tag{4}$$

$$\frac{\sigma_0}{\text{MPa}} = -0{,}2919 \cdot \left(\frac{L}{\text{mm}}\right)^2 + 2{,}9309 \cdot \left(\frac{L}{\text{mm}}\right) + 27{,}497 \tag{5}$$

[4] The quantities are divided by their unit to obtain a non-dimensional variable.

$$m = 0{,}000815 \cdot \left(\frac{L}{\text{mm}}\right)^2 - 0{,}000985 \cdot \left(\frac{L}{\text{mm}}\right) + 1{,}205 \qquad (6)$$

These dependencies are illustrated in Figure 10.

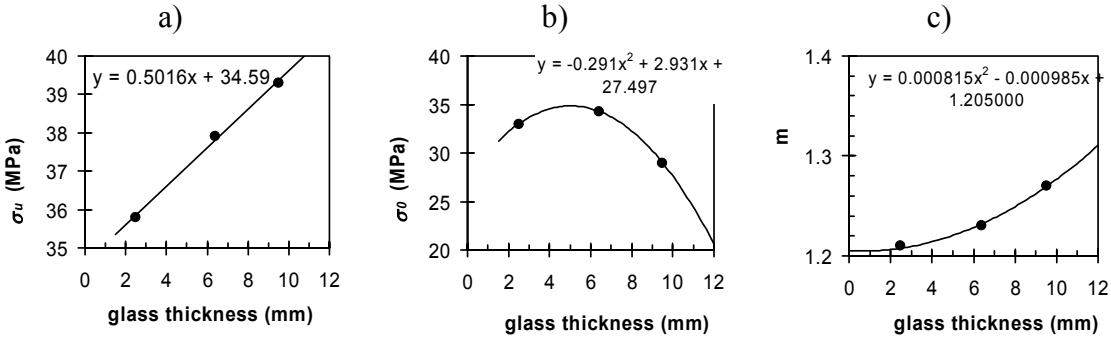

Figure 10. Dependence of σ_u, σ_0 and m on the glass thickness: a) σ_u, b) σ_0 and c) m.

According to Pagni (2003), Prime has established a relation of the breaking stress of full-scale windows σ_b and the breaking stress σ_t corresponding to the windows of size 178 mm × 25,4 mm × 2,5 mm:

$$\sigma_b = \sigma_u + (\sigma_t - \sigma_u) \cdot (2a/\ell_e)^{1/m} \qquad (7)$$

where a = 38,6 mm is the length of the uniform bending moment in the four point test apparatus (Joshi & Pagni 1994) and ℓ_e is the total length of window edges. For example, for a window with height and width equal to 1 m, ℓ_e = 8 m; the resulting full-scale breaking stress distribution is illustrated in Figure 11b.

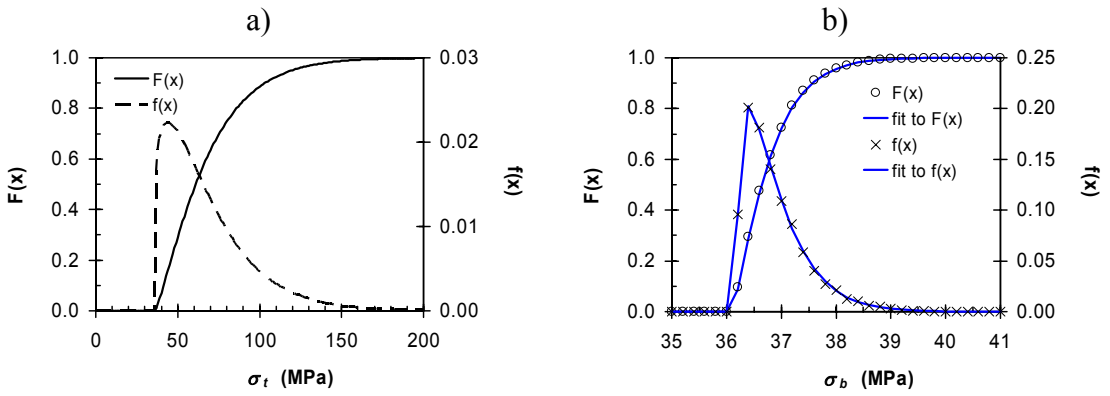

Figure 11. Characterisation of the mechanical properties of glass: a) breaking stress σ_t observed in tests Joshi and Pagni (1994) with glass panes of size 178 mm × 25,4 mm × 2,5 mm and b) example of the breaking stress for full-scale windows σ_b obtained on the basis of the quantity σ_t (window size1 m × 1 m and thickness 3 mm). In Fig. b, the data points are calculated by equation (7) and the solid curves are least-squares fits using a 3-parameter Weibull distribution with parameters a = 1.211, b = 0.737MPa and x_{min} = 36.1 MPa. The curves shown depict the cumulative frequency function F(x) and the probability density function f(x) with the argument x standing for the relevant quantity.

The Youngs modulus of the glass is treated as a deterministic parameter with value equal to E = 72 GPa (Pagni 2003).

3.1.4 Calculation of direct heat flux from the flames

3.1.4.1 Selection of the deterministic calculation model

If the fire starts close to the window, the direct heat flux from the flames to window may be high enough to cause fracture of the window pane. Evaluation of the heat flux emitted by flames is one of most common problems encountered in fire safety engineering and, thus, there are several models developed to quantify the radiative heat flux. These models are described in fire engineering handbooks (Beyler 2002, Lattimer 2002, Tien et al. 2002) and textbooks (Drysdale 1999, Karlsson & Quintiere 2000). The simplest models involve only the distance between the exposed target and the fire and the size of the fire expressed in terms of the diameter D of the fire (the power-law expression by Shokri and Beyler [1989]) or the heat release rate $\dot{Q}$ of the fire such as the point-source model (Drysdale 1999, p. 148) or the model developed by Back et al. (1994) while more elaborate models include the geometrical configuration factors describing the situation in more details. The latter models include, e.g., the model

developed by Dayan and Tien (1974) or the Mudan method (Mudan 1984). The methods employing the configuration factors usually involve evaluation of the emissive power of the flames via the flame temperature T_f and due to the strong 4th power dependence, the selection of the flame temperature is of crucial importance to the results produced by the model.

In this treatise we choose the model developed by Back et al. (1994). In particular we use the expressions corresponding to the lower part of the fire, i.e., the radiation heat flux $\dot{q}''_f$ (kW/m^2) from the fire with heat release rate (HRR) $\dot{Q}$ (in kW) and diameter D (in m) depends on the horizontal distance L from the fire centreline as

$$\begin{aligned} \dot{q}''_f &= \dot{q}''_{cl} \cdot \exp\left[-\left(\frac{L}{D/2} \right)^2 \right], \text{ for } L \le D/2 \\ \dot{q}''_f &= 0{,}38 \cdot \dot{q}''_{cl} \cdot \left(\frac{L}{D/2} \right)^{-1{,}7}, \text{ for } L > D/2 , \end{aligned} \tag{8}$$

where

$$\dot{q}''_{cl} = 200 \cdot \left[1 - \exp\left(-0{,}09 Q^{1/3} \right) \right]. \tag{9}$$

The diameter of the fire D can be assessed using the concept that the fire releases heat at a constant rate $\mathrm{RHR_f}$ (kW/m^2) per unit area:

$$D = \sqrt{\frac{4 \cdot \dot{Q}}{\pi \cdot \mathrm{RHR_f}}} . \tag{10}$$

The reasons for selecting this particular model are the following:

- The model is simple.
- It can be used down to zero distances while many other models (e.g. the point-source model and the Dayan & Tien model) are valid only beyond some certain distance (e.g. $d > 2D$ for the point-source model and $d > 1{,}5D$ the Dayan & Tien model).
- Heat flux depends on the heat release rate, not on the flame temperature.
- There is data readily available to assess the uncertainty of the model.

The results of the selected model agree also well with results of other models, see Figure 12. It may seen that with large HRR values (Figure 12c and Figure 12d) the model by Back et al. predicts higher radiative heat flux values than the two other models considered for all distances from the fire[5]. At lower HRR (~ 10–100 kW) the model by Back et al. (1994) gives slightly smaller radiative heat flux values than the Dayan and Tien (1974) model for a certain range of distance. However, the values of heat flux at this distance range are small and the slight underestimation is not significant considering the present application. At HRR values ~ 1 kW, the point source model gives highest values of heat flux while the results of the other two models are practically the same. However, also in this HRR range, the model of Back et al. (1994) is sufficient for the purposes of the present study[6].

[5] Point-source model radiative fraction equals 35% and the κ value of the Dayan & Tien model is 1,0 m^{-1}.

[6] In this particular example we use a value $RHR_f = 250$ kW/m^2. The point-source model is very sensitive to this value and also the Dayan and Tien model exhibits some dependence on the selection of RHR_f. The Back et al. model results when plotted against the value L/(D/2) are not affected by the choice of RHR_f.

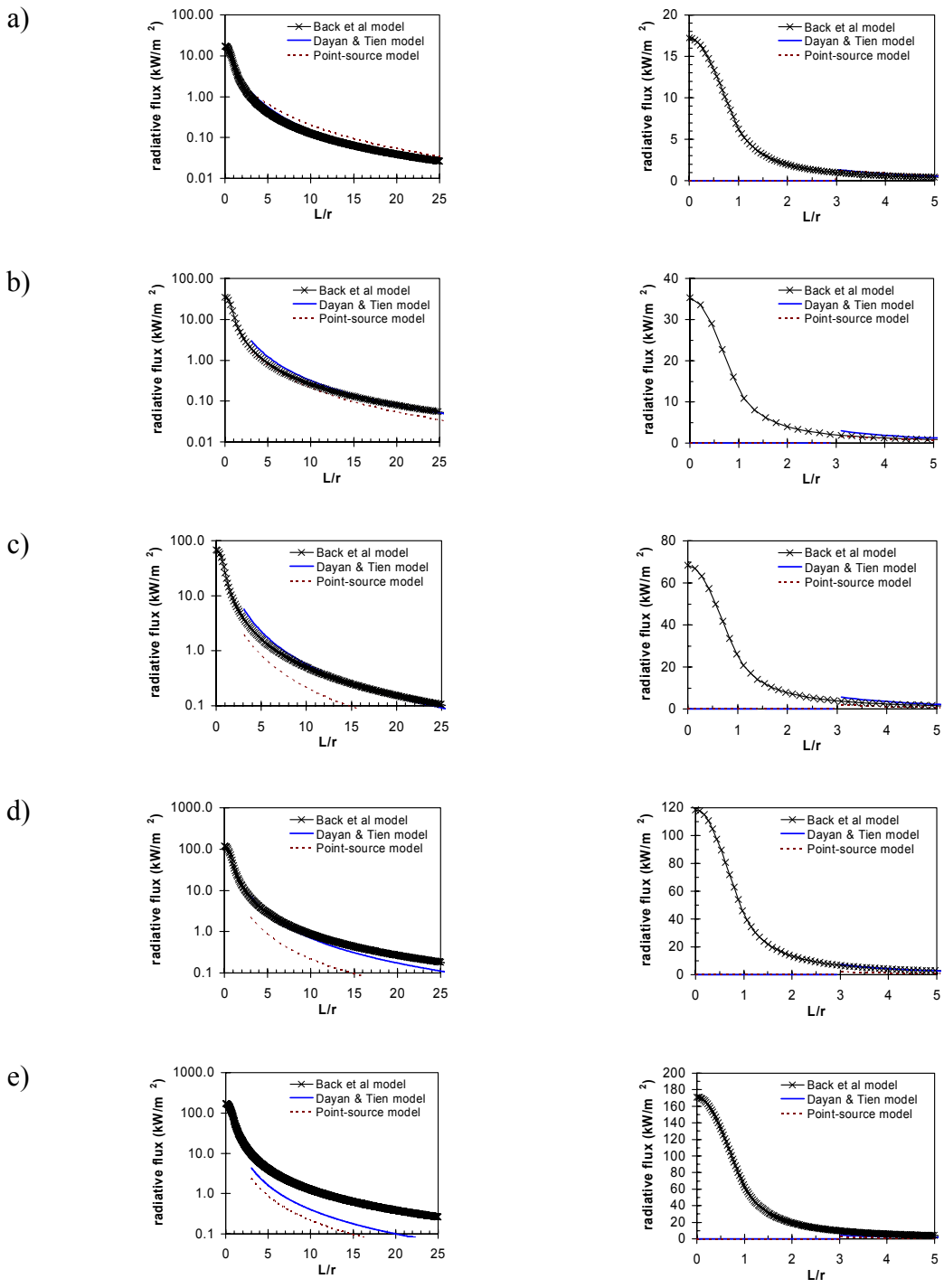

Figure 12. Comparison of three models to calculate the radiative heat flux from a fire: 1) Back et al. (1994) model, 2) Dayan & Tien (1974) model and the point-source model (Drysdale 1999, p. 148). Five different HRR values of the fire are considered: a) 1 kW, b) 10 kW, c) 100 kW, d) 1 000 kW and e) 10 000 kW. Charts on the left hand side are plotted using a logarithmic scale for the ordinate and the charts on the right hand side with a normal ordinate scale (r = D/2 and RHR_f = 250 kW/m^2 in this example).

3.1.4.2 Converting the deterministic model to a stochastic model

In order to be able to take into account the uncertainties in the selected heat flux model, we modify the expressions for $\dot{q}''_f$ by introducing two additional model parameters a and A. The modified equations read

$$\begin{aligned} \dot{q}''_f &= \dot{q}''_{cl} \cdot a \cdot \exp\left[-\left(A \cdot \frac{L}{D/2} \right)^2 \right], \text{ for } L \le D/2, \\ \dot{q}''_f &= \dot{q}''_f \cdot a \cdot \exp\left(-A^2\right) \cdot \left(\frac{L}{D/2} \right)^{-1,7}, \text{ for } L > D/2, \end{aligned} \tag{11}$$

where $\dot{q}''_{cl}$ is calculated on the basis of the heat release in the same way as in the original formulation of Back et al. (Eq. [11]).

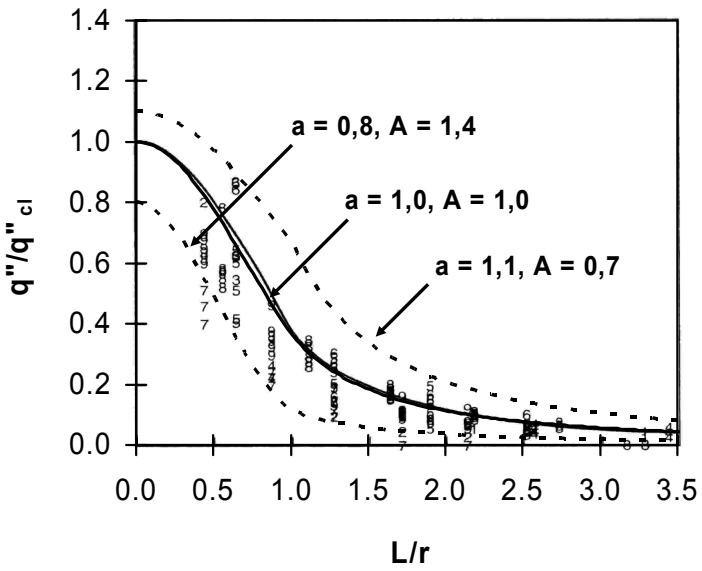

Figure 13. Characterising the uncertainty in the heat flux calculation model. The data points are obtained from Fig. 2-14-4 of the Lattimer's article in the SFPE Handbook (Lattimer 2002) and the dotted curves are calculated using Eq. 11 by tuning the parameters a and A so that they enclose majority of the data points (by visual judgement).

The parameters a and A are treated as random numbers with their ranges determined from the data of Back et al. (1994). A visual analysis procedure (see Figure 13) gives the results that $a \in [a_{\min}, a_{\max}] = [0{,}8;1{,}1]$ and $A \in [A_{\max}, A_{\min}] = [1{,}4;0{,}7]$. It should be noted that in the further development of the stochastic model one must retain the order relationship between the two parameters, i.e., values of a in its lower range correspond to values of A in its higher range. This means that only either a or A can be selected

randomly while the other is dependable variable. Another requirement is that the most probable value of both a and A should be unity. These requirements can be fulfilled by a simple monotonous bilinear mapping between the two parameters. Let us select a to be the random variable and A the dependable variable. Then a suitable mapping between a and A, which fulfils the following requirements

- for the range $a \in [a_{\min}, 1]$ when $a = a_{\min}$ then $A = A_{\max}$
- for the range $a \in [1, a_{\max}]$ when $a = a_{\max}$ then $A = A_{\min}$
- for $a = a_{\text{peak}}$, $A = A_{\text{peak}}$

is shown in Figure 14, i.e.,

$$\begin{aligned} &\text{when } a \in \lfloor a_{\min}, a_{peak} \rfloor,\ A = -\frac{\left(A_{\max} - A_{peak}\right)}{\left(a_{peak} - a_{\min}\right)}\left(a - a_{\min}\right) + A_{\max}, \\ &\text{when } a \in \lfloor a_{peak}, a_{\max} \rfloor,\ A = -\frac{\left(A_{peak} - A_{\min}\right)}{\left(a_{\max} - a_{peak}\right)}\left(a - a_{peak}\right) + A_{peak}. \end{aligned} \tag{12}$$

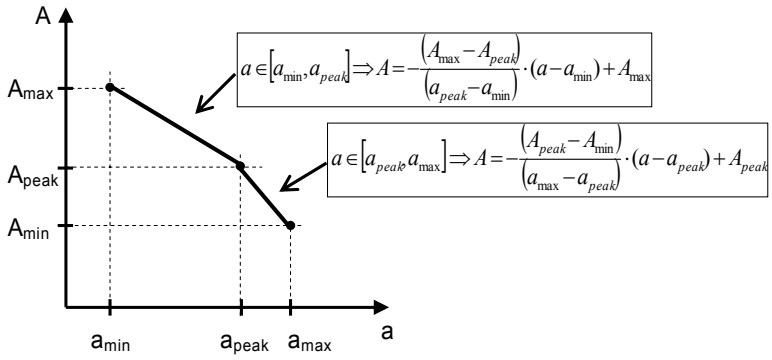

Figure 14. Relationship between parameters a and A of Eq. (3).

Examples of stochastic heat flux curves are shown in Figure 15.

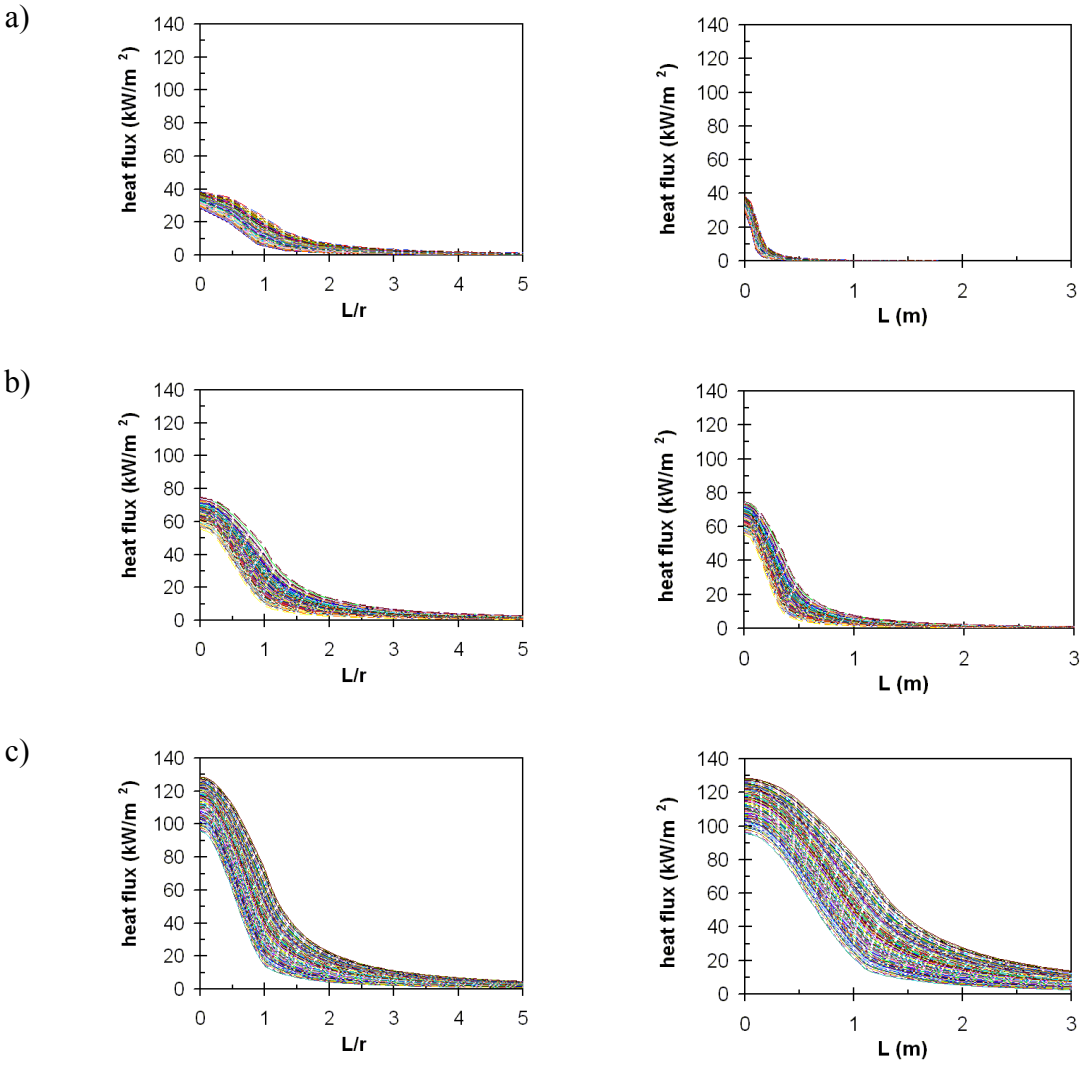

Figure 15. Stochastic heat fluxes as a function of the distance from the fire: a) 10 kW, b) 100 kW and c) 1 000 kW. Charts on the left hand side are plotted against normalised distance L/(D/2) and the charts on the right hand side against the distance L.

3.2 Computer implementation of the Monte-Carlo BREAK1: MCB.for

The Monte Carlo version of the BREAK1 is implemented as a Fortran program MCB.for (Fortran 90 language). The listing of this program is attached as Appendix C of this report. Appendix C presents also the format and contents of the input parameter file MCB.config as well as the format and contents of the time series fire characteristics data file. The format of the latter is the same as that of the **.pri* file generated by the Ozone fire zone model (Cadorin & Franssen 2003).

The BREAK1 glass fracture calculation module is implemented as a function on the MCB.for. Input required is read from a file MCB.config with one exception: the shading thickness is given as an interactive response to the program prompting.

3.3 Example calculations of the occurrence of the first cracking by the Monte Carlo BREAK1 model

In this section we demonstrate the use of the MCB.for program. We consider a fire in the small room depicted in Figure 16. The floor and ceiling are assumed to be made on normal-weight concrete and the walls of gypsum board. We consider only one opening, the doorway with dimensions of 2 m × 0,8 m. The fire density is assumed to be 750 MJ/m^2. The maximum HRR is taken to be 3 MW (fuel limited, but on the brink of being ventilation limited). In these examples, the heating is assumed to be due to the hot gas layer only.

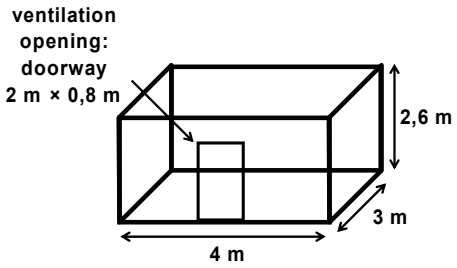

Figure 16. The simple small room considered in the example MCB runs in this section.

Figure 17 shows results concerning the first occurrence of glass fracture in a fire in the room shown in Figure 16 with HRR growth time equal to 300 s (normal fire growth rate). The glass pane height is assumed to be 1 m and its width 1,2 m. The glass thickness is assumed to be 3 mm and the shading thickness equal to 15 mm. It is seen that the first crack forms at 3,5–4 minutes (Figure 17e) and that the hot gas layer temperature at the time of the first glass cracking is about 160–220 °C (Figure 17f). The corresponding average glass temperature, i.e., the quantity ΔT_g of the conceptual model presented in the previous Chapter, varies between 75 °C and 85 °C (Figure 17g). The distributions in Figure 17 can be fitted well with the Weibull distribution (see the previous sections for the particular form of the Weibull distribution used in this study): for the time of the first cracking the Weibull distribution parameters are $\alpha = 5{,}61$, $\beta = 0{,}55$ min and $x_{\min} = 3{,}2$ min (mean value 3,7 min); for the hot gas layer temperature at the first cracking the Weibull distribution parameters are $\alpha = 4{,}75$, $\beta = 38{,}6$ °C and $x_{\min} = 156{,}9$ °C (mean value 192 °C) and for the average glass temperature at the first cracking the Weibull distribution parameters are $\alpha = 2{,}26$, $\beta = 3{,}70$ °C and $x_{\min} = 75{,}4$ °C (mean value 78,7 °C).

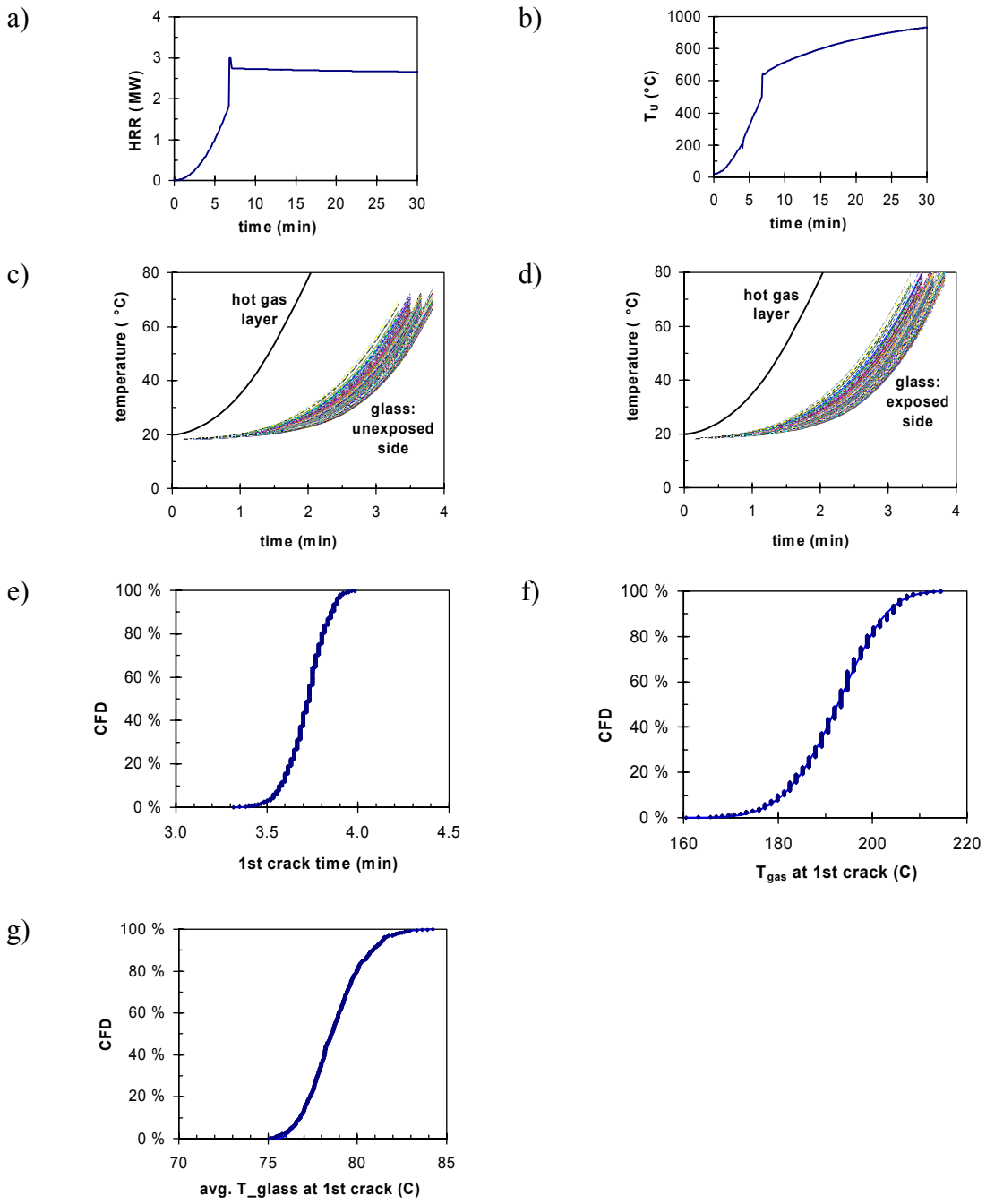

Figure 17. Occurrence of the first cracking of the glass in the example room fire with HRR growth rate equal to 300 s: a) HRR, b) hot gas layer temperature, c) glass surface temperature on the unexposed side (sample of 200 curves), d) glass surface temperature on the fire-exposed side (sample of 200 curves), e) distribution of the time to the first glass cracking, f) distribution of the hot gas layer temperature at the first glass cracking and g) distribution of the average glass temperature (ΔT_g) the first glass cracking.

The influence of the fire growth rate on the occurrence of the first glass cracking is studied in Figure 18, Figure 19 and Figure 20, which show the time to the first glass cracking, the hot gas layer temperature at the first cracking and the average glass temperature at the first cracking, respectively.

It is seen that in slowly growing fire (growth time 600 s), the first glass crack appears between 5,5 minutes and 7 minutes (Figure 18a) while in the ultrafast growing fire (growth time 75 s), it takes only about 1,3–1,4 min (Figure 18d) for the first crack to appear. In a rapidly growing fire, however, the hot gas layer temperature at the first glass cracking reaches a much higher level, 280–340 °C (Figure 19d), than in a slowly growing fire which reaches ca. 130–180 °C (Figure 19a).

While the time to the first crack of the window pane and the hot gas layer temperature at this moment depend very strongly on the fire growth rate, the average glass temperature at the first cracking is virtually invariant with respect to the fire growth rate as evidenced by Figure 20: the distribution vary between 75 °C and 85 °C (Figure 20a–Figure 20e) and the mean values of the distributions lie all within 2 °C (78 °C–80 °C, Figure 20f). The invariance of the temperature rise ΔT_g required to create the first crack with respect to the hot gas rise rate supports the conceptual model of glass fallout presented in Chapter 2: although the rising rate of the hot gas layer temperature varies during the fire, we can assume that the average glass temperature increment required to create subsequent cracks and eventually a glass fallout, remains virtually constant.

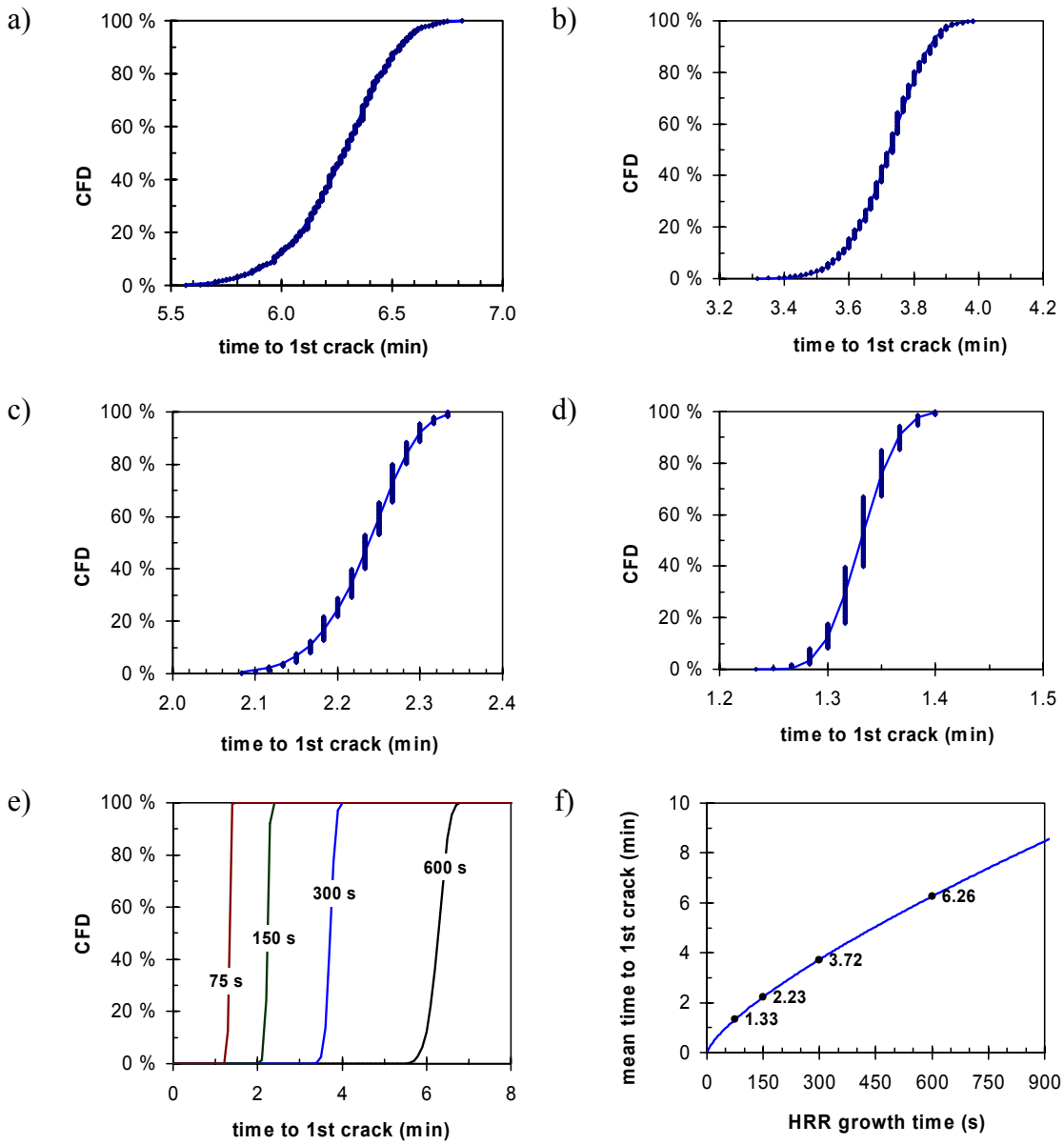

Figure 18. Distributions of the time to the first glass cracking in a fire in the example room with different HRR growth rates equal to a) 600 s, b) 300 s, c) 150 s and d) 75 s. Figure e) presents comparison of all distributions and f) shows the dependence of the mean time to the first crack on the fire HRR growth time in the example room shown in Figure 16.

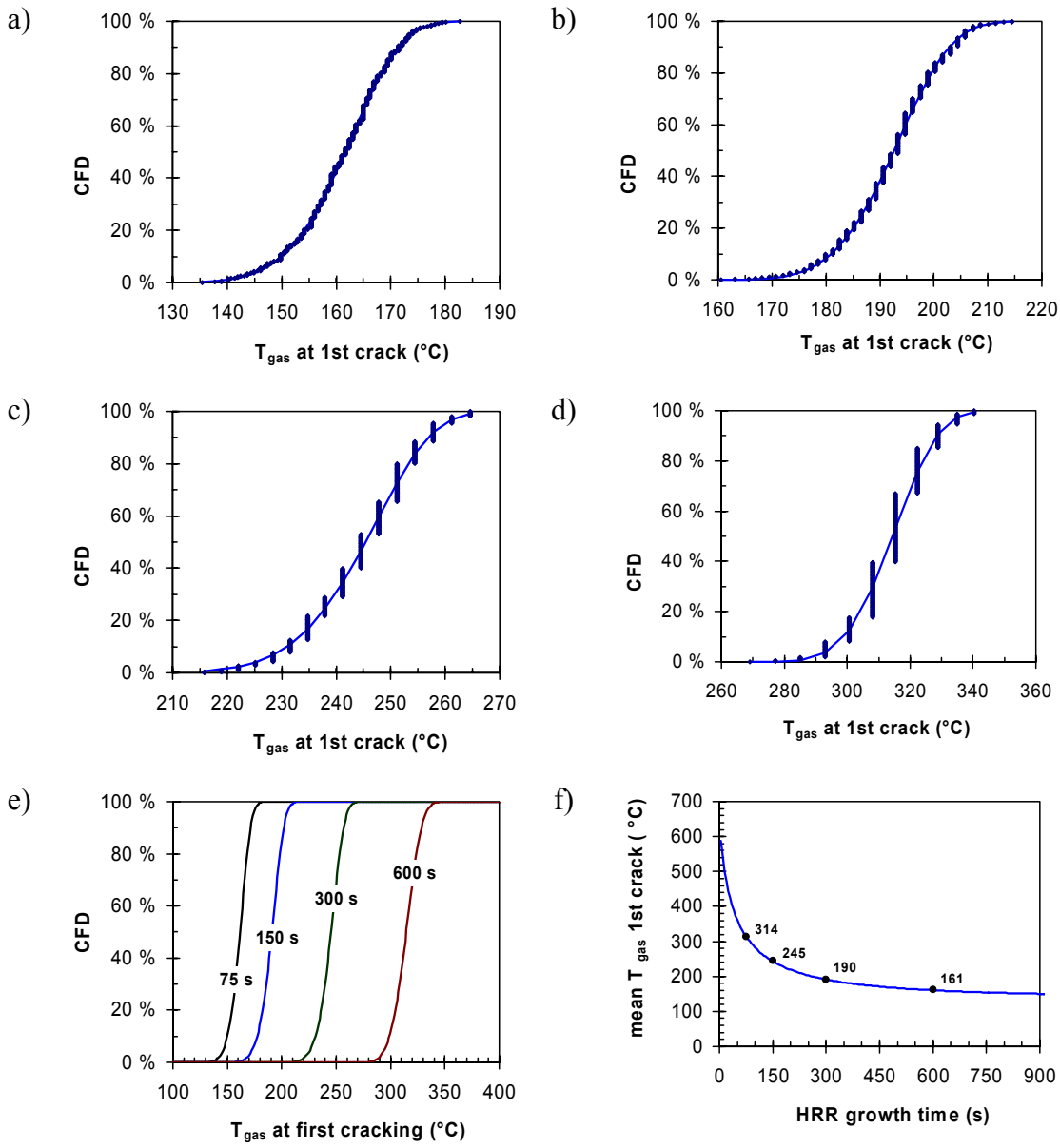

Figure 19. Distributions of the hot gas layer temperature at the first glass cracking in a fire in the example room with different HRR growth rates equal to a) 600 s, b) 300 s, c) 150 s and d) 75 s. Figure e) presents comparison of all distributions and f) shows the dependence of the mean time to the first crack on the fire HRR growth time in the example room shown in Figure 16.

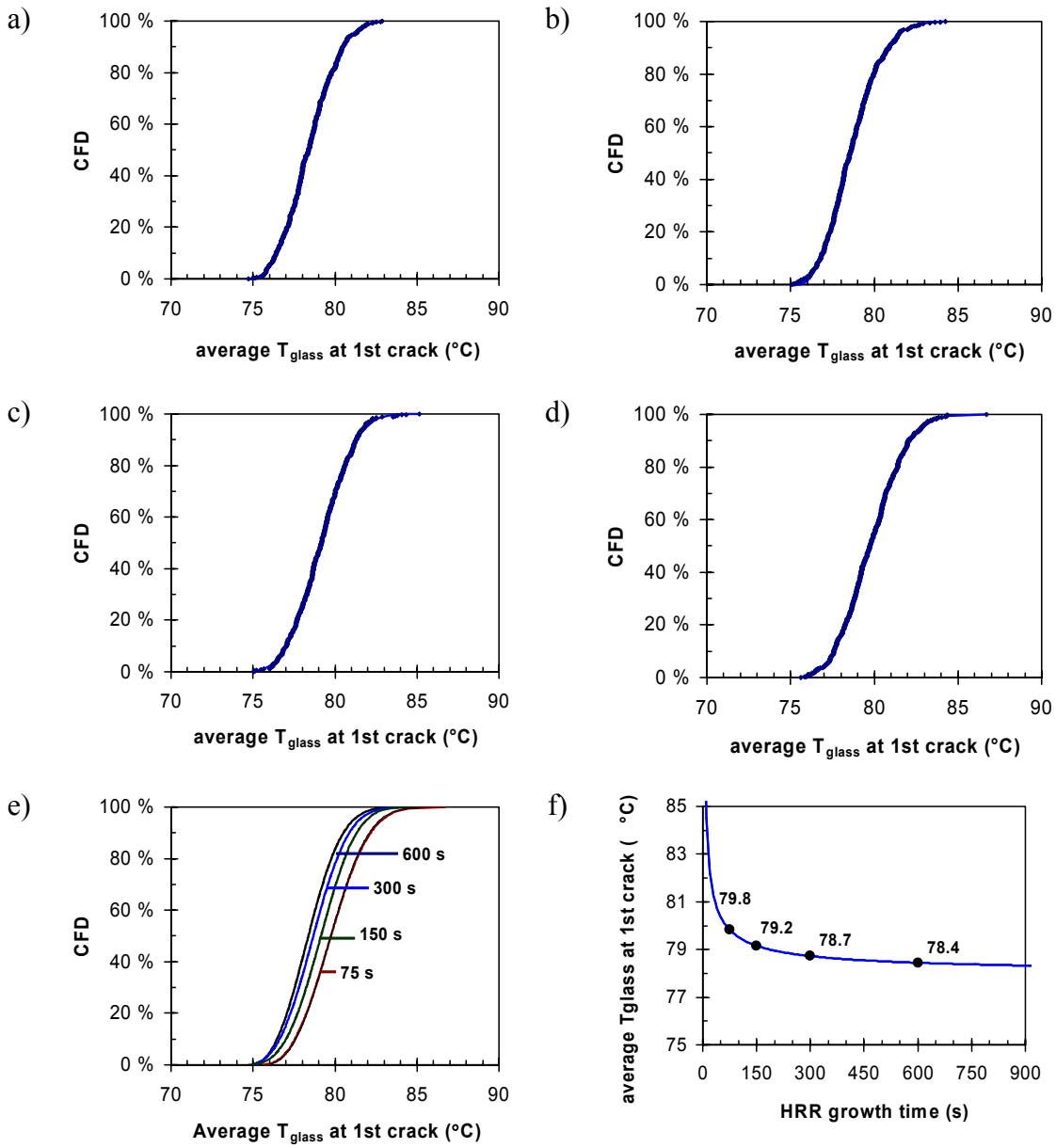

Figure 20. Distributions of the average glass temperature at the first glass cracking in a fire in the example room with different HRR growth rates equal to a) 600 s, b) 300 s, c) 150 s and d) 75 s. Figure e) presents comparison of all distributions and f) shows the dependence of the mean time to the first crack on the fire HRR growth time in the example room shown in Figure 16.

4. Window fallout creating a ventilation opening: modelling based on series of consecutive heat-induced fractures

In this Chapter we complete the conceptual model described in Chapter 2 by evaluating the heating up of the glass after the first cracking and assessing how many crackings will lead to a catastrophic failure and fallout of the glass pane.

4.1 Glass heating described using the lumped heat-capacity model

The philosophy of the treatise in section is to keep the modelling simple. Thus, we omit any influence of direct radiation effect of the flames and assume that only the hot gas layer temperature T_{hot} contributes to the glass heating. Then, within the lumped heat-capacity model the governing equation for the glass temperature T_g reads:

$$\rho\delta C\frac{dT_g}{dt} = h_{hot}\cdot\left(T_{hot}-T_g\right)+\varepsilon_{hot}\varepsilon_{g,hot}\sigma\left(T_{hot}^4-T_g^4\right)- \\ -\left[h_{cold}\cdot\left(T_g-T_\infty\right)+\varepsilon_{cold}\varepsilon_{g,cold}\sigma\left(T_g^4-T_\infty^4\right)\right] \tag{13}$$

where

- ρ = glass density (random parameter)
- δ = glass thickness (given value)
- C = glass specific heat (random parameter)
- h_{hot} = heat transfer coefficient on the exposed side (random parameter)
- ε_{hot} = hot layer emissivity (assumed to be equal to unity, $\varepsilon_{hot} = 1$)
- $\varepsilon_{g,hot}$ = glass emissivity on the exposed side (random parameter)
- h_{cold} = heat transfer coefficient on the unexposed side (random)
- $\varepsilon_{g,cold}$ = glass emissivity on the cold side, assumed to be equal to $\varepsilon_{g,hot}$ (random)
- ε_{cold} =emissivity of the ambient (assumed to be equal to unity, $\varepsilon_{cold} = 1$)
- T = ambient temperature (given value).

The random parameters are the same as those described in section 3.1.

Equation (13) is readily integrated numerically using the forward-Euler method to give

$$T_{g,k+1} = T_{g,k}+\Delta t\cdot\left(\frac{1}{\rho\delta C}\right)\left\{\begin{matrix} h_{hot,k}\cdot\left(T_{hot,k}-T_{g,k}\right)+\varepsilon_{hot.k}\varepsilon_{g,hot,k}\sigma\left(T_{hot.k}^4-T_{g.k}^4\right)- \\ \left[h_{cold.k}\cdot\left(T_{g,k}-T_\infty\right)+\varepsilon_{cold,k}\varepsilon_{g,cold,k}\sigma\left(T_{g,k}^4-T_\infty^4\right)\right] \end{matrix}\right\} \tag{14}$$

where Δt is the integration time step (of the order of 5–10 s).

The lumped heat-capacity model applies the better the more constant the temperature distribution within the solid is. As glass is a poor heat conductor, a temperature gradient builds up along its thickness and thus, the lumped heat capacity model is intrinsically a poor model to describe glass heating. However, the glass panes that we usually are interested in fire safety engineering are thin, with thickness typically ranging between 3 mm and 6 mm. In such a thin solid, the lumped heat-capacity model gives a *working approximation* of the heating of the solid. This notion is corroborated by Figure 21 and Figure 22 which show that the lumped heat-capacity approach gives a decent approximation of results calculated by the more rigorous heat-transfer model implemented in the BREAK1 program.

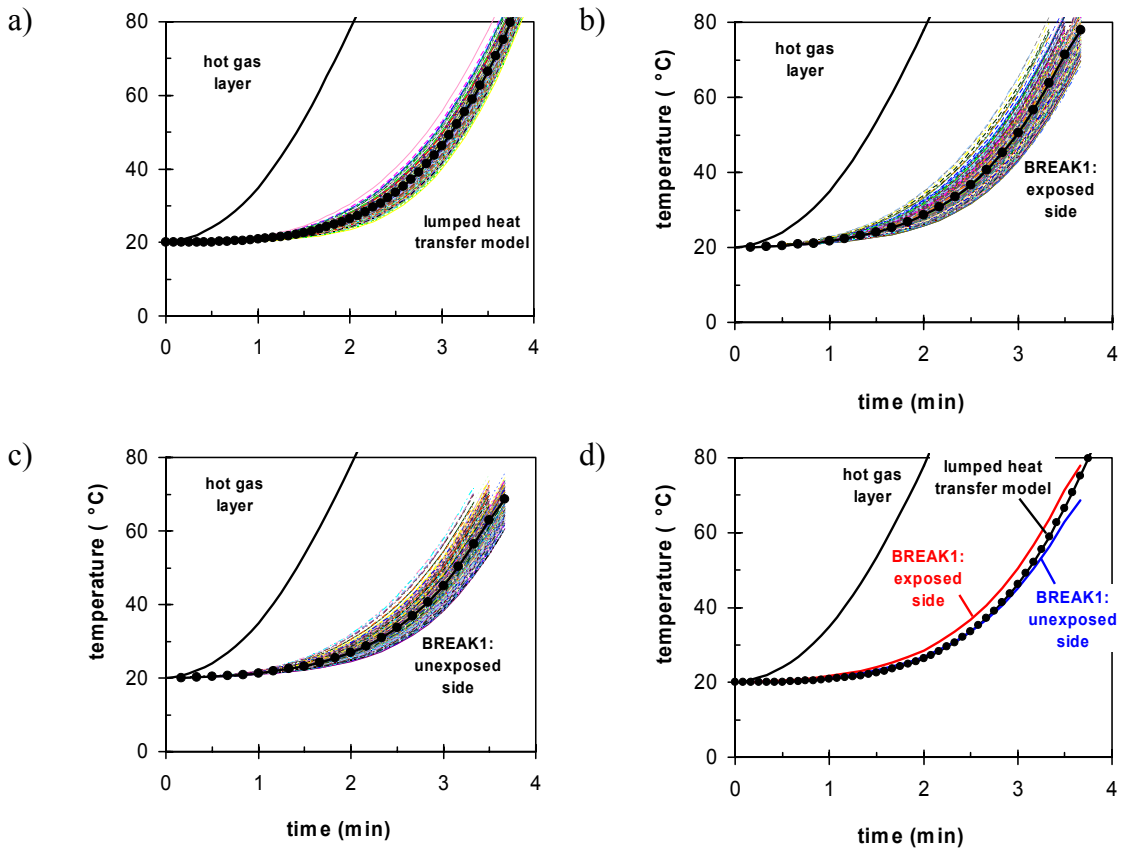

Figure 21. 3 mm thick glass: comparison of glass temperatures calculated using the simple lumped heat-capacity model and the more rigorous heat transfer model implemented in the BREAK1 program (glass pane with dimensions of 1 m (height) and 1,2 (width) and shading thickness of 15 mm): a) results of the lumped heat-capacity model, b) BREAK1 result for the exposed side temperature, c) b) BREAK1 result for the unexposed side temperature and d) comparison of the average temperatures calculated using the both models.

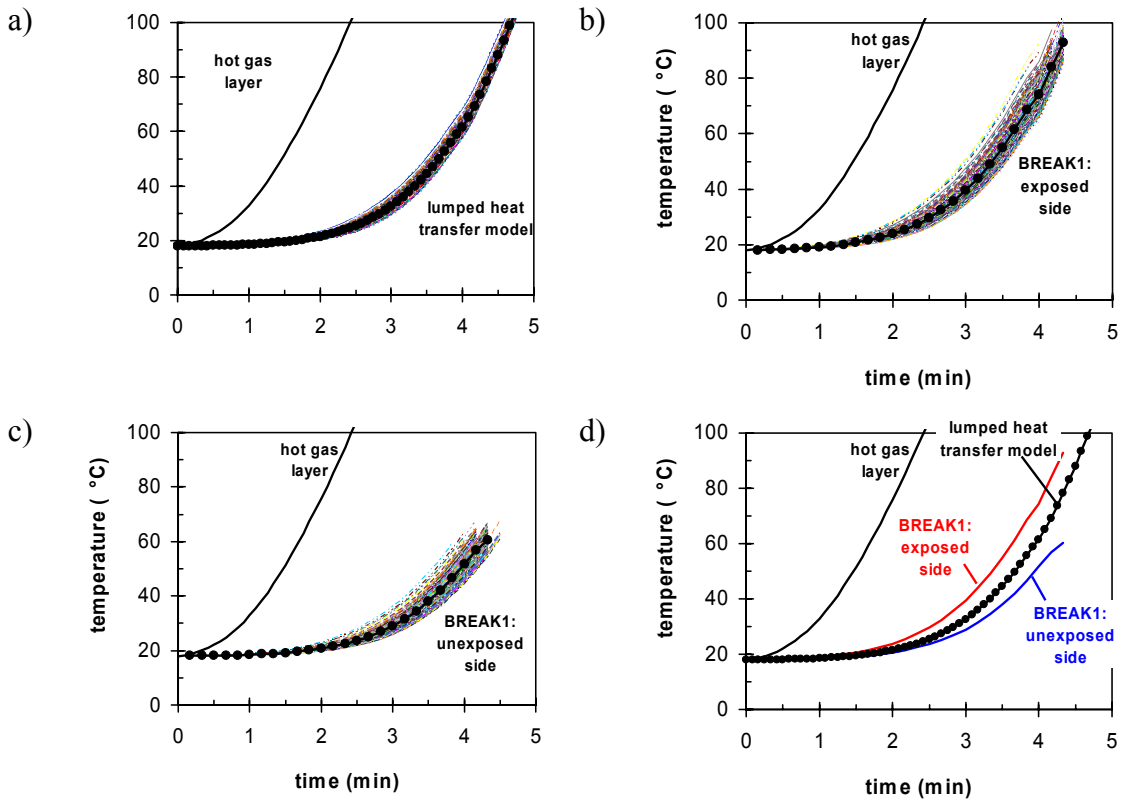

Figure 22. 6 mm thick glass: comparison of glass temperatures calculated using the simple lumped heat-capacity model and the more rigorous heat transfer model implemented in the BREAK1 program (glass pane with dimensions of 1 m (height) and 1,2 (width) and shading thickness of 15 mm): a) results of the lumped heat-capacity model, b) BREAK1 result for the exposed side temperature, c) b) BREAK1 result for the unexposed side temperature and d) comparison of the average temperatures calculated using the both models.

4.2 Example of the application of the simple heat up model

To exemplify the use of the simple heating model described above, we consider again a fire in the small room shown in Figure 16. The characteristics of the room and the fire are assumed to be the same as those considered in section 3.3. The fire HRR growth rate is taken to be 300 s. The results are shown in Figures 23–25.

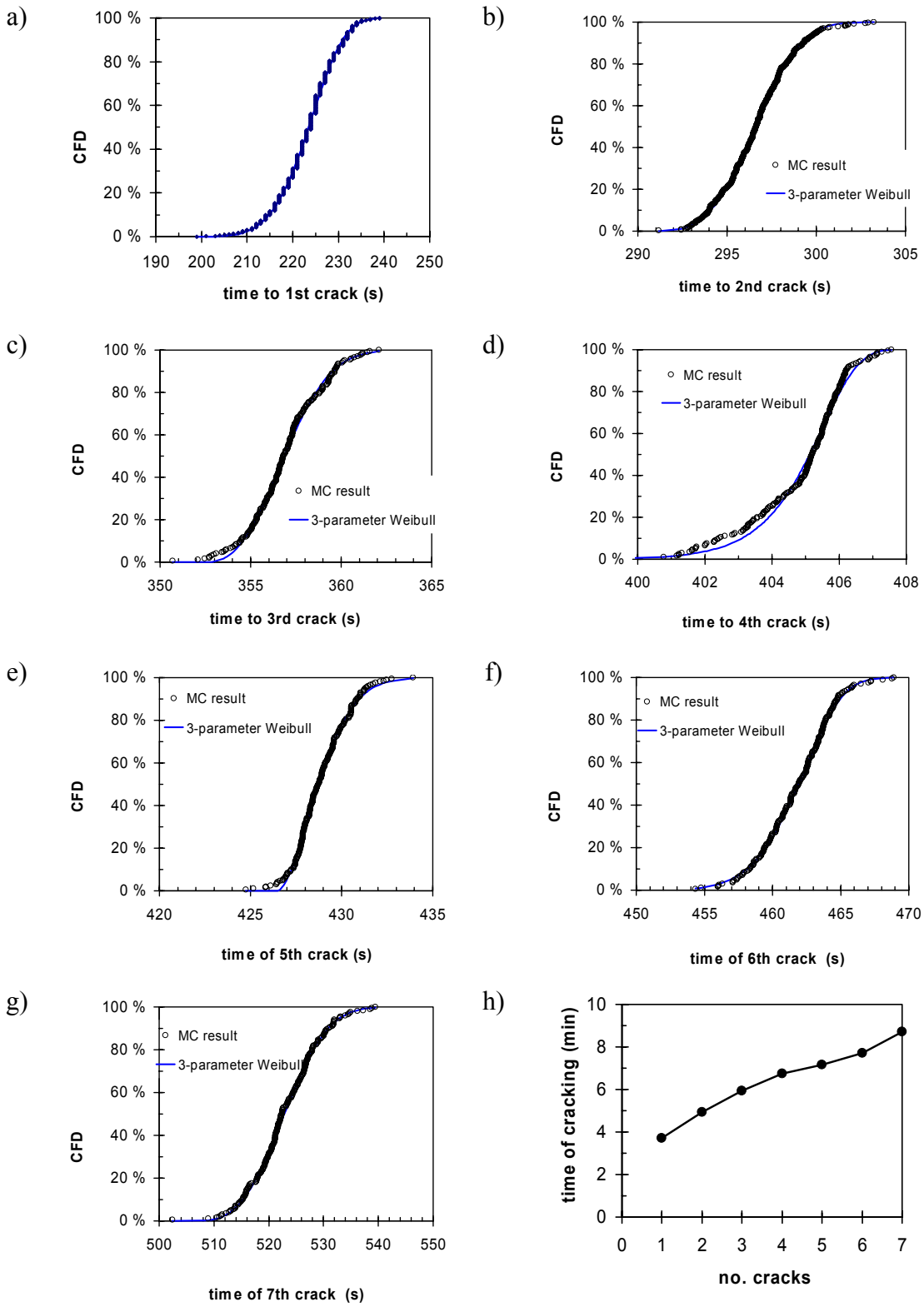

Figure 23. Times of occurrence of glass crackings in a fire in the example room shown in Figure 16 with HRR growth rate equal to 300 s. a)–g) cracks no. 1–7 and h) summary of mean times to creation of cracks.

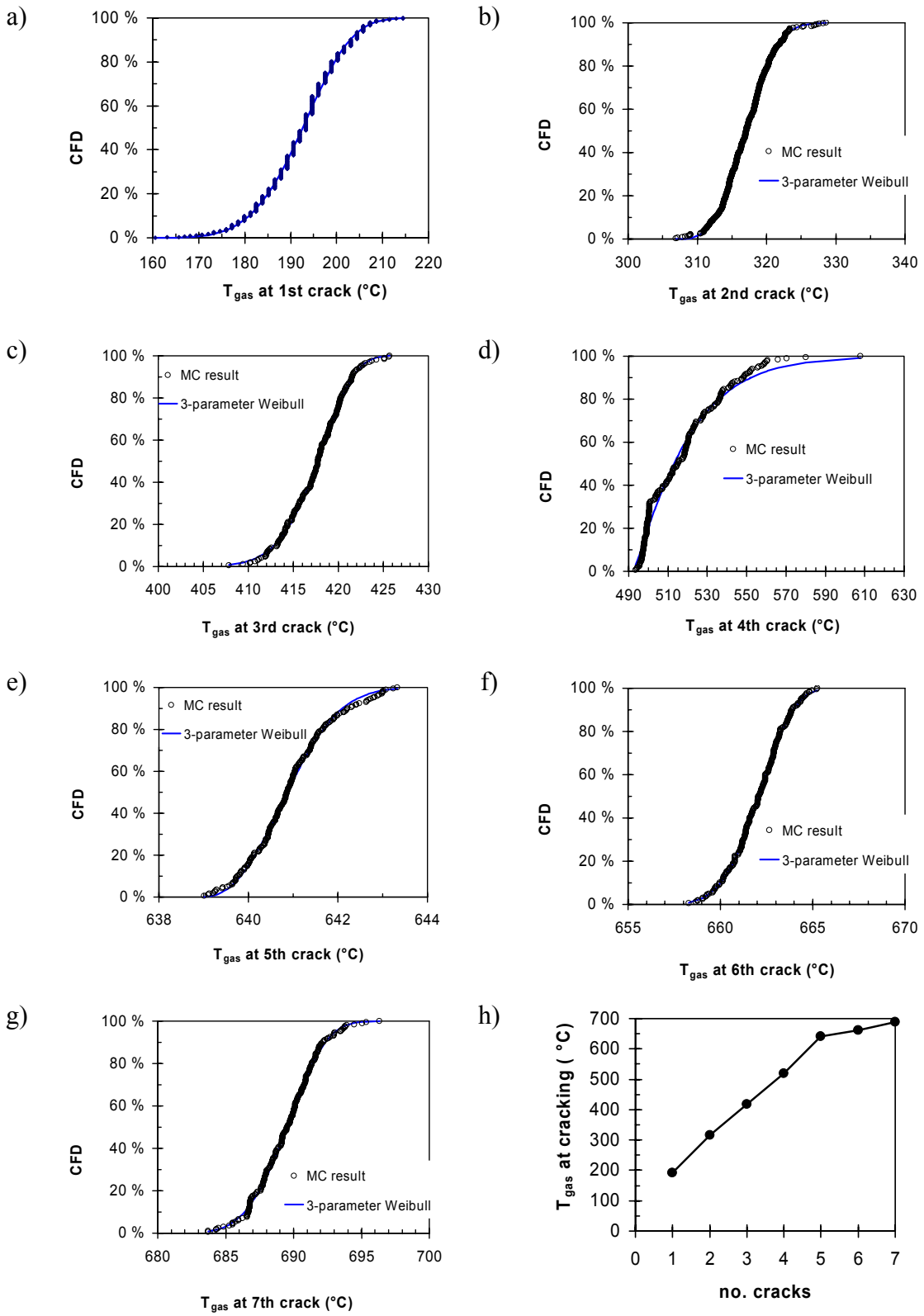

Figure 24. Hot gas layer temperatures at the occurrence of glass crackings in a fire in the example room shown in Figure 16 with HRR growth rate equal to 300 s. a)–g) cracks no. 1–7 and h) summary of the mean values of hot gas layer temperatures.

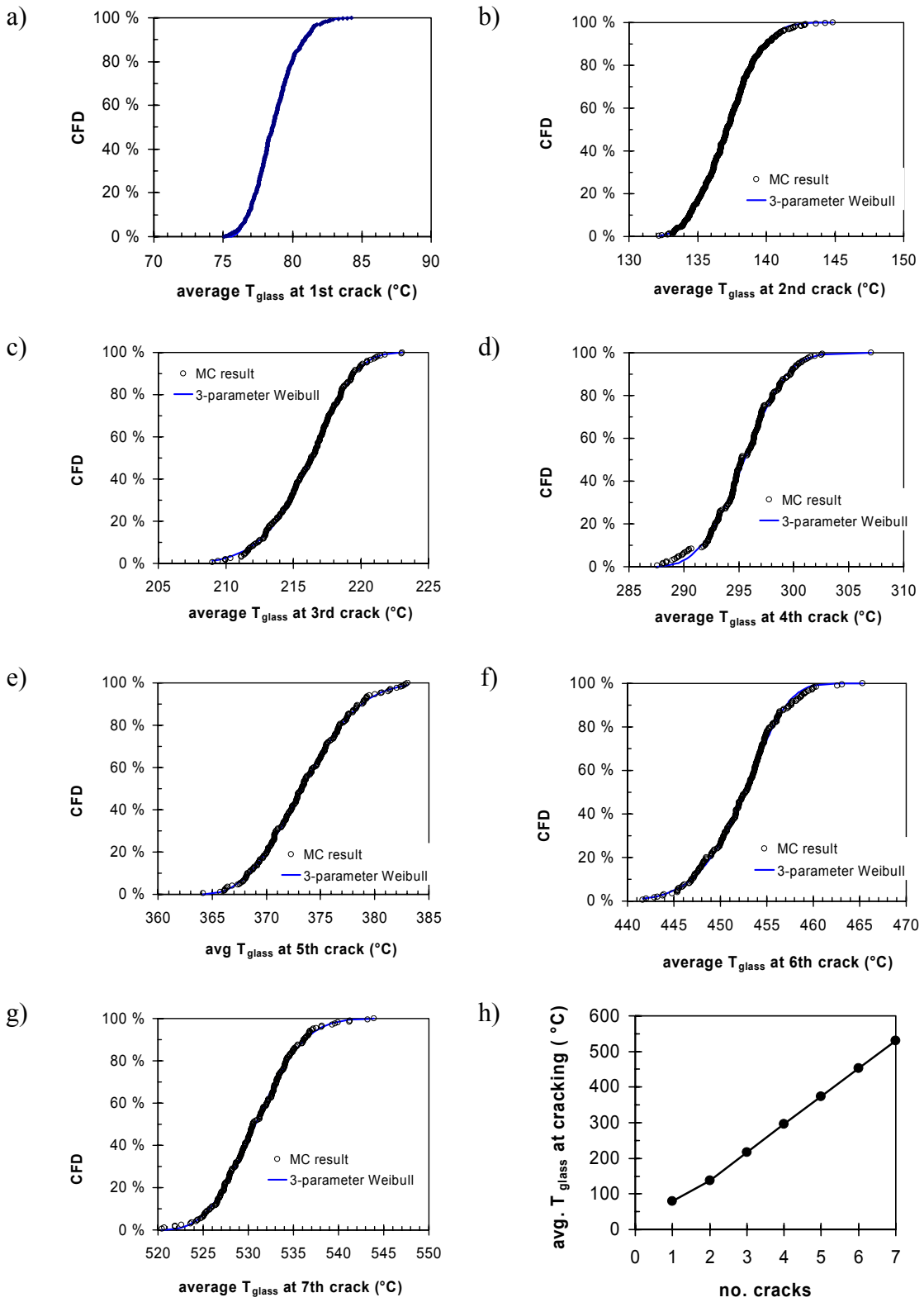

Figure 25. Average glass temperatures at the occurrence of glass crackings in a fire in the example room shown in Figure 16 with HRR growth rate equal to 300 s. a)–g) cracks no. 1–7 and h) summary of the mean values of the average glass temperatures.

4.3 Elucidating the number of crackings needed for glass fallout on the basis of experimental findings

In this section we analyse with our model the pieces of experimental findings listed below on the glass fracture and fallout to establish the number of crackings required take into account in our to assess the glass fallout conditions. The analysis is carried out by using the reported hot gas layer temperatures in out model. It should be noted that as our approach considers only enclosure fires with heating coming from the hot gas layer we have not included the several outstanding studies with radiant heating (e.g. Mowrer 1998 and Harada et al. 2000) in our analysis.

The experimental studies that we have subjected to an in-depth analysis are the following:

1. Skelly et al. (1991): An experimental investigation of glass breakage in compartment fires.

2. Hassani et al. (1994/1995): An experimental investigation into the behaviour of glazing in enclosure fire.

3. Loss Prevention Council (Anon. 1999): Study concerning fire spread in multi-storey buildings with glazed curtain wall facades.

4. Shields et al. (2001): Study on the performance of single glazing elements exposed to enclosure corner fires of increasing severity.

5. Shields et al. (2002): Study on the performance of a single glazing assembly exposed to a fire in the centre of an enclosure.

6. Hietaniemi et al. (2002): An investigation of fire safety issues related to building cavity spaces, Appendix F: glass-breaking study using a fire-resistance furnace.

7. MeHaffey et al. (2004): Fire experiments in furnished houses (test 1 and 2).

There are some studies which we could not subject to such in-depth analysis as the results of the studies listed above, such as Richardson and Oleszkiewicz (1987) and Tanaka et al. (1998).

4.3.1 An experimental investigation of glass breakage in compartment fires by Skelly et al. (1991)

Skelly et al. (1991) carried out experiments on glass-breakage using the small-scale enclosure fire test set-up shown in with compartment dimensions of 150 cm × 120 cm × 100 cm (Figure 26). The glass panes studied were 50 cm wide, 28 cm high and 2,4 mm thick. The shading thickness was 25 mm.

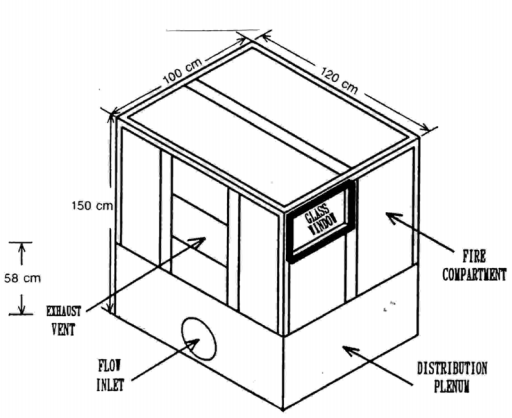

Figure 26. Schematic presentation of the experimental set-up of Skelly et al. (1991).

We consider tests 3 and 4 of Skelly et al. (1991). The temperature curves of these tests are reproduced in Figure 27 with the compartment gas temperature curves used as input to our calculations emphasised by thick blue curves.

The results on the occurrence of the crack initiation of the glass panes calculated by the Monte Carlo BREAK program are shown in Figure 28 (test no. 3) and Figure 29 (test no. 4). For test no. 3 the agreement between the calculated results the observed results (summarised in Table 1 of Skelly et al.) is good. For the test no. 4 the agreement is considerably worse. The latter discrepancy was revealed also in the study by Larsson (1999). While the reason for this discrepancy can not be unveiled on the basis of the information of the article by Skelly et al. (1991), perhaps the note made Babrauskas (2004) concerning the experiments of Skelly et al., i.e., that "one peculiarity of his tests was that the windows were never exposed to a vertical temperature gradient" may explain at least some of the discrepancy.

The events that take place at 48 s in test no. 3 and 100 s in test no. 4 are characterised in the Figures as "catastrophic window collapse", but the phrasing used in Table 1 is "crack initiation". It seems to us that these two characterisations are quite different so that "catastrophic window collapse" would mean substantial glass fallout but "crack initiation" would suggest only an occurrence of a fracture in the window pane. At least in test no. 3, the compartment temperature rises steeply with no sign of changes of the

rate of rising at 48 s, which would suggest that the performance of the window would not have changed dramatically at this moment. In test no. 4, a clear deflection towards slower rate of compartment temperature rising can be discerned after 100 s, which would suggest that the performance of the window changes at this time. Nevertheless, not knowing exactly the nature of the glass performance, we choose not to use data of Skelly et al. (1991) to elucidate the number of crackings that is needed for partial or complete glass fallout in fire.

a)

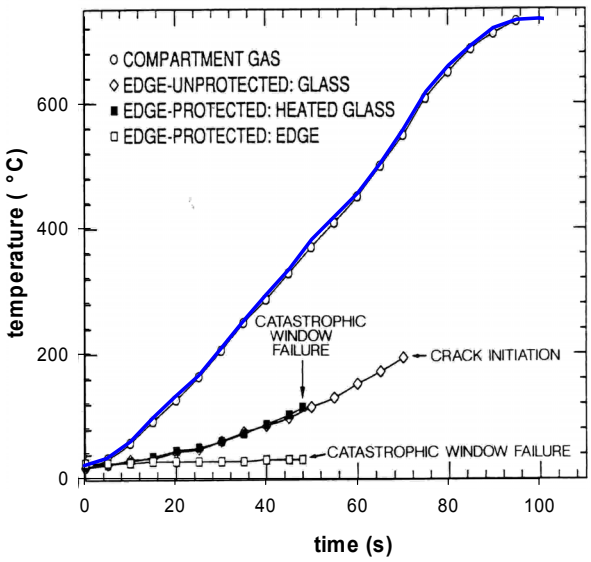

b)

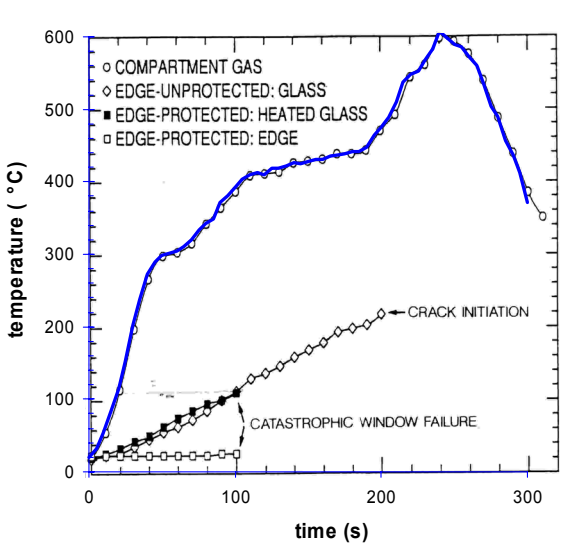

Figure 27. a) Temperature readings reported by Skelly et al. (1991) from their test no. 3 and b) temperature readings from the test no. 4. The compartment gas temperature curves are emphasised by thick blue curves because they are used as input to our modelling.

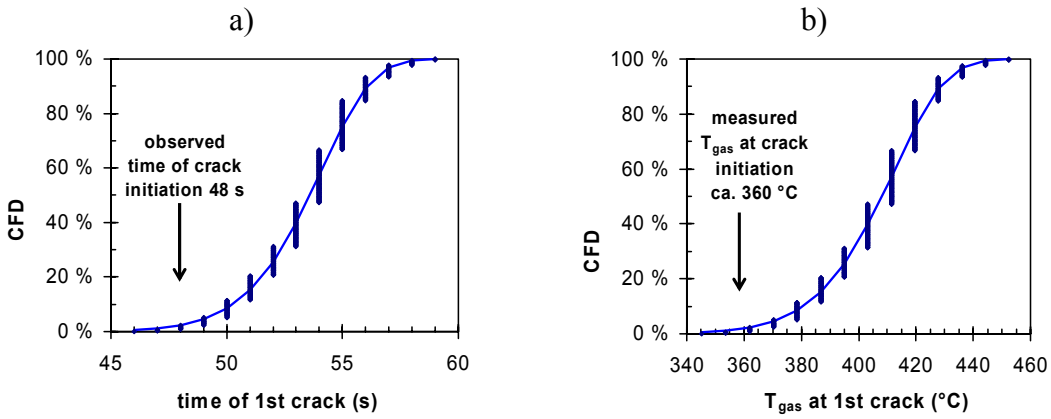

Figure 28. Modelling of the glass crack initiation in test 3 of Skelly et al. (1991): a) time of crack initiation and b) compartment gas temperature at crack initiation.

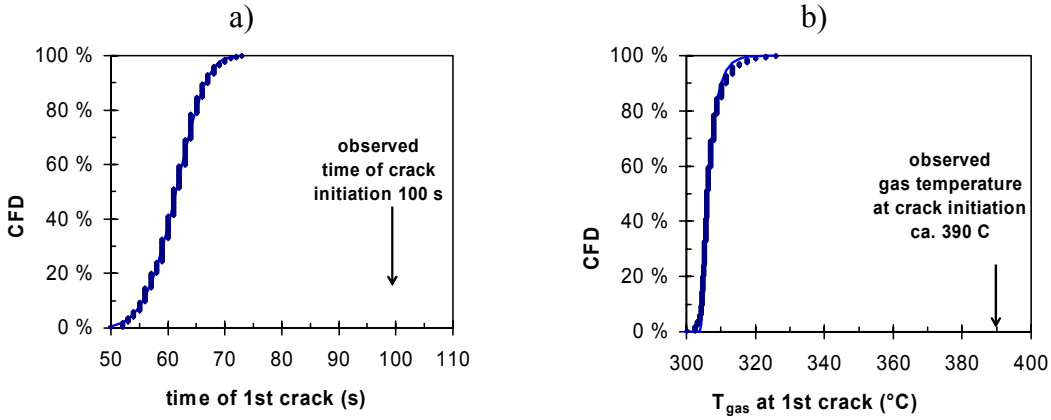

Figure 29. Modelling of the glass crack initiation in test 4 of Skelly et al. (1991): a) time of crack initiation and b) compartment gas temperature at crack initiation.

4.3.2 An experimental investigation into the behaviour of glazing in enclosure fire by Hassani et al. (1994/1995)

Hassani et al. (1994/1995) made experiments on glass breaking in fire using a half-scale room with dimensions of 1705 mm (depth) 1525 mm (width) and 1180 mm (height). Three different wall constructions were used, a heavyweight construction made of concrete, a "normalised" construction with a double plaster-board construction on the concrete wall and a lightweight construction with a single plaster-board construction on the concrete wall. Here we concentrate on the results pertaining to the lightweight construction because that is the one of which the authors have provided the time-temperature graphs of the hot gas layer temperature (Figure 10 of ref. Hassani et al.

[1994/1995]).The glazing was of size 0.9 m × 1.6 m and it had only a single pane with two different thicknesses: 4 mm and 6 mm. The shading thickness was 18 mm (p. 317 of Hassani et al. [1994/1995]).

The results concerning the occurrence of the first crack in the single glass panes of thickness of 4 mm or 6 mm obtained by the Monte Carlo BREAK1 program are presented in Figure 31 (4 mm thick glass) and Figure 32 (6 mm thick glass). In both cases, there is a clear difference between the observed time and hot gas layer temperature as the first crack occurs: in the 4 mm thick glass, the observed first cracking occurs about 3 minutes later than the calculations suggest (mean calculated value = 283 s) and in the in the 6 mm thick glass, the observed first cracking occurs about 3,3 minutes later than the calculations suggest (mean calculated value = 266 s). The differences in the first crack times are also reflected in the hot gas layer temperatures: for the 4 mm thick glass, the calculated hot gas layer temperature at the first cracking is 90 °C lower than the observed one and 130 °C lower for the 6 mm thick glass.

Hassani et al. (1994/1995) has provided data on glass fallout. It was observed that only in one test out of six tests glass fallout appeared during the 20 minute test period. This one test was the case b with single 6 mm thick glass and the glass fallout took place at about 15 minutes leaving 50 % of the glass in place. From Figure 30 it can be seen that the glass panes endured temperature exposure of about 500 °C with the probability of glass fall out at this temperature level being around 16 % (1 out of six).

In the following we analyse the glass fallout results of Hassani et al. (1994/1995) from the point of view of our glass fallout model. We consider only the single glass pane cases with 4 and 6 mm thick glasses. The basic quantity of our conceptual model (see Chapter 2), i.e., the average glass temperature rise required for the creation of the first crack ΔT_g, for these two cases is shown in Figure 33: the distributions of ΔT_g for the two cases are almost the same: the mean values differ only by 2 °C with the mean value for the 4 mm glass being ΔT_g = 66 °C and 68 °C for the 6 mm glass.

In the experiment with the single 4 mm thick glass, there was no glass fall out. When we apply our model, we see that in the hot gas layer temperature exposure shown as case a in Figure 30, the heating up process of the glass consists of 5 steps of magnitude ΔT_g: the 6th and further steps do not occur in that particular heat exposure. Associating the heat-up steps by the amount of ΔT_g, we conclude that 4 mm glass will not fall out by 5 cracks.

In the experiment with the single 6 mm thick glass, there was glass fall out at ca. 15 minutes[7]. When we apply our model, we see that in the hot gas layer temperature exposure shown as case b in Figure 30, we see that the 15 minutes fallout time corresponds to occurrence of 5 cracks, see Figure 34. Thus, our calculation model tells us that the glass fallout has taken place at the 5th crack.

The glass crack patterns observed by Hassani et al. (1994/1995) (and reproduced here as Figure 35 for the convenience of the reader) show that for the lightweight case analysed above, there appears 4 cracks in the experiment with the single 4 mm thick glass and also 4 cracks in the experiment with the single 6 mm thick glass (Figure 35a). Presumably in latter case, the 5th crack leads to glass fallout. These findings can be considered to be in good agreement with the prediction of our model.

In the double-glazing cases, the glazing systems have sustained 4 or 5 cracks without fallout. In the experiments with the normalised construction (Figure 35b), in 3 cases there are 4 cracks and in 1 case 3 cracks.

[7] The hot gas layer temperature starts to rise a bit before 15 minutes suggesting that the fallout time of 15 minutes quoted in the text is a rounded value and that in exact numbers, the fallout ime might be a bit shorter than 15 minutes.

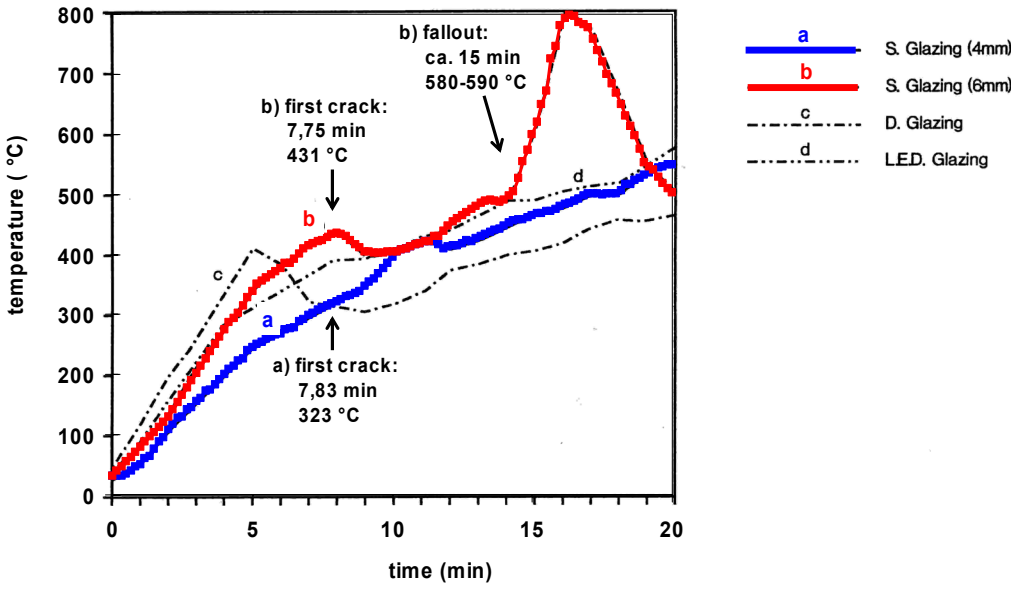

Figure 30. Hot gas layer temperature curves presented in Figure 10 by Hassani et al. (1994/1995). The cases a) and b) with single 4 mm or 6 mm thick glass pane, respectively, which we analyse in more details are emphasised by the thick blue and red curves. The graph contains also the data concerning the occurrence of the first crack given in Table 1 by Hassani et al. (1994/1995) as well the information concerning the glass fall out at about 15 minutes observed in the case b.

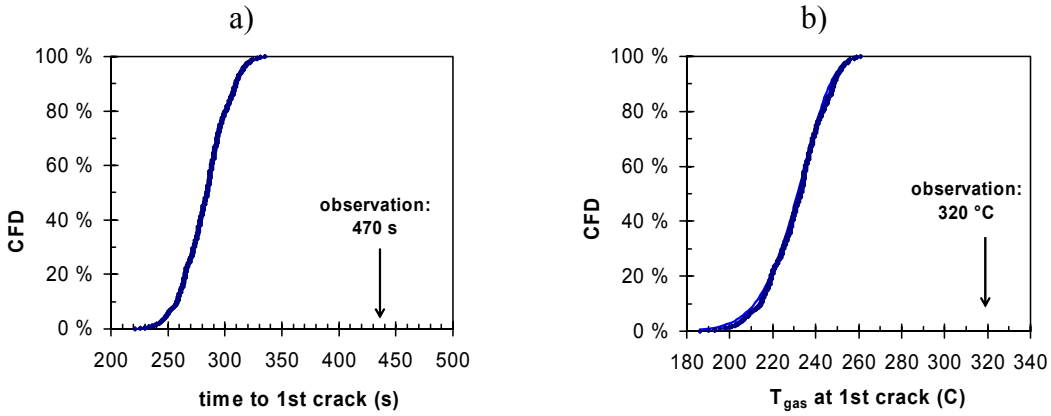

Figure 31. Modelling of the first glass crack in case a of Hassani et al. (1994/1995) with a 4 mm thick glass pane: a) time of the first crack and b) hot gas layer temperature at the first crack.

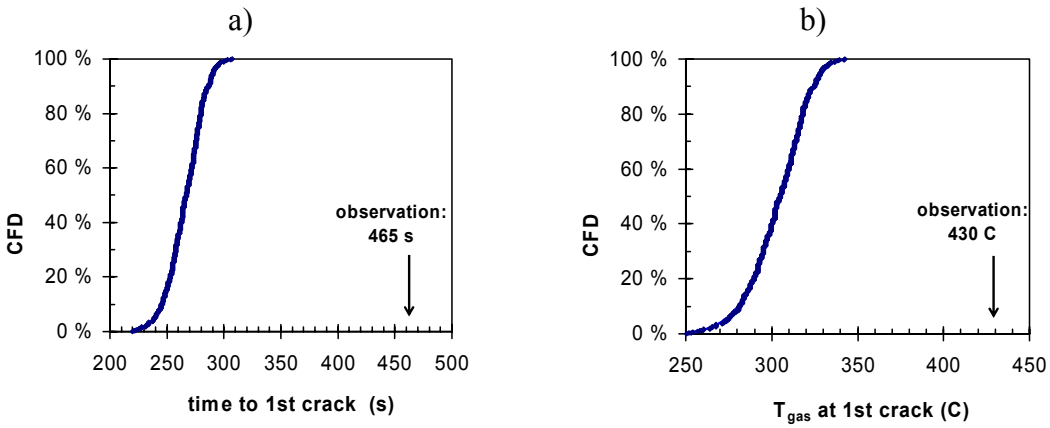

Figure 32. Modelling of the first glass crack in case b of Hassani et al. (1994/1995) with a 6 mm thick glass pane: a) time of the first crack and b) hot gas layer temperature at the first crack.

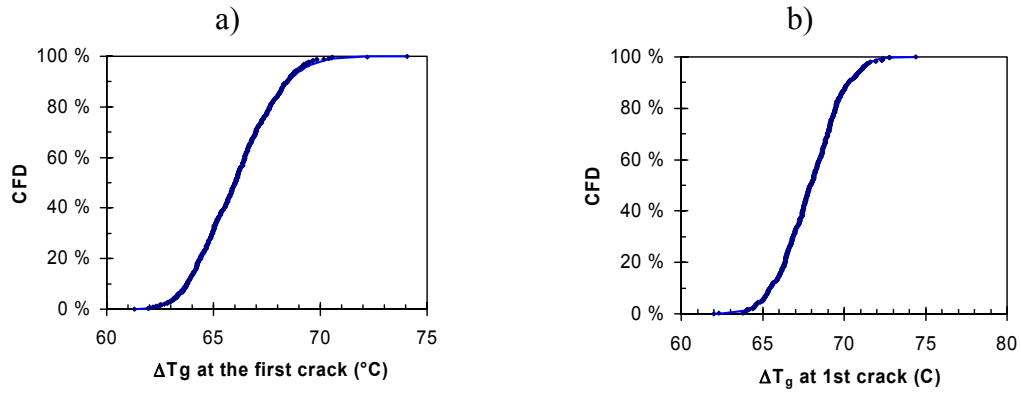

Figure 33. The average glass temperature rise ΔT_g required for the first cracking for the two single-glazed cases studied by Hassani et al. (1994/1995): a) 4 mm thick glass and b) 6 mm thick glass. The ΔT_g distributions are very similar: the mean value of ΔT_g for the 6 mm thick glass is only 2 °C higher than that of the 4 mm glass.

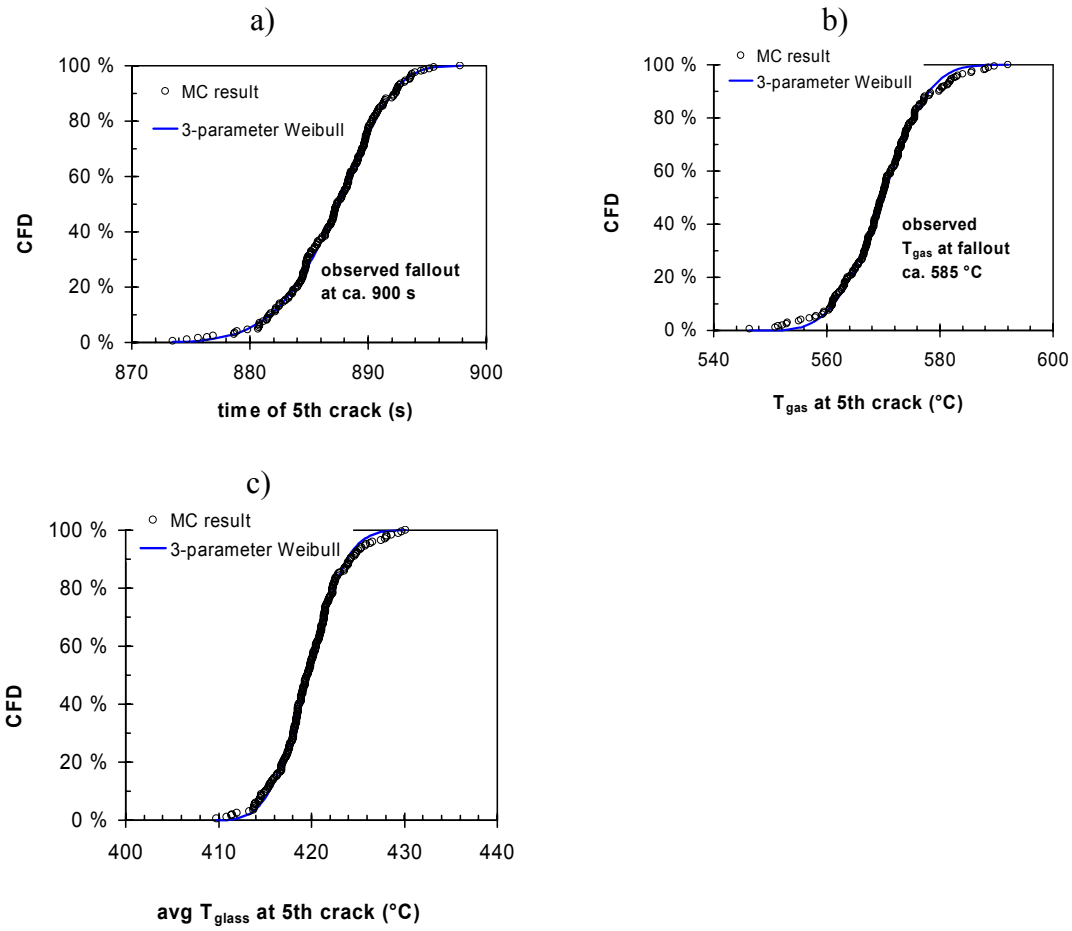

Figure 34. Analysis of the 6 mm thick single-glass experiment of Hassani et al. (1994/1995): a) the fallout time of 15 minutes (or 900 s) coincides with 5 cracks within our model. b) At the 5th crack, the calculated hot gas layer temperature is ~550–590 °C, which agrees with the observed value. c) The average glass temperature at the 5th crack is ~410–430 °C.

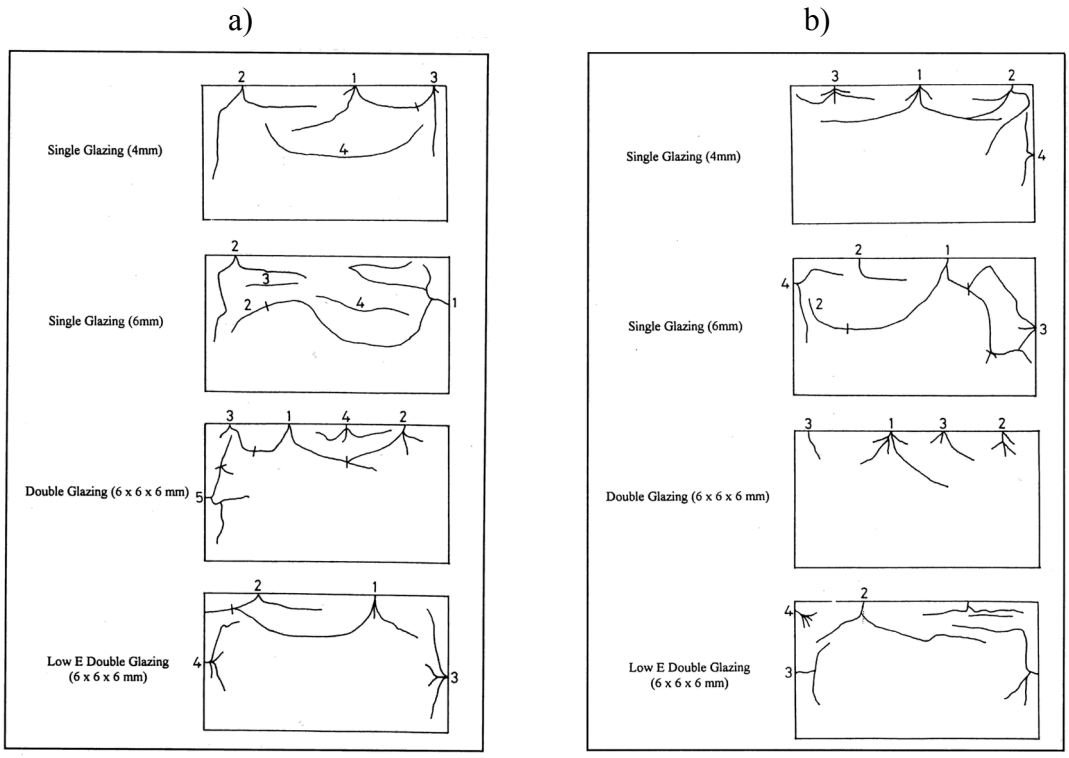

Figure 35. Glass crack patterns observed by Hassani et al. (1994/1995): a) the lightweight room construction and b) the normalised room construction. Glass fallout took place only in the experiment with the single 6 mm glass in the lightweight room construction.

4.3.3 Study concerning fire spread in multi-storey buildings with glazed curtain wall facades carried out for the Loss Prevention Council (Anon. 1999)

The principal objective of the study carried out for the Loss Prevention Council (LPC) (Anon. 1999) was to study fire spread in a glazed curtain wall facade typical to, e.g., to many office buildings. The results provide also excellent information on the glass breakage and fallout in a fire.

The experiments we consider here were carried out using two kinds of fire loads, the other consisting of wooden cribs and in the other case the fire load consisted of a materials and items of a fully-furnished office. Below we analyse these two cases separately with respect to the glass fallout. As it is part of our procedure we also calculate the occurrence of the first crack although there is no experiment observations concerning this event, but the observations relate to a catastrophic glass failure associated with glass fallout.

4.3.3.1 Experiment with fire load consisting of wooden cribs

The temperature curves of LPC report for the wood crib file load are reproduced in Figure 36. We use the highest temperature curve as input to our analysis. The results concerning the occurrence of the first crack are shown in Figure 37 and the average glass temperature rise required for the first crack ΔT_g is shown in Figure 38. Starting from these results, we apply our approach and it is noted that the observed time of glass fallout, 13 minutes, corresponds to the 8th crack formation in the glass, Figure 39a. The calculated hot gas layer temperature at the occurrence of the 8th crack is ~820–880 °C which agrees with the experimental result of about 740–870 °C which can be read from Figure 36. The calculated average glass temperature at the 8th crack is ~620–650 °C (Figure 39c).

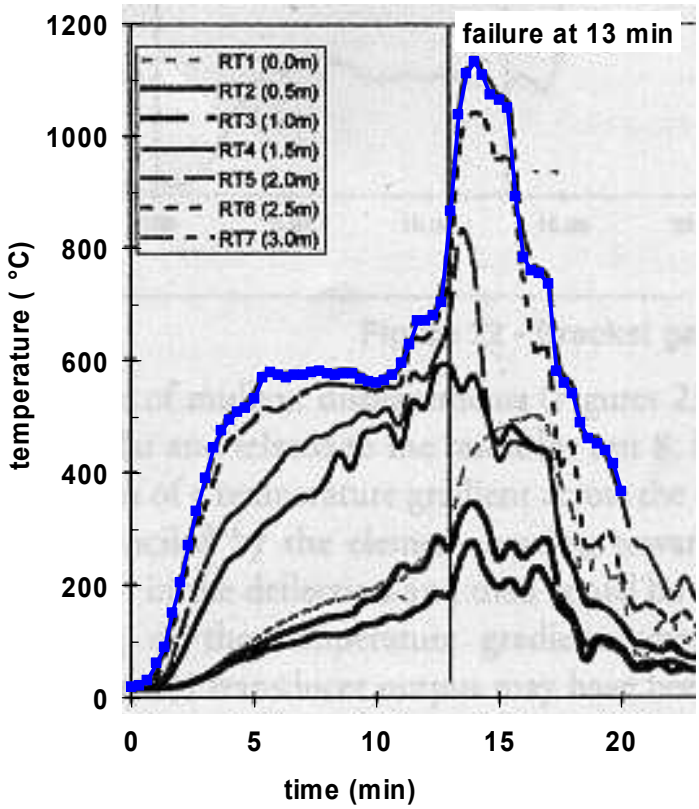

Figure 36. Temperature data of the experiments carried for the LPC (Anon. 1999): fire load consisting of wooden cribs. The thick blue curve emphasised by markers is used as input temperature data in our analysis.

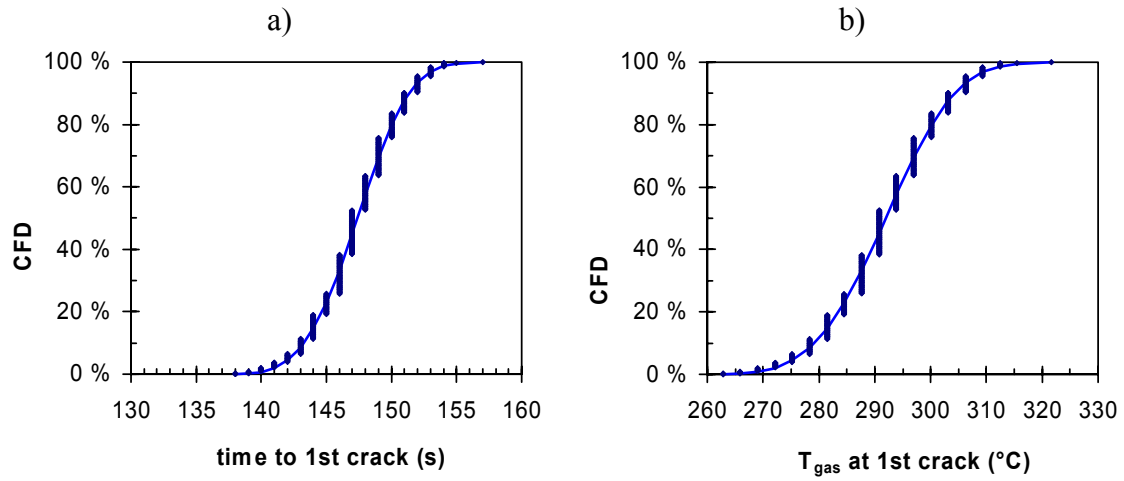

Figure 37. Modelling of the first glass crack in the LPC fire experiments with fire load consisting of wooden cribs: a) time of the first crack and b) hot gas layer temperature at the first crack.

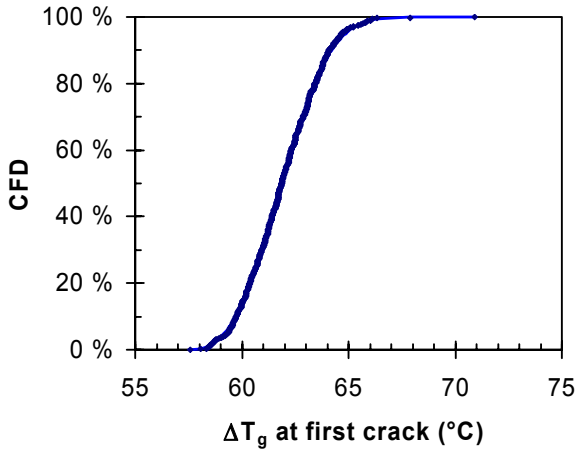

Figure 38. The average glass temperature rise ΔT_g required for the first glass cracking in the LPC fire experiments with fire load consisting of wooden cribs.

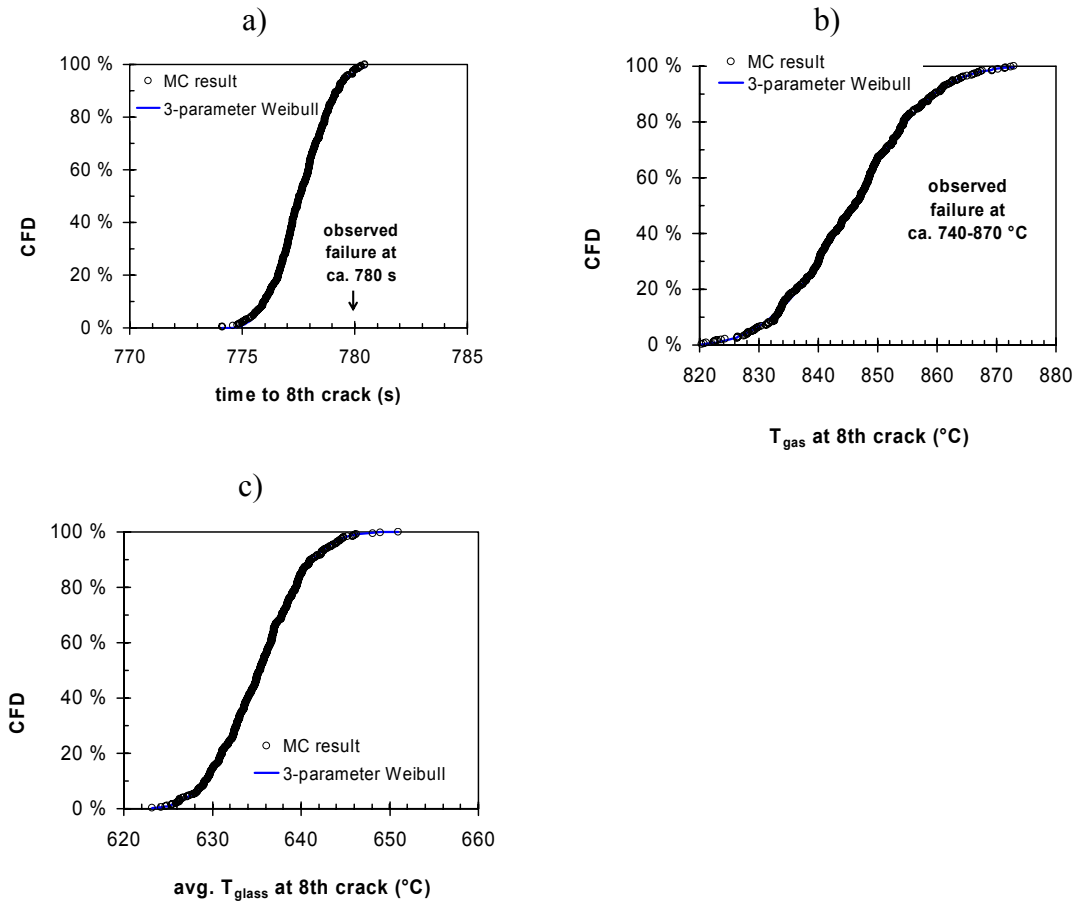

Figure 39. Analysis of the LPC fire experiments with fire load consisting of wooden cribs: a) the fallout time of 13 minutes (or 780 s) coincides with 8 cracks within our model. b) At the 8th crack, the calculated hot gas layer temperature is ~820–880 °C, which agrees with the observed value. c) The average glass temperature at the 8th crack is ~620–650 °C.

4.3.3.2 Experiment with fire load consisting of a fully-furnished office configuration

The temperature curves of LPC report for the file load consisting of materials and items of a fully-furnished office are reproduced in Figure 40. The highest temperature curve is used as input to our analysis. The results concerning the occurrence of the first crack are shown in Figure 41 and the average glass temperature rise required for the first crack ΔT_g is shown in Figure 42. The observed time of glass fallout, only 5 minutes, corresponds to formation the 7th crack within our formalism Figure 43a. The calculated hot gas layer temperature at the occurrence of the 7th crack is ~730–760 °C which agrees with the experimental result of about 700–800 °C which can be read from Figure 40. The calculated average glass temperature at the 7th crack is ~545–570 °C (Figure 43c).

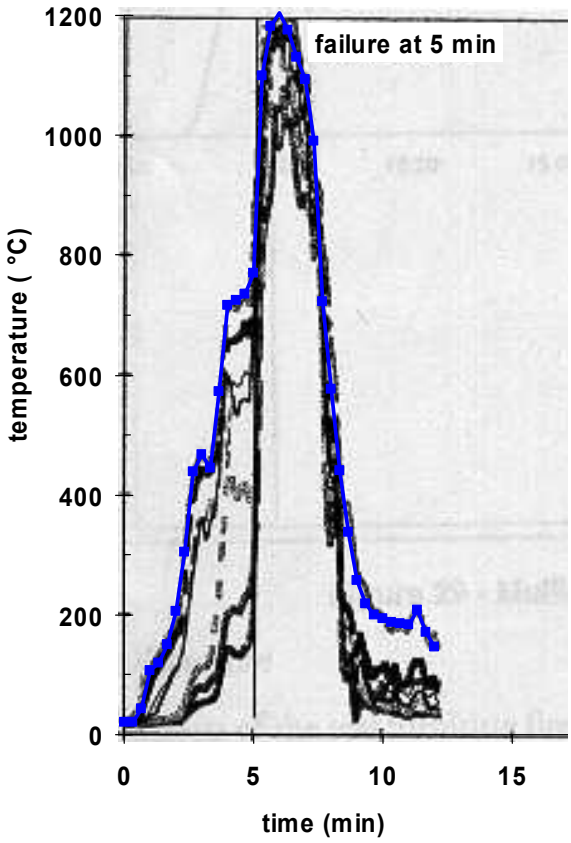

Figure 40. Temperature data of the experiments carried for the Loss Prevention Council (Anon. 1999): fire load consisting of a materials and items in a fully-furnished office. The thick blue curve emphasised by markers is used as input temperature data in our analysis.

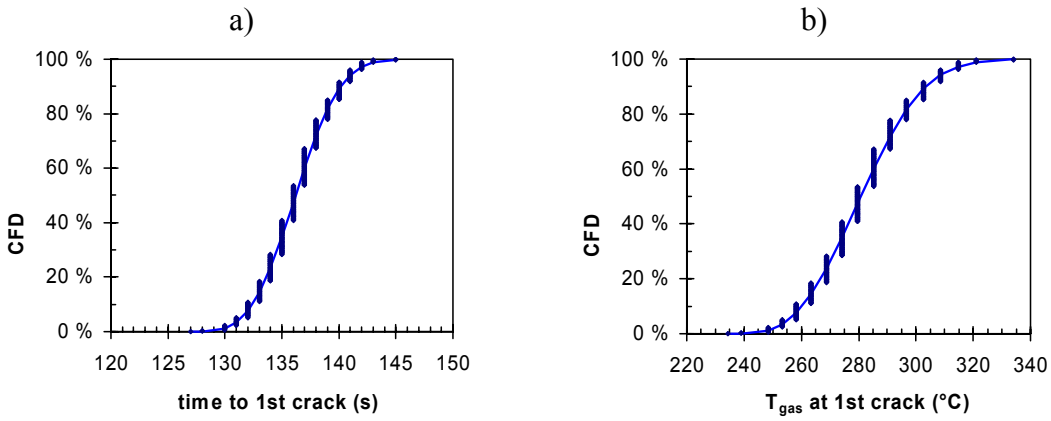

Figure 41. Modelling of the first glass crack in the LPC fire experiments with fire load consisting of a materials and items in a fully-furnished office: a) time of the first crack and b) hot gas layer temperature at the first crack.

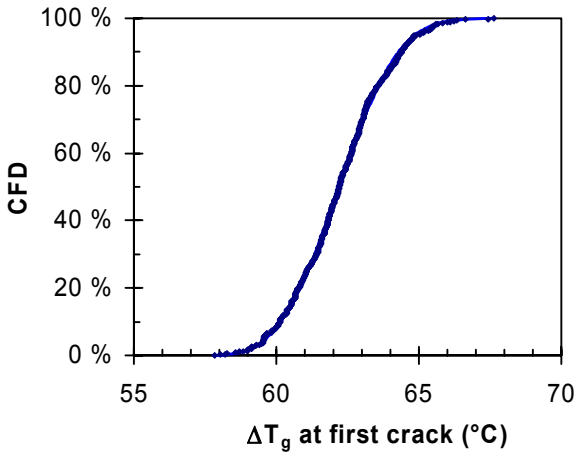

Figure 42. The average glass temperature rise ΔT_g required for the first glass cracking in the LPC fire experiments with fire load consisting of a materials and products in a fully-furnished office.

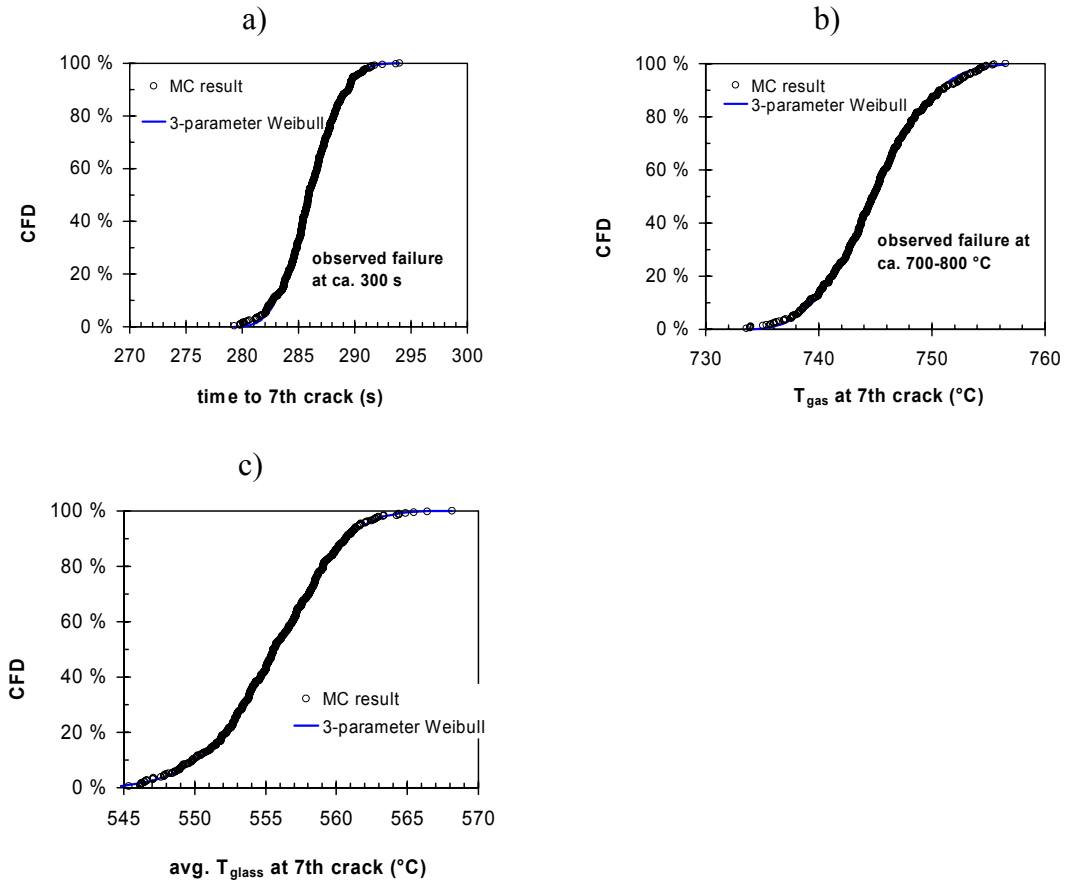

Figure 43. Analysis of the LPC fire experiments with fire load consisting of a materials and items in a fully-furnished office: a) the fallout time of 5 minutes (or 300 s) coincides with 7 cracks within our model. b) At the 7th crack, the calculated hot gas layer temperature is ~735–760 °C, which agrees with the observed value. c) The average glass temperature at the 7th crack is ~545–570 °C.

4.3.4 Study on the performance of single glazing elements exposed to enclosure fires of increasing severity (Shields et al. 2001 & 2002)

Shields, Silcock and Flood (2001 & 2002) have carried out comprehensive research work on glass performance in fire using an enclosure with floor area of 3,6 m × 2,4 m and height of 2,4 m, constructed and instrumented to ISO room standards. The window system was placed on the long wall of the enclosure as shown in Figure 44a. It has of three panes as shown in Figure 44b with two panes of size 85 cm × 85 cm on top of each other (the upper one is labelled pane 1 and the lower one pane 2) and one pane of size 85 cm × 191 cm (labelled pane 3). The window panes were of single 6 mm thick float glass. The shading thickness was 20 mm.

Experiment series were carried out with two fire locations, one series with the fire located in the corner of the enclosure opposite to the glazing system (Shields et al. 2001) and the other with the fire located in the centre of the room (Shields et al. 2002). The fuel was mineralized methylated spirits and several different fuel pan sizes varying from 500 mm × 500 mm to 900 mm × 900 mm corresponding to different fire severities were used.

Below we analyse the experiments carried out using the 900 mm × 900 mm pan size for the two fire positions, corner and centre, separately.

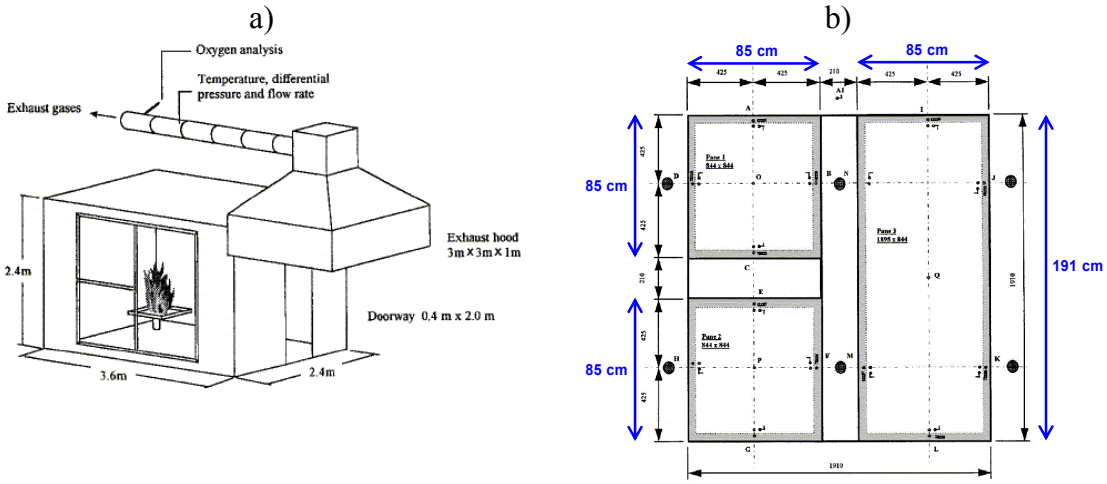

Figure 44. The experimental set up of Shields et al. (2001 & 2002): a) the fire room constructed and instrumented according to the ISO room standard (this particular figure shows the configuration with the fire in the corner of the enclosure [Shields et al. 2001]) and b) the window system with two panes of size 85 cm × 85 cm on top of each other (upper = pane 1 and lower = pane 2) and one pane of size 85 cm × 191 cm (pane 3).

4.3.4.1 Single glazing elements exposed to enclosure corner fire (Shields et al. 2001)

With the 900 mm × 900 mm pan size, the heat release rate of the fire in the corner increased above 0,5 MW. The corresponding hot gas layer temperatures at different measuring positions are shown in Figure 45. We base our analysis of the glass breakage to the highest temperature curve (denoted by Shields et al. [2001] by A1). In the calculation of the occurrence of the first crack we take into account besides the hot gas layer heat exposure also the heat radiation from the flames.

The results of the calculation of the occurrence of the first crack in pane 1 are presented in Figure 46 and Figure 47. It is seen that the time of the first crack is predicted well and also the calculated temperature of the hot gas layer at the first crack compares reasonably favourably with the observed value. The calculations give a range of ca. 57–70 °C for the glass temperature rise ΔT_g required for the first crack to occur.

The results of the calculations concerning the major glass fallout of the pane 1, which in the experiments takes place at ca. 250 s, are presented in Figure 48. The closest agreement between the observed results and the results of our model is obtained by selecting 5 calculated crackings to describe the glass fallout. The agreement is fair but not very good, though: the calculated time of fallout is about half a minute shorter than the observed one and the calculated hot gas temperature is about 100 °C lower than the experimental value. The calculated average glass temperature at fallout is ~380–410 °C.

As there is not major fallout in the pane 3, we model only the occurrence of the first crack. The results are shown in Figure 49 and Figure 50. With respect to the time of the first crack, the calculated and observed ranges agree fairly well and this is the case also with respect to the hot gas layer temperatures. The calculations give a range of ca. 58–68 °C for the glass temperature rise ΔT_g required for the first crack to occur.

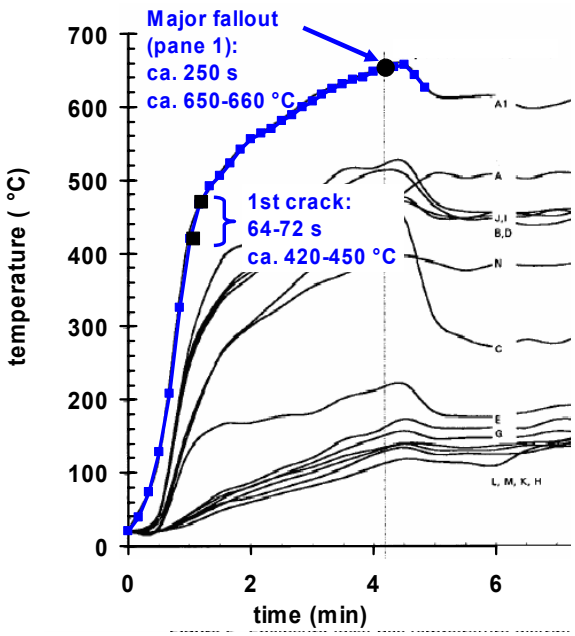

Figure 45. Temperature data of the experiments of Shields et al. (2001) carried using the corner-fire configuration with pan size of 900 mm × 900 mm (only the first 7 minutes are shown). The thick blue curve with markers is used as input temperature data in our analysis. Also the occurrence of the first crack read from Table 1 of Shields et al. (2001) as well as the occurrence of major glass fallout are depicted.

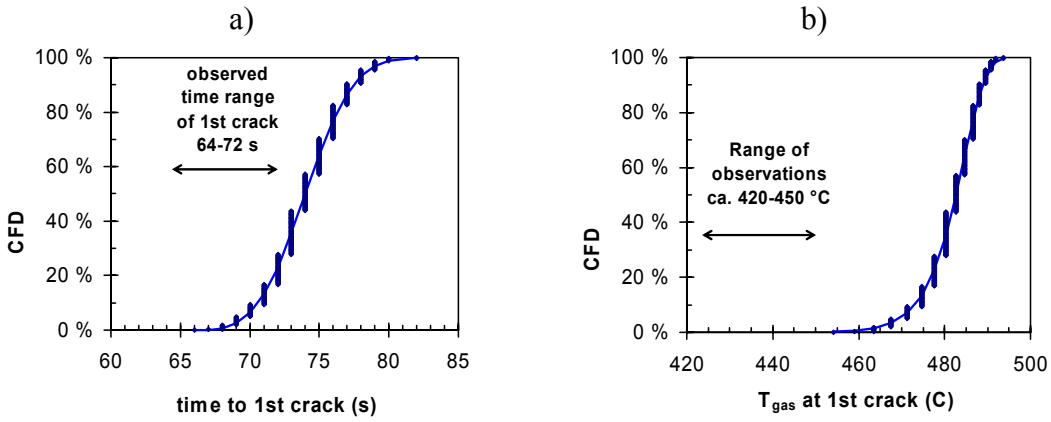

Figure 46. Modelling of the first glass crack in the experiments of Shields et al. (2001) carried using the corner-fire configuration with pan size of 900 mm × 900 mm, pane 1: a) time of the first crack and b) hot gas layer temperature at the first crack. The calculated time of the 1st crack ranging between ca. 65 s and 80 s agrees well with the observed range of 64–72 s. Also the agreement with hot gas layer temperature ranges (calculated 450–490 °C and observed 420–460 °C s) is reasonably good.

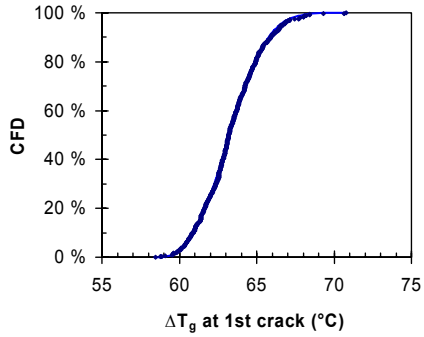

Figure 47. The average glass temperature rise ΔT_g required for the first glass cracking in the experiments of Shields et al. (2001) carried using the corner-fire configuration with pan size of 900 mm × 900 mm, pane 1.

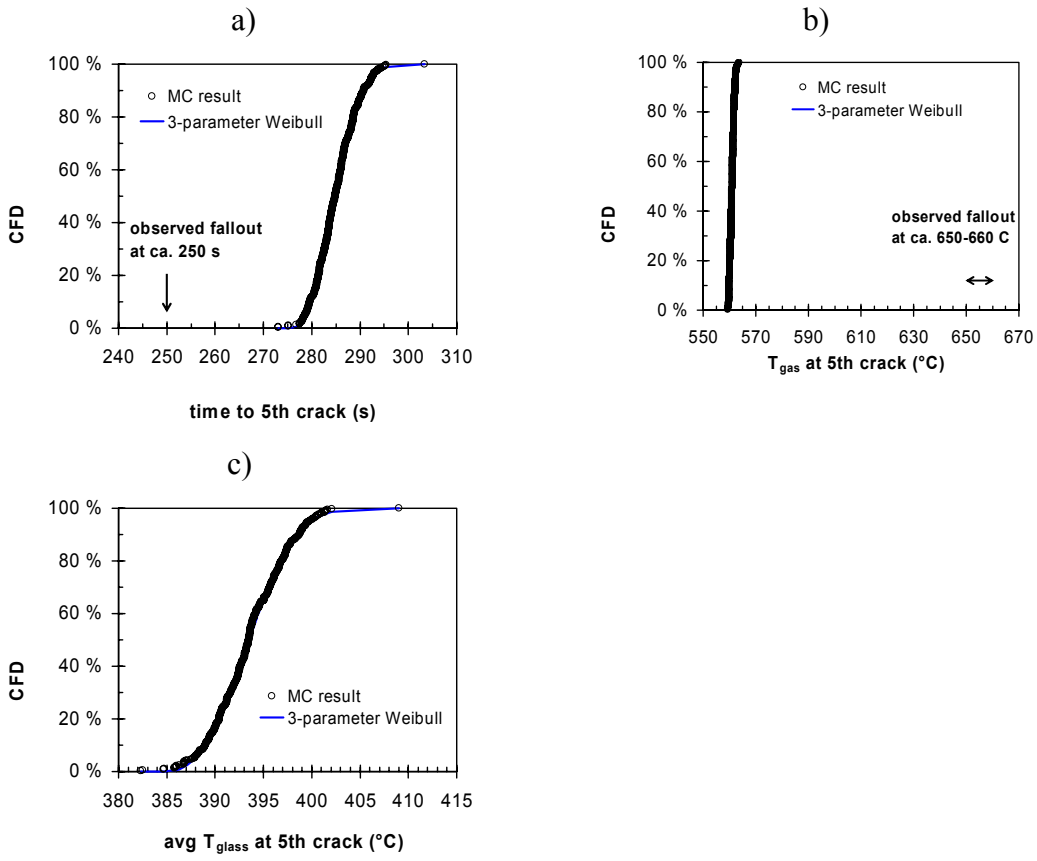

Figure 48. Analysis of the experiments of Shields et al. (2001) carried using the corner-fire configuration with pan size of 900 mm × 900 mm, pane 1: a) the fallout time of 250 s is closest to the time when 5 cracks occur within our model. b) At the 5th crack, the calculated hot gas layer temperature is ~710–730 °C, which is somewhat higher than the observed range of 650–660 °C. c) The average glass temperature at the 5th crack is ~380–410 °C.

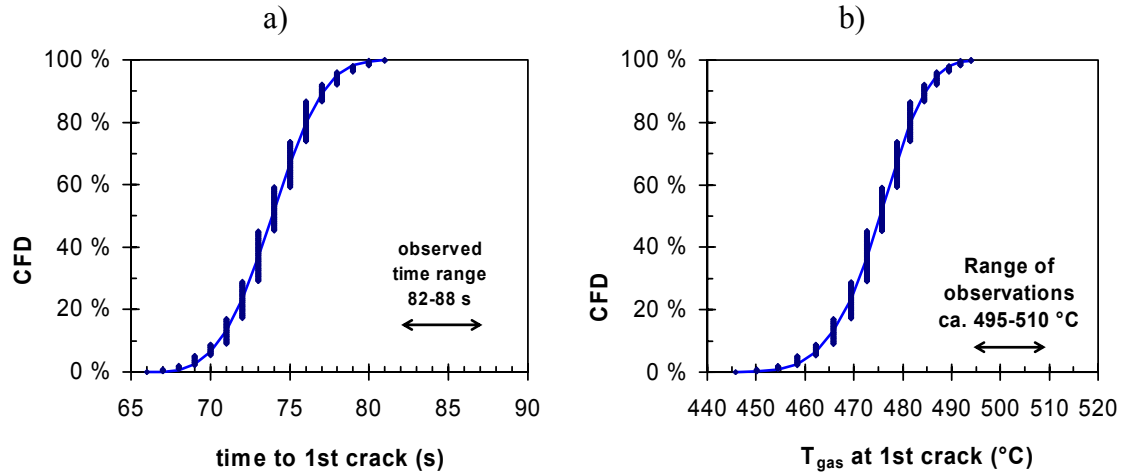

Figure 49. Modelling of the first glass crack in the experiments of Shields et al. (2001) carried using the corner-fire configuration with pan size of 900 mm × 900 mm, pane 3: a) time of the first crack and b) hot gas layer temperature at the first crack. The calculated time of the 1st crack ranges between ca. 65 s and 80 s which is a bit lower than the observed range of 82–88 s. Similar a small discrepancy is observed also in the comparison to the calculated and measured hot gas layer temperature ranges (calculated 440–490 °C and observed 495–510 °C s).

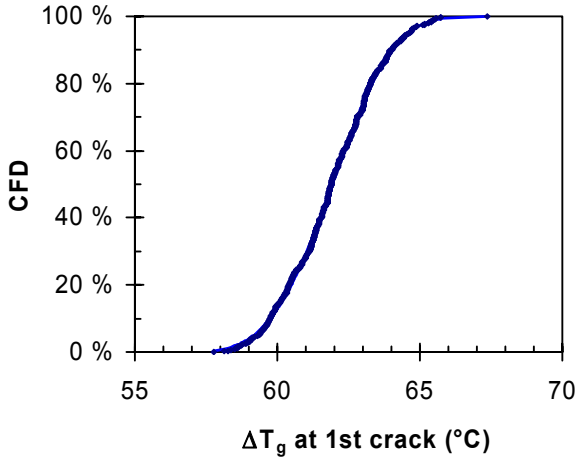

Figure 50. The average glass temperature rise ΔT_g required for the first glass cracking in the experiments of Shields et al. (2001) carried using the corner-fire configuration with pan size of 900 mm × 900 mm, pane 3.

4.3.4.2 Single glazing assembly exposed to a fire in the centre of an enclosure (Shields et al. 2002)

With the 900 mm × 900 mm pan size, the heat release rate of the fire in the centre of the enclosure reaches a peak of about 0,7 MW. The corresponding hot gas layer temperatures at different measuring positions are shown in Figure 51. We base our analysis of the glass breakage to the highest temperature curve (denoted by Shields et al. [2002] by A1). In the calculation of the occurrence of the first crack we take into account besides the hot gas layer heat exposure also the heat radiation from the flames.

The results of the calculation of the occurrence of the first crack in pane 3 are presented in Figure 52 and Figure 53. It is seen that both the calculated time of the first crack and the calculated temperature of the hot gas layer at the first crack are below the observed values. Yet, the agreement between the calculated and the measured values may be considered as fair rather than poor. The calculations give a range of ca. 58–70 °C for the glass temperature rise ΔT_g required for the first crack to occur.

The results of the calculations concerning the major glass fallout of the pane 3, which in the experiments takes place at ca. 440 s, are presented in Figure 54. As the glass fallout takes place during the cooling phase of the fire and our model tacitly assumes that the fallout, if it is going to happen, will occur when the hot gas temperature rises, our model can not reproduce this fallout case. Nevertheless, we have applied our model and looked at the hot gas temperature (Figure 54b, range 650–680 °C) to deem the number of cracks required to cause the fallout. A close agreement between the observed results and the results of our model is obtained by 5 calculated crackings. The calculated time to the glass fallout is less than half of the observed value to above described reason. The calculated average glass temperature at fallout is ~385–410 °C.

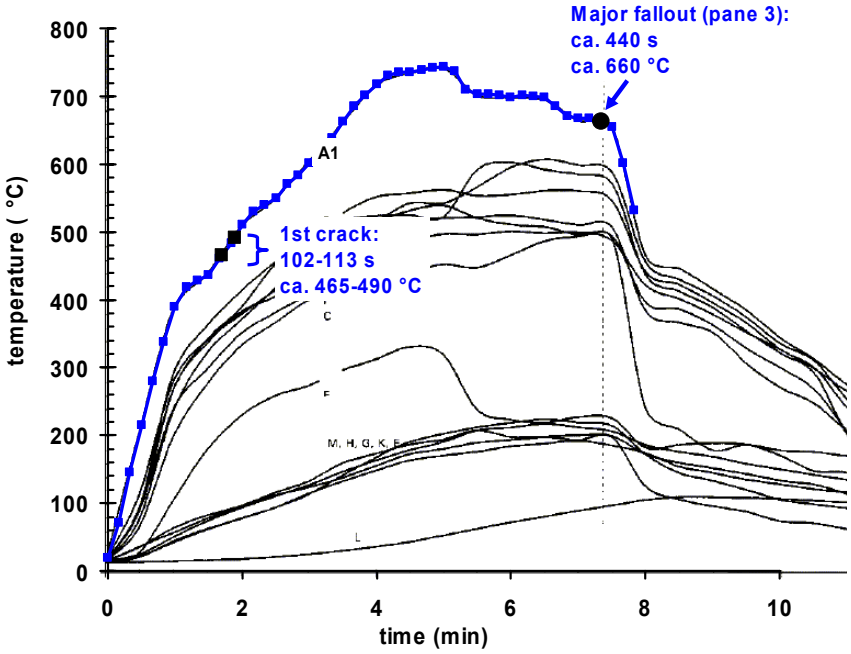

Figure 51. Temperature data of the experiments of Shields et al. (2002) carried out using the enclosure centre fire configuration with pan size of 900 mm × 900 mm (only the first ca. 11 minutes are shown). The thick blue curve with markers is used as input temperature data in our analysis. Also the occurrence of the first crack read from Table 1 of Shields et al. (2002) as well as the occurrence of major glass fallout are depicted.

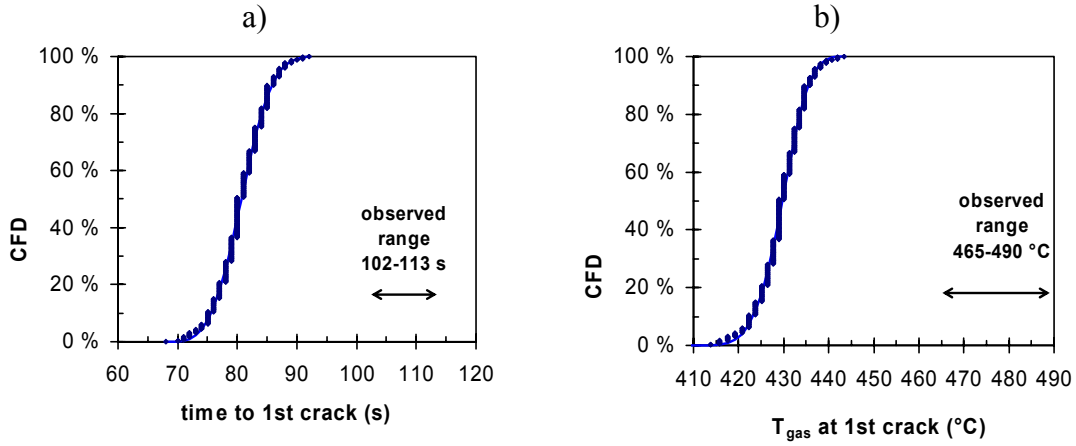

Figure 52. Modelling of the first glass crack in the experiments of Shields et al. (2002) carried using the enclosure centre fire configuration with pan size of 900 mm × 900 mm, pane 3: a) time of the first crack and b) hot gas layer temperature at the first crack. The calculated time of the 1st crack ranging between ca. 70 s and 90 s is a bit shorter than the observed range of 102–113 s. Also the calculated hot gas layer temperature range, 410–445 °C, lies below the observed range of 465–490 °C.

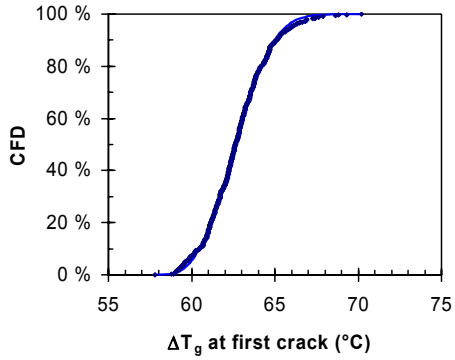

Figure 53. The average glass temperature rise ΔT_g required for the first glass cracking in the experiments of Shields et al. (2002) carried using the enclosure centre fire configuration with pan size of 900 mm × 900 mm, pane 3.

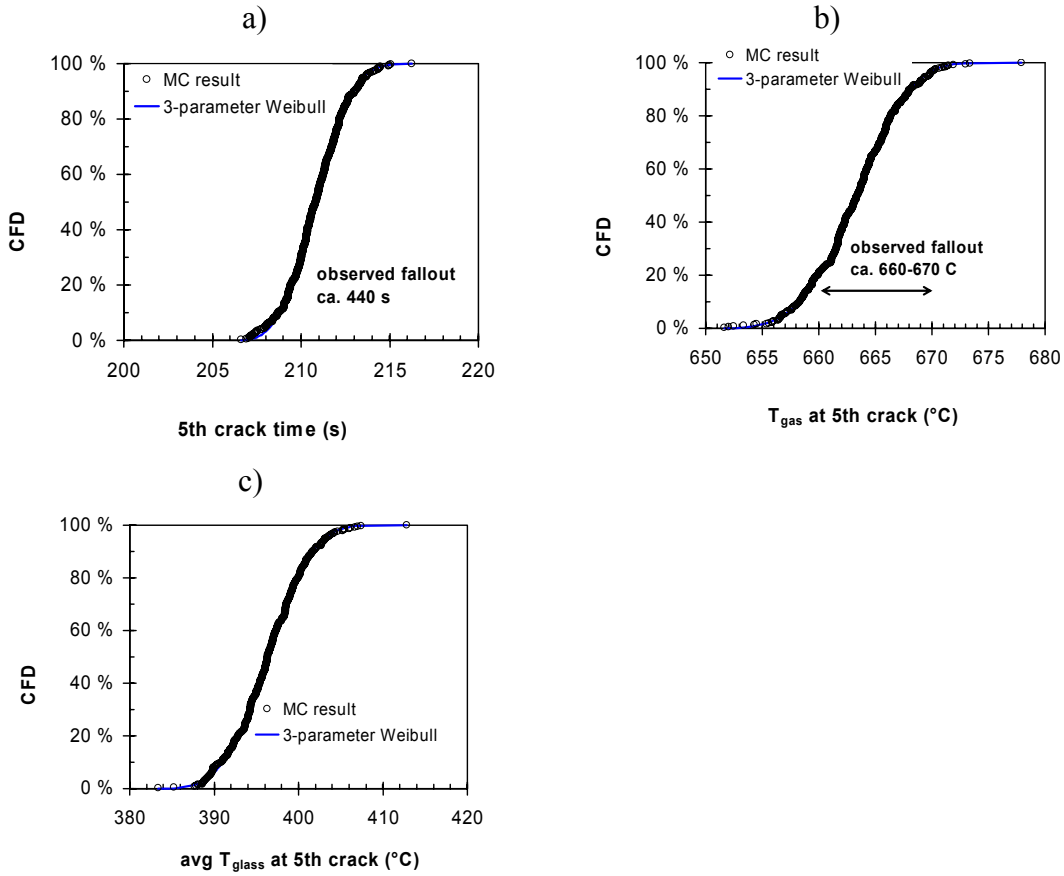

Figure 54. Analysis of the experiments of Shields et al. (2002) carried using the enclosure centre fire configuration with pan size of 900 mm × 900 mm, pane 3: a) the fallout time of 250 s is closest to the time when 5 cracks occur within our model. b) At the 5th crack, the calculated hot gas layer temperature is ~650–680 °C (adjusted to fit the data). c) The average glass temperature at the 5th crack is ~380–410 °C.

4.3.5 Glass-breaking study using a fire-resistance furnace (Hietaniemi et al. 2002)

VTT carried out an experimental study of glass-breaking in fire in a research project aimed at improving fire safety of building void spaces; the particular hazard address being the danger of fire spread within the cavity space formed by the inner and outer glass pane of a double-glass facade (Hietaniemi et al. 2002). The glass system studied was an aluminium-framed float glass of size of 800 mm × 1000 mm and thickness of 6 mm (Figure 55a). The shading thickness was 10 mm. The experiment was carried in the model fire-resistance furnace of VTT using the standard temperature-time curve. Figure 56 shows the time-temperature curve of the experiment as well as the timings of the initial glass crackings and the occurrence of glass fallout: initial cracks appeared after 105–130 s of temperature exposure (furnace temperature at first cracks was ca. 350–420 °C) and the first minor glass fallout took place after 590 s of temperature exposure (furnace temperature ca. 670 °C) and major fallout occurred after 800 s of temperature exposure (furnace temperature ca. 720 °C).

The results of the analysis concerning the initial crackings in the VTT glass-breaking experiment are shown in Figure 57 and Figure 58. The calculated time of the 1st crack ranges between ca. 75 s and 105 s which is in fair agreement with the observed time range of 105–130 s. The calculated gas temperature at the first crack ranges between 380 °C and 445 °C which is in a rather good agreement with the measured values, i.e., the range of 350–420 °C. The calculations give a range of ca. 60–70 °C for the glass temperature rise ΔT_g required for the first crack to occur.

The results of the calculations concerning the minor glass fallout at 590 s are presented in Figure 59. Within our model, this fallout corresponds to occurrence of the 7th crack. With respect to the time of the minor glass fallout, the calculated and the observed result agree well. Also the agreement between the ranges of the calculated and measured gas temperatures can be considered to be in a reasonably good agreement. The calculated average glass temperature at the minor fallout is ~520–540 °C.

The results of the calculations concerning the major glass fallout at 800 s are presented in Figure 60. This fallout corresponds to occurrence of the 8th crack in our model. The calculated and the observed time of the major fallout agree well. The agreement between the ranges of the calculated and measured gas temperatures is less satisfactory but can be considered reasonably good. The calculated average glass temperature at the minor fallout is ~595–625 °C.

a)

b)

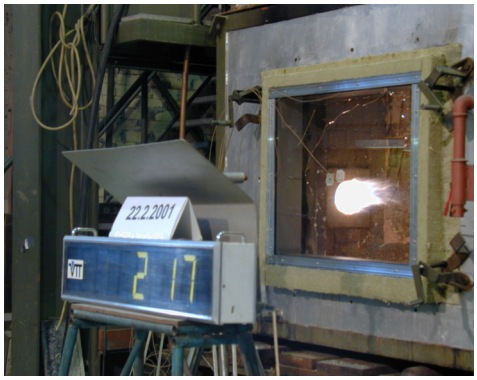

c)

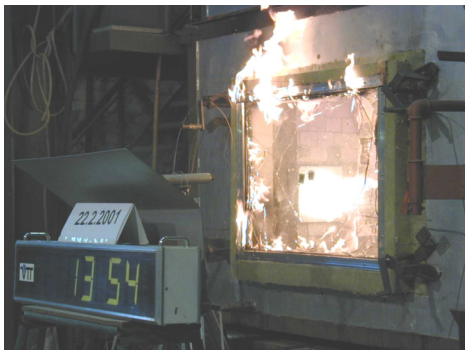

Figure 55. Glass-breaking study in the VTT model fire-resistance furnace: a) the glass system, b) picture taken just after the occurrence of the first crack at 2 min 14 s from time zero and c) major glass fallout at close to 14 minutes from time zero. The time zero and the time when the temperature started to rise differ by ca. half a minute.

a)

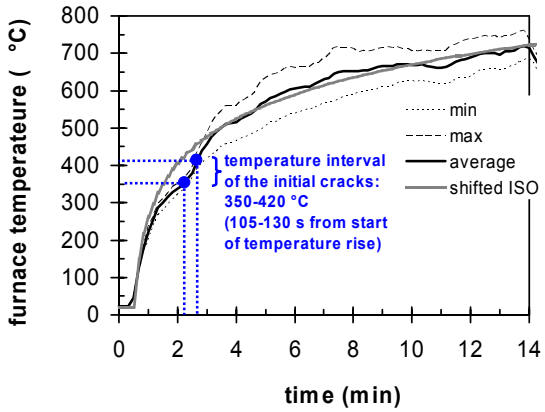

b)

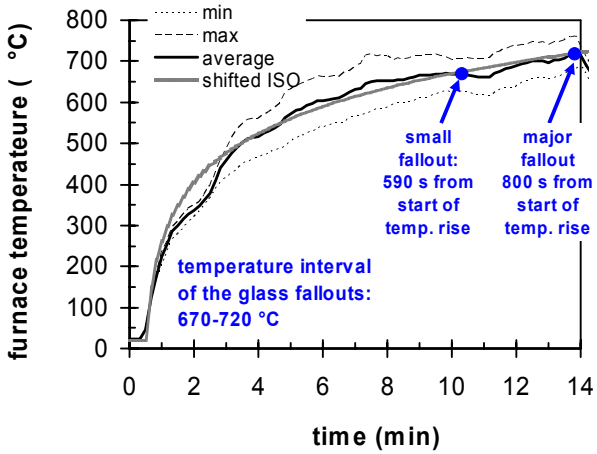

Figure 56. The temperature exposure in the VTT glass-breaking experiment: a) timing of the first crack and b) timing of the glass fallouts. The times shown in the legends are counted from the time when the furnace temperature started to rise.

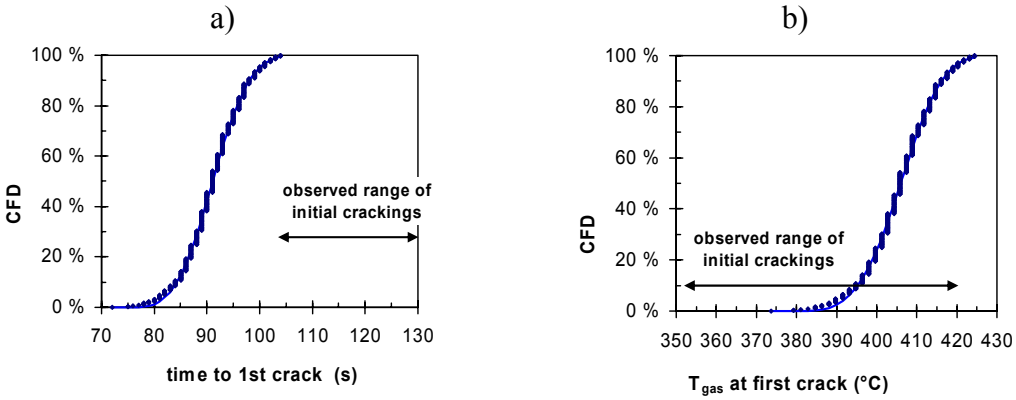

Figure 57. Modelling of the first glass crack in the VTT glass-breaking experiment: a) time and b) gas temperature at the first crack. Both the calculated time (~75–105 s) and the calculated gas temperature (~380 °C–445 °C) agree reasonably well with the measured ranges of values, i.e., 105–130 s and 350–420 °C, respectively.

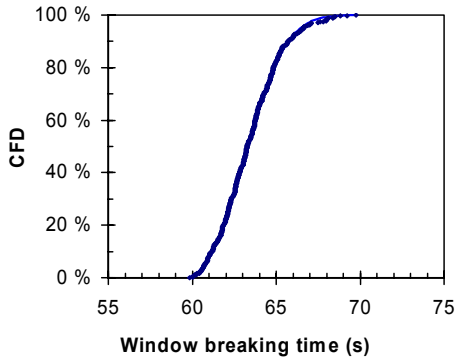

Figure 58. The average glass temperature rise ΔT_g required for the first glass cracking in the VTT glass-breaking experiment.

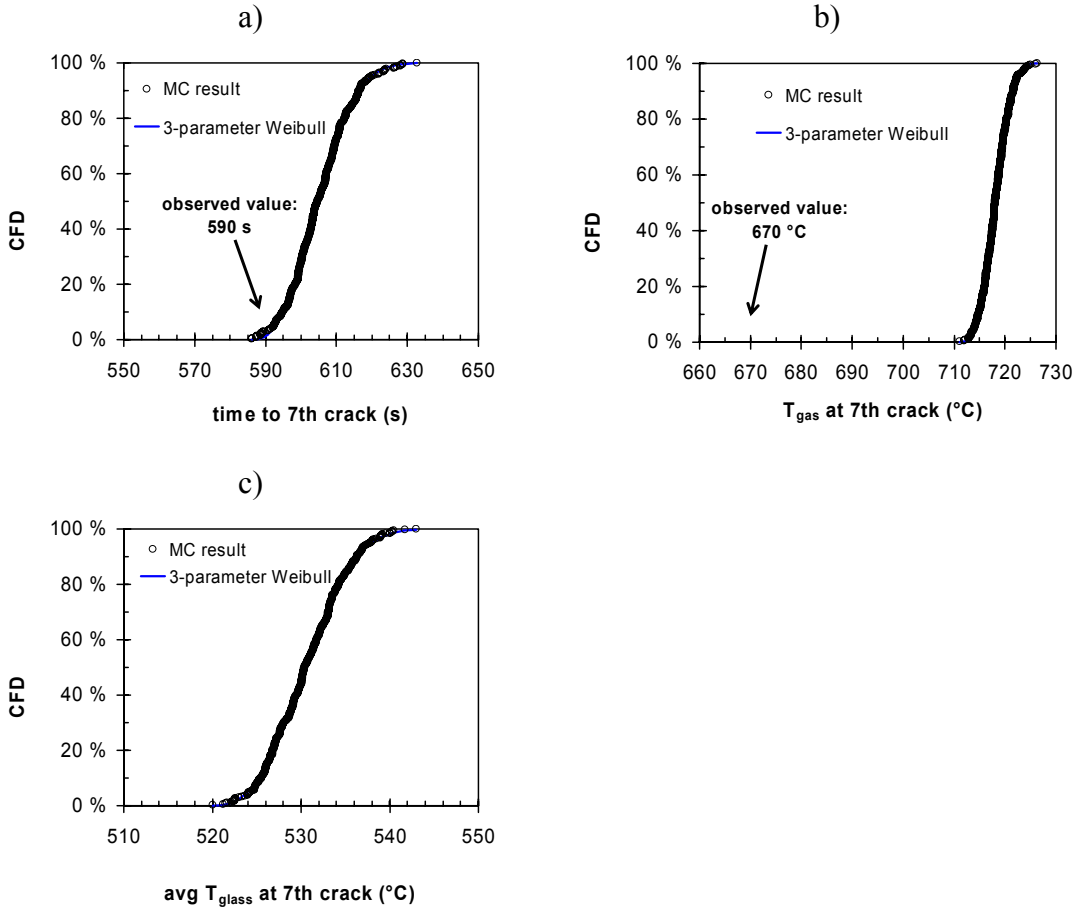

Figure 59. Analysis of the minor glass fallout at 590 s in the VTT glass-breaking experiment: a) the observed fallout time of 590 s is closest to the time when 7 cracks occur within our model. b) At the 7th crack, the calculated gas temperature is ~710–730 °C, which is somewhat higher than the observed value of 670 °C. c) The average glass temperature at the 7th crack is ~520–540 °C.

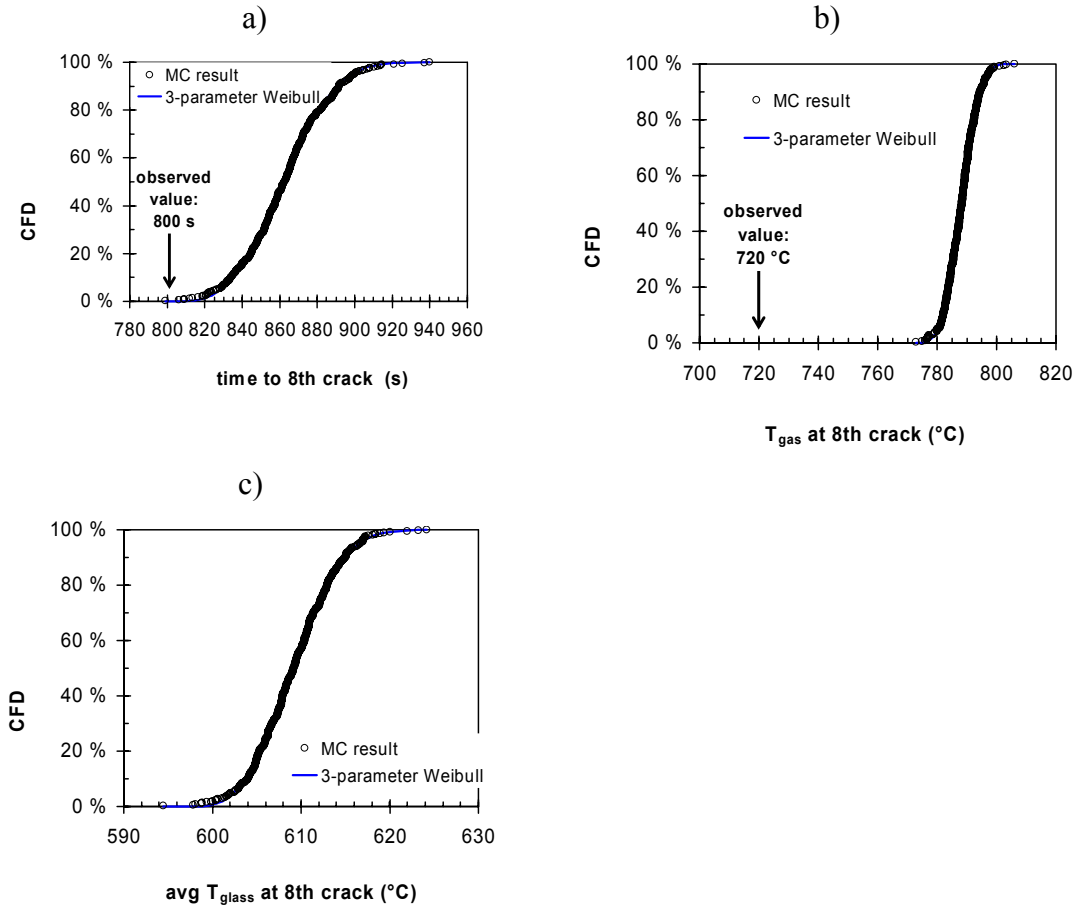

Figure 60. Analysis of the major glass fallout at 800 s in the VTT glass-breaking experiment: a) the observed fallout time of 800 s is closest to the time when 8 cracks occur within our model. b) At the 8th crack, the calculated gas temperature is ~770–810 °C, which is a bit higher than the observed value of 720 °C. c) The average glass temperature at the 7th crack is ~595–625 °C.

4.3.6 Fire experiments in furnished houses by MeHaffey et al. (2004)

MeHaffey et al. (2004) performed six experiments to assess the performance of wood-frame assemblies exposed to fires in furnished houses. Here we consider their tests 1 and 2 for which the performance of the window panes is reported. A schematic presentation of the fire room in these tests is shown in Figure 61. The room size and openings in the two tests were similar with difference between the two tests being the gypsum board on the ceiling and the walls (with ordinary gypsum board in the 1st test and fire-rated gypsum board in the 2nd test) The window consisted of the central pane (1,47 m wide and 1,42 m high) which was closed in the beginning of the tests and eventually fell out due to the fire exposure as well as two side panes (each 0,55 m wide and 1,42 m high) which were open from the beginning of the tests to provide ventilation

to the developing fire. The temperature data of these tests as well as the temperature input to our analyses are shown in Figure 62.

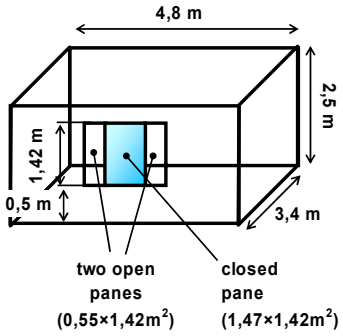

Figure 61. Schematic presentation of the experimental set-up in tests 1 ands 2 of MeHaffey et al. (2004).

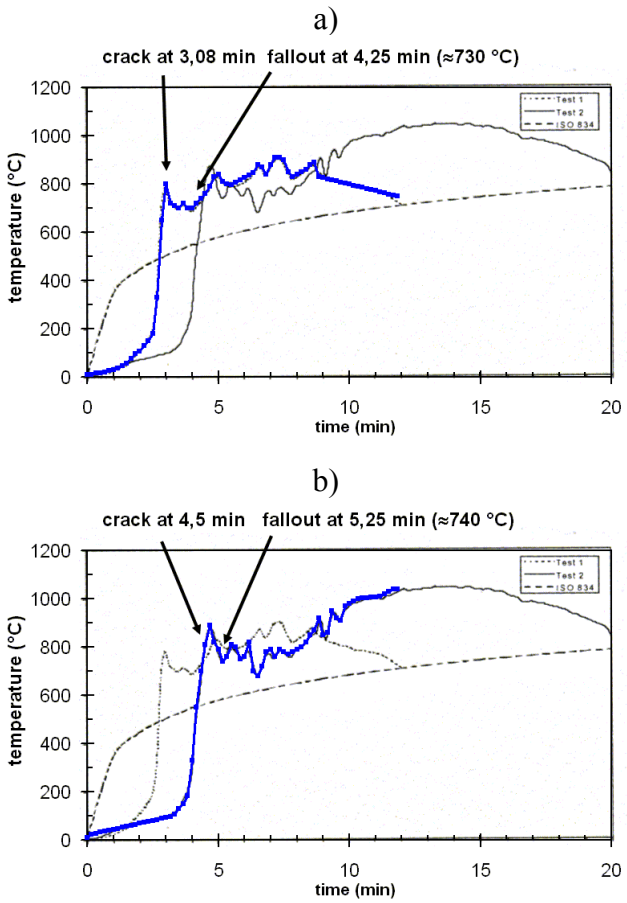

Figure 62. Temperature data of the tests 1 and 2 of MeHaffey et al. (2004) with the thick blue curves with markers is used as input temperature data in our analysis. Also the occurrence of the first crack read from Table 3 of MeHaffey et al. (2004) as well as the occurrence of major glass fallout are depicted.

4.3.6.1 Analysis of test 1 of MeHaffey et al. (2004)

In the analysis of the occurrence of the 1st crack in the test 1 we adjusted the glass thickness (6 mm) and the shading thickness (10 mm) which were not given in the reporting of the test so that the mean value of the calculated time (*ca*. 175 s) of the occurrence of the first crack was reasonably close to the observed time (185 s), see Figure 63a. The corresponding temperature of the hot gas layer is shown in Figure 63b and the average glass temperature in Figure 64.

The observed time of the glass fallout of 255 s corresponds closest to the occurrence of the 6th crack in our model (Figure 65). The calculated gas temperature at glass fallout ranges between 700 °C and 720 °C in quite good agreement with observed temperature of ca. 730 °C. The model predicts that the average glass temperature at the fallout is 460–490 °C.

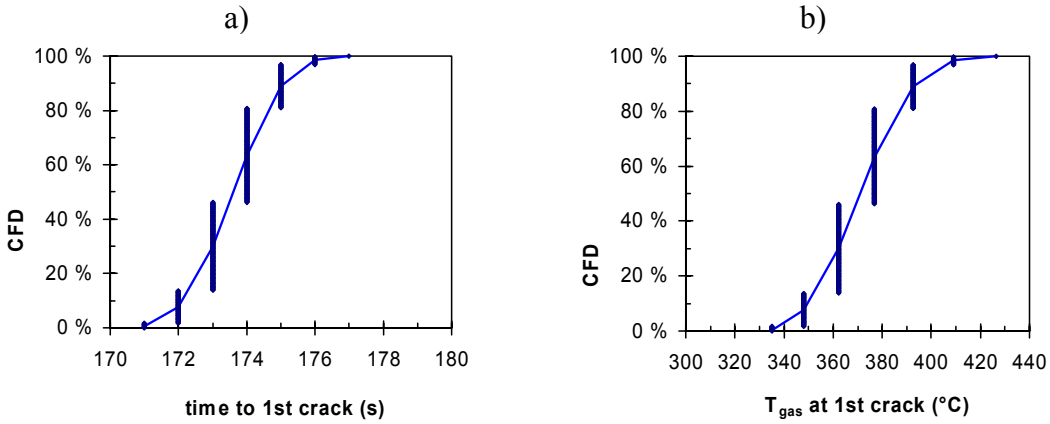

Figure 63. Modelling of the first glass crack in the test 1 of MeHaffey et al. (2004): a) time of the first crack and b) hot gas layer temperature at the first crack. In this case, the glass thickness and the shading thickness were adjusted so that the mean value of the calculated time (ca. 175 s) is reasonably close to the observed value of 185 s.

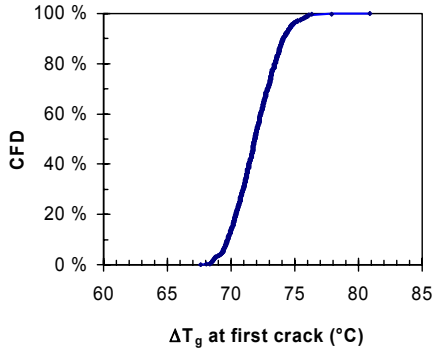

Figure 64. The average glass temperature rise ΔT_g required for the first glass cracking in the test 1 of MeHaffey et al. (2004).

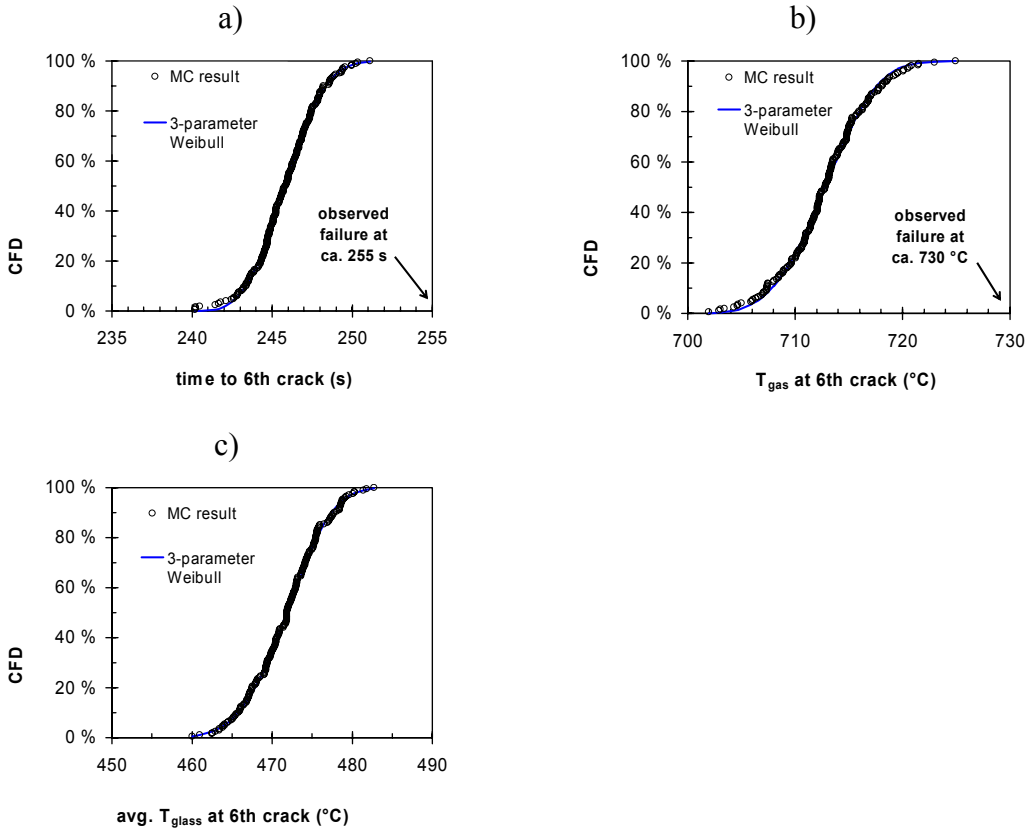

Figure 65. Analysis of the test 1 of MeHaffey et al. (2004): a) the observed fallout time of 255 s is closest to the time when 6 cracks occur within our model. b) At the 6th crack, the calculated hot gas layer temperature is ~700–730 °C, which is in good agreement with observed value of ca. 730 °C. c) The average glass temperature at the 6th crack is ~460–480 °C.

4.3.6.2 Analysis of test 2 of MeHaffey et al. (2004)

In the analysis of the occurrence of the 1st crack in the test 2 we used the same parameters as in analysis of the test 1. The calculated time ranging between ca. 250-260 s agrees quite well with the observed value of 270 s (Figure 66a). The calculated hot gas layer temperature ranging between *ca*. 330 and 430 °C (Figure 66b) is clearly lower than that recorded value of about 800 °C at the time of the first crack. However, the gas temperature rises rapidly just before the first window cracking time and hence it is possible that the temperature at the location of the window pane lags behind the recorded temperature value which presumably reflects the temperature close to the ceiling level and hence, the calculated value may not be as bad as it seems. The average glass temperature in is shown in Figure 67.

The observed time of the glass fallout of 315 s corresponds closest to the occurrence of the 4th crack in our model (Figure 68). At this moment the calculated gas temperature ranges between 740 °C and 800 °C in good agreement with observed temperature of ca. 740 °C. The model predicts that the average glass temperature at the fallout is 500–540 °C.

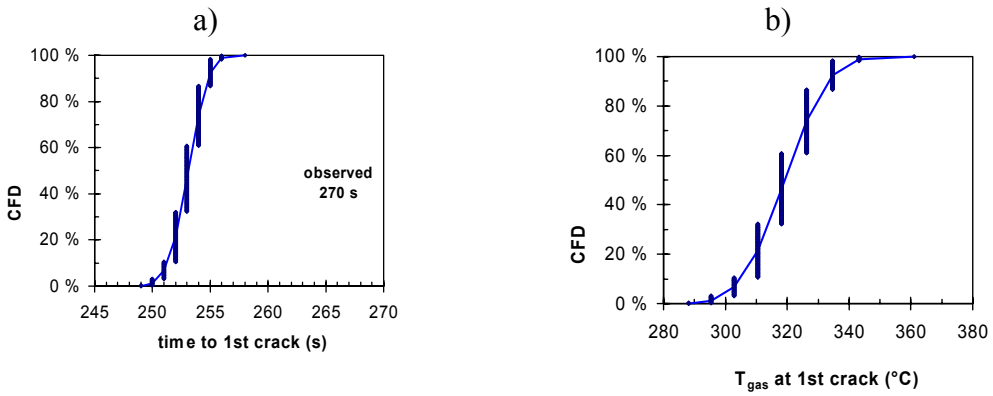

Figure 66. Modelling of the first glass crack in the test 2 of MeHaffey et al. (2004): a) time of the first crack and b) hot gas layer temperature at the first crack. The calculated time ranging between ca. 250–260 s agrees quite well with the observed value of 270 s. The hot gas layer temperature is lower than that recorded at the time of the first crack.

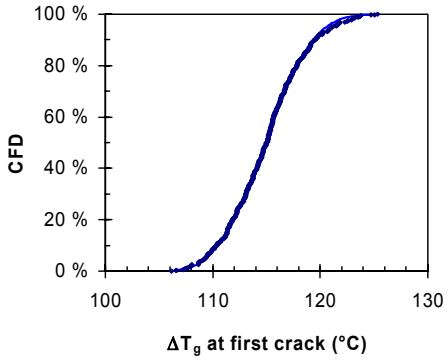

Figure 67. The average glass temperature rise ΔT_g required for the first glass cracking in the test 2 of MeHaffey et al. (2004).

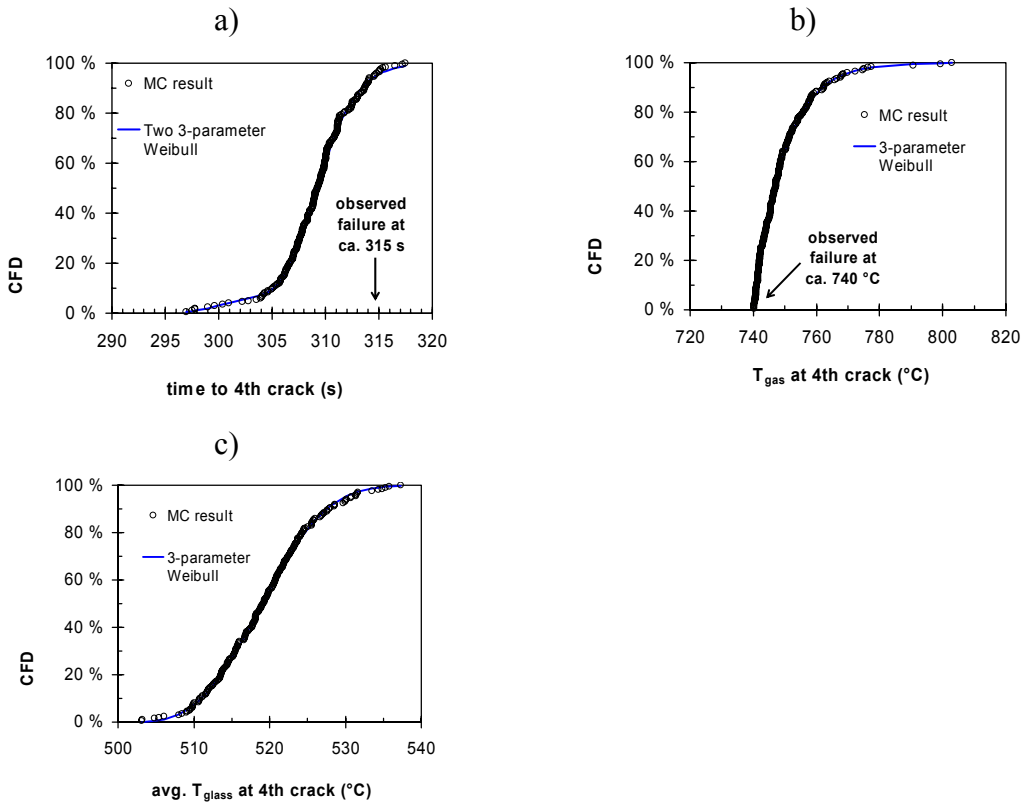

Figure 68. Analysis of the test 2 of MeHaffey et al. (2004): a) the observed fallout time of 315 s is closest to the time when 4 cracks occur within our model. b) At the 4th crack, the calculated hot gas layer temperature is ~740–800 °C, which is in good agreement with observed value of ca. 740 °C. c) The average glass temperature at the 6th crack is ~500–540 °C.

4.3.7 Summary of results on the glass fallout

The principal objective of the analyses presented in the previous sections of this Chapter is to establish how many cracks within our model are required for catastrophic galls failure leading to major window fallout and ventilation opening formation. These results are summarised in Table 1. It can be seen that the number of crack occurrences needed for glass fallout varies between four and eight and, taking into account the approximate nature of our approach, the distribution of these numbers is quite uniform.

Table 1. Summary of the results of the glass-fallout analyses presented in this Chapter.

Source of experimental data	**No. of cracks**	**Calculated hot gas layer temperature (°C)**	**Calculated average glass temperature (°C)**
Hassani et al. (1994/1995): An experimental investigation into the behaviour of glazing in enclosure fire.	5	550–590	410–430
Loss Prevention Council (Anon. 1999): Study concerning fire spread in multi-storey buildings with glazed curtain wall facades.	8	820–880	620–650
	7	730–760	545–570
Shields et al. (2001): Study on the performance of single glazing elements exposed to enclosure corner fires of increasing severity.	5	ca. 560	380–410
Shields et al. (2002): Study on the performance of a single glazing assembly exposed to a fire in the centre of an enclosure.	5	650–680	380–410
Hietaniemi et al. (2002): An investigation of fire safety issues related to building cavity spaces, Appendix F: glass-breaking study using a fire-resistance furnace.	7[a)]	710–730	520–540
	8[a)]	770–810	595–625
MeHaffey et al. (2004): Tests 1 and 2 of the series of fire experiments in furnished houses.	6	700–720	460–490
	4	740–800	500–540

a) Seven cracks correspond to a minor glass fallout and 8 cracks to a major fallout.

Table 1 incorporates also the ranges of the calculated hot layer gas temperatures and average glass temperatures at glass fallout. In fact, as can be seen from the plots of the hot gas layer temperature and average glass temperature distributions, i.e., Figure 34c, Figure 39c, Figure 43c, Figure 48c, Figure 54c, Figure 59c, Figure 60c, Figure 65c and Figure 68c, there is a statistical distribution fitted to each calculated distribution. The particular distribution used is the three-parameter Weibull distribution, the functional shape has been presented already in the context of the glass parameters (section 3.1.2). When one makes a Monte Carlo simulation based on these distributions, i.e. draws values for the hot gas layer temperatures and average glass temperatures at glass fallout randomly from either of the nine distributions shown in the above-mentioned distributions, one arrives at the distributions shown in Figure 69 (hot gas layer temperature distribution) and Figure 70 (average glass temperature distribution). Two cases are shown: the first one expressing the Monte Carlo sampled distribution with no further processing fitted by a triangular distribution and the second one expressing the

Monte Carlo sampled distribution with 10% model uncertainty attached to each data value fitted by a three-parameterWeibull distribution. Technically, the 10% model uncertainty is incorporated by multiplying each value in the Monte Carlo sample by a normally distributed factor with mean value equal to unity and standard deviation equal to 10%.

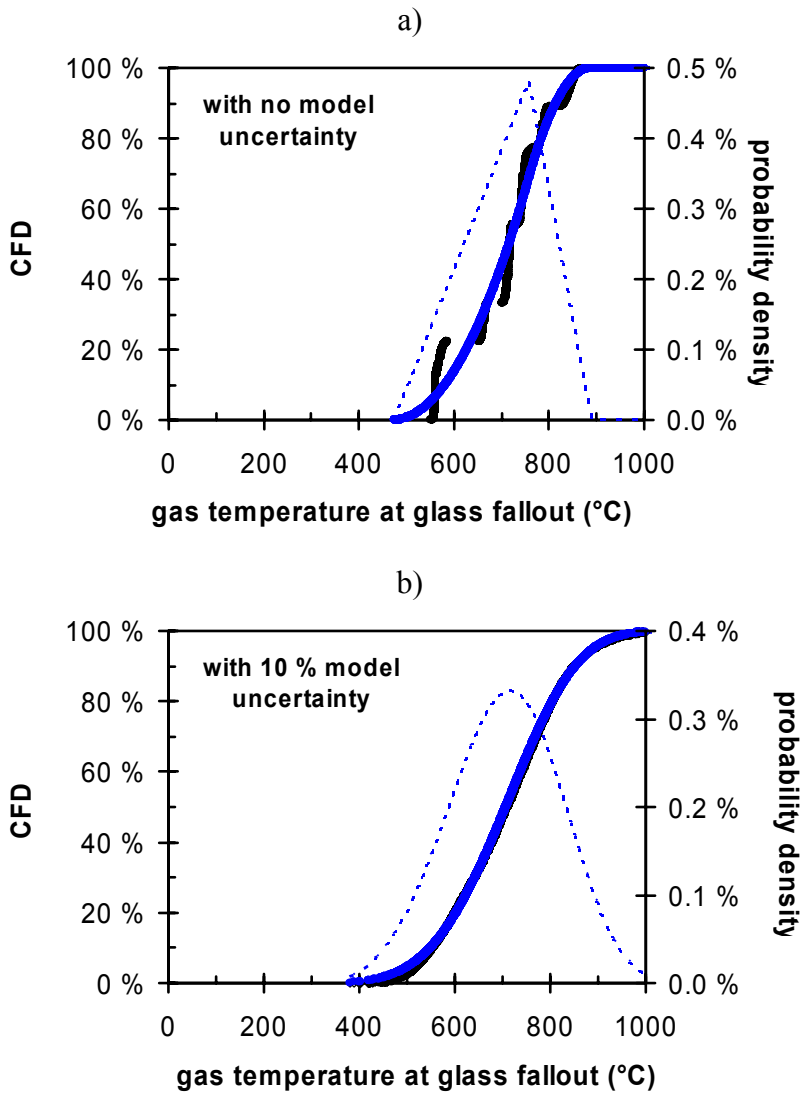

Figure 69. Monte Carlo sampling estimate of the hot gas layer temperature at glass fallout based on the distributions established on the basis of the analyses presented in this Chapter: a) the Monte Carlo sampled distribution with no further processing fitted by a triangular distribution and b) the Monte Carlo sampled distribution with 10% model uncertainty attached to each data value fitted by a three-parameter Weibull distribution.

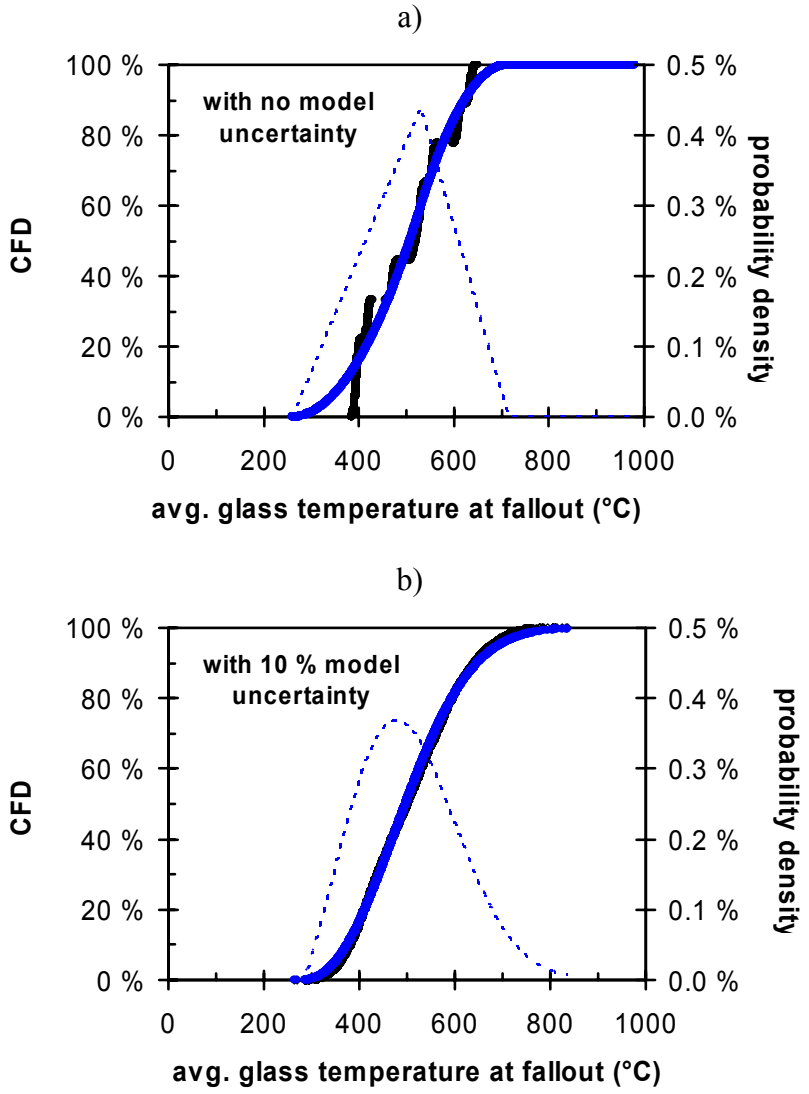

Figure 70. Monte Carlo sampling estimate of the average glass temperature at fallout based on the distributions established on the basis of the analyses presented in this Chapter: a) the Monte Carlo sampled distribution with no further processing fitted by a triangular distribution and b) the Monte Carlo sampled distribution with 10% model uncertainty attached to each data value fitted by a three-parameter Weibull distribution.

Table 2. Characteristics of the distributions shown in Figure 69 and Figure 70.

Quantity analysed	**Modelling using triangular distribution**	**Modelling using three-parameter Weibull distribution (with 10% model uncertainty added)**
Hot gas layer temperature at glass fallout	min. value = 474 °C peak value = 758 °C max. value = 889 °C mean = 707 °C standard deviation = 87 °C 2% fractile = 522 °C 5% fractile = 551 °C 10% fractile = 582 °C 20% fractile = 627 °C	α = 4,05 β = 464 °C x_{min} = 284 °C mean = 704 °C median = 707 °C mode = 716 °C standard deviation = 116 °C 2% fractile = 460 °C 5% fractile = 506 °C 10% fractile = 550 °C 20% fractile = 604 °C
Average glass temperature at fallout	min. value = 260 °C peak value = 530 °C max. value = 715 °C mean = 502 °C standard deviation = 93 °C 2% fractile = 310 °C 5% fractile = 339 °C 10% fractile = 371 °C 20% fractile = 417 °C	α = 2,28 β = 255 °C x_{min} = 280 °C mean = 506 °C median = 497 °C mode = 478 °C standard deviation = 105 °C 2% fractile = 326 °C 5% fractile = 350 °C 10% fractile = 375 °C 20% fractile = 412 °C

5. Example of the use of the glass-fallout model combination with the PFS probabilistic fire simulation tool

The principal use of the modelling presented in this report is to provide input data for probabilistic fire simulations (Hietaniemi et al. 2004, Hostikka & Keski-Rahkonen 2003, Hostikka et al. 2005), which at VTT are usually carried out by the Probabilistic Fire Simulator (PFS) tool (Hostikka et al. 2003). In this Chapter we present an example of the use of the probabilistic approach to glass breaking and fallout in combination with the PFS tool.

The building that we consider is a 6-level office building with an area of 1320 m2 and level height of 3,80 m. The floors consist basically of open-space offices. The façade is fully glazed by double glazing with 6-mm thick panes. The internal walls are of normal-weight concrete. Statistics (e.g., Holborn et al. 2002) show that a typical office fire is one that ignites due to electrical causes in the office space and hence we consider such fire scenario, i.e., a fire that ignites electrically in a workstation in the open-space office. We consider only the fire development within the compartment-of-fire-origin and leave out considerations of fire spread beyond this space.

The fire safety objective that we set out to analyse in this example is the load-bearing capacity of unprotected steel beams. We assume that the beams considered are of the type HE 400 B made of the S460 steel grade. The length of the beams is 9 m and their separation 10 m. The combined load equals 5,7 kN/m^2. In the standard temperature exposure, the fire resistance of these beams would be about 24 minutes, which corresponds to a failure temperature of 635 °C.

As we are dealing with practically a single-space room, we use the PFS-Ozone tool, i.e., the version of the PFS tool that runs the Ozone (Cadorin & Franssen 2003) fire zone model. The execution of the PFS-Ozone tool is principally controlled via the two EXCEL sheets shown in Figure 71 and Figure 72 which define the characteristics of the fire load, the fire and other relevant factors. Any of these factors can be treated as a stochastic factor. Descriptions of the stochastic fire characteristics are given in Table 3.

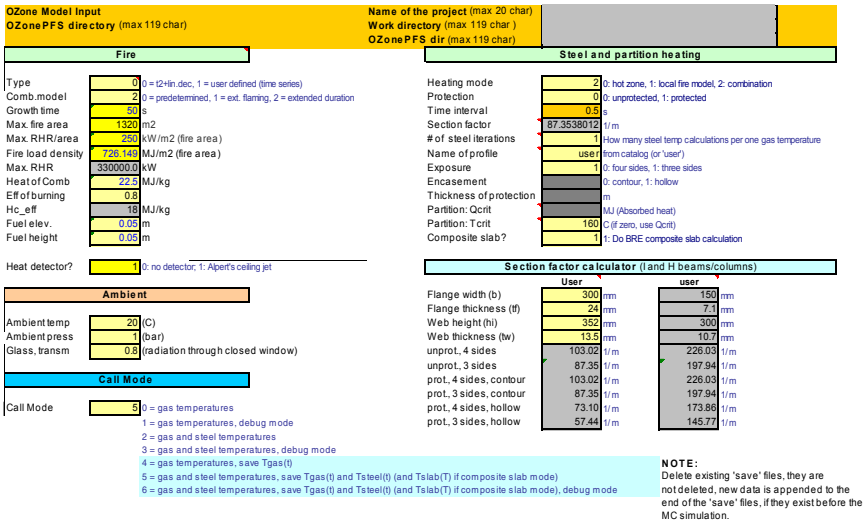

Figure 71. The first PFS-Ozone control sheet.

Create Ozone Input Data File Current Iteration 0

Input for the room geometry and openings

Title of the case (max 30 char)				
Running directory (max 119 char)				
Strategy	1	(1: 1-zone, 2: 2-zone, 3: combination of 1- and 2-zones)		
Flashover temperature	550	C	823	K
Fuel ignition temperature	325	C	598	K
Fuel area criterion	25	%	0.25	
Zone height criterion (z/H)	0.1		0.38	m
Room data				
Room height	3.8	m		
Room length	40	m		
Room depth	33	m		
Room area	1320	m2		
Fire elevation	0.05	m		
Fuel height	0.05	m		
Ceiling height (pitched roofs)		m		
Ambiet temperature	20	C	293	K
Ambient pressure	1	bar	100000	Pa
Eff. heat of combustion (DHc)	18000000	J/kg		
Glass: epsilon	0.8			

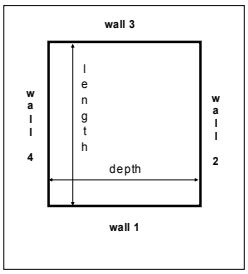

Time parameters:

xtimestep	printstep	timemax	timepoints
10	10	3600	361

Control parameters:

iceiling	ifloor	nbwall	nbmat	nbopen
1	1	4	1	2

irmf	nbptrmf	iceiltype	icomb	iairent
0	0	0	2	2

nbsmokeext	nbHVgroup	iExtPrint
0	0	1

Fire source (NFSC2 type)

Growth time (s)	50	s		
growth ends (tplateau)	908.295106	s		
decay starts (tendplate)	2638.74741	s	70% of fire load is consumed	
fire ends (tendfire)	4381.50513	s		
max. fire area (rfirearea)	1320	m2		
max. RHR/area (RHRf)	250	kW/m2	max. RHR	330000 kW
max. pyrolysis rate (rmfmax)	18.3333333	kg/s		
fire load density (fire area)	726.149049	MJ/m2	fire load	958516.745 MJ

Parameters for Time and Temperature Dependent Vents

	ropper1 (%)	ropT2 (C)	ropper2 (%)	ropT3 (C)	ropper3 (%)	
stepwise temp. dep.	0	280	35	350	100	iopevol=1
linear temp. dep.	0	280	0	350	100	iopevol=2
time dep., initial vent	0					iopevol=3
time dep., opening time	roptime2 (s)	1200				iopevol=3
	ropT0 (C)					
opening temperature	500					iopevol=4

Materials for partitions nbmat 1

	rho [kg/m3]	rk [W/m.K]	rc [J/kg.K]	repsilint []	repsilext []	rhint [W/m2.K]	rhext [W/m2.K]
Light weigth concrete	2300	1	1000	0.8	0.8	25	9
Cerablanket [25mm-128kg/m3]	128	0.035	800	0.8	0.8	25	9
CaSi - board	450	0.069	748	0.8	0.8	25	9
Brick	2000	1.04	1114	0.8	0.8	25	9
Wood	450	0.1	1113	0.8	0.8	25	9
Structural steel	7850	54	425	0.8	0.8	25	9
Normal weight concrete	2300	2	900	0.8	0.8	25	9
Middle weight concrere	2000	1	840	0.8	0.8	25	9
Average concrete	2300	1.3	1087	0.8	0.8	25	8
Gypsum	800	0.15	2750	0.8	0.8	25	8

Openings nbopen 2

	rsill	rsoffit	rwidth	rcvent	nopwall	(0,1,2,3,4) iopevol	(0,1) iadia	A (m2)	Q (MW)	Fo (m0,5)
1	0	1	6.66	0.7	1	0	1	6.66	9.99	0.002085
2	0.4	3.6	146	0.7	3	4	0	467.2	1253.63	0.261598

PARTITIONS

	Ceiling d=	0.16	Floor d=	0.16	Wall 1 d=	0.16	Wall 2 d=	0.16	Wall 3 d=	0.16	Wall 4 d=	0.16
		nbeleC		nbeleF	walllength	nbeleW	walllength	nbeleW	walllength	nbeleW	walllength	nbeleW
Max. number of nodes:		7		7	33	7	40	7	33	7	40	7
7	rlelem	nmat	rlelem	nmat	rlelem	nmat	rlelem	nmat	rlelem	nmat	rlelem	nmat
	0.02285714	7	0.02285714	7	0.02285714	7	0.02285714	7	0.02285714	7	0.02285714	7
Note: Only up to 7 elements	0.02285714	7	0.02285714	7	0.02285714	7	0.02285714	7	0.02285714	7	0.02285714	7
can be used in the wall	0.02285714	7	0.02285714	7	0.02285714	7	0.02285714	7	0.02285714	7	0.02285714	7
calculation is tested.	0.02285714	7	0.02285714	7	0.02285714	7	0.02285714	7	0.02285714	7	0.02285714	7
If more elements are needed,	0.02285714	7	0.02285714	7	0.02285714	7	0.02285714	7	0.02285714	7	0.02285714	7
then the original OZone user	0.02285714	7	0.02285714	7	0.02285714	7	0.02285714	7	0.02285714	7	0.02285714	7
interface should be used to get	0.02285714	7	0.02285714	7	0.02285714	7	0.02285714	7	0.02285714	7	0.02285714	7
the number and positions of the elements. These should then be used here.												

Figure 72. The second PFS-Ozone control sheet.

Table 3. Description of the principal quantities of our office fire simulation example.

Quantity	**Description**	**Basis**
Growth time of the t^2 HRR model	Triangular distribution with minimum at 40 s, peak at 50 s and maximum at 65 s	FDS4 simulations, see Figure 73
HRR per unit floor area	Triangular distribution with minimum at 150 kW/m^2 , peak at 250 kW/m^2 and maximum at 390 kW/m^2	FDS4 simulations, see Figure 73
Fire load density	Gumbel distribution with mean of 420 MJ/m^2 and 80 % fractile of 510 MJ/m^2	Eurocode 1 (CEN 2002)
Flashover temperature	Uniform distribution between 500 ˚C and 600 ˚C	Expert judgement
Fuel ignition temperature	Uniform distribution between 300 ˚C and 350 ˚C	Expert judgement
Heat of combustion	Uniform distribution between 20 MJ/kg and 25 MJ/kg	Expert judgement

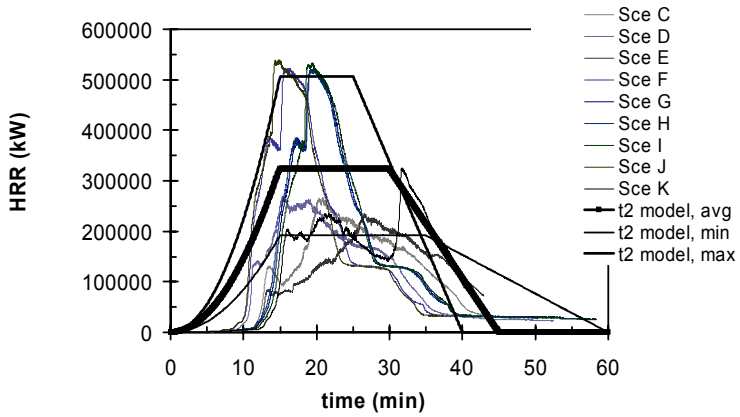

Figure 73. The stochastic description of the heat release as compared with HRR curves obtained from several FDS4 simulations.

There several options to model the window fire behaviour in the Ozone: the opening may be constantly open, the window may be modelled to break and fallout when the calculated hot-gas layer temperature reaches a single user-given value or it may break and fallout in several steps corresponding to user-given hot-has layer temperature values (Cadorin & Franssen 2003). In this study we use the single-value criteria approach. In a probabilistic approach the value of the hot-gas layer temperature required to cause window breakage break and fallout can be modelled in two ways:

- The simpler approach is to use a hot-gas layer temperature value obtained from the Weibull distribution given in Table 2. In this approach, however, one can not incorporate the particular properties of the windows used in building.

- The longer way is to use the procedure developed in this report to assess the breakage and fallout performance of the windows. In this approach one has to assess the hot-gas layer temperature development, *e.g.*, by executing deterministic fire simulation runs and after this, using the hot-gas layer temperature to carry out the probabilistic calculations of the window fire performance to obtain a probability distribution for the window breakage and fallout specific to the particular case analysed.

In the following we employ the former, simpler approach. The results obtained are compared with a deterministic approach which uses a single predefined window breakage and fallout temperature of 400 ˚C. The results of an exemplary Monte Carlo analysis of these two approaches are shown in Figure 74. As we are just giving an example, not presenting a thorough fire-safety analysis, we have kept the Monte Carlo sample size small, consisting of only 250 PFS-Ozone runs. The simulations have been terminated at 90 minutes since 1) in the case of the of the probabilistic window-breakage and fallout approach, the heat release rate (HRR) at this time is so small, about 10 MW, that the fire brigade which in reality would almost certainly be present at this time would also be able to extinguish the fire and 2) in the case of the deterministic window-breakage and fallout approach, in most the fire load has been consumed or at least the fires are in the decay phase. The probability of a failure of the steel structures can be assessed from the maximum temperatures reached by the steel beams. The steel temperature curves depicted in Figure 74e show that for the probabilistic window-breakage and fallout approach, most cases the maximum steel temperatures are relatively low, below ~300 ˚C, and in the few cases in which the steel temperatures grow higher than this, they still remain considerably below the failure temperature of 635 ˚C so that the failure probability is negligible. In the case of the deterministic window-breakage and fallout approach, the steel temperature curves may reach the failure temperature. The analysis of the (small) Monte Carlo sample shown in Figure 75 suggests that the failure probability is of the order 0,1% per fire.

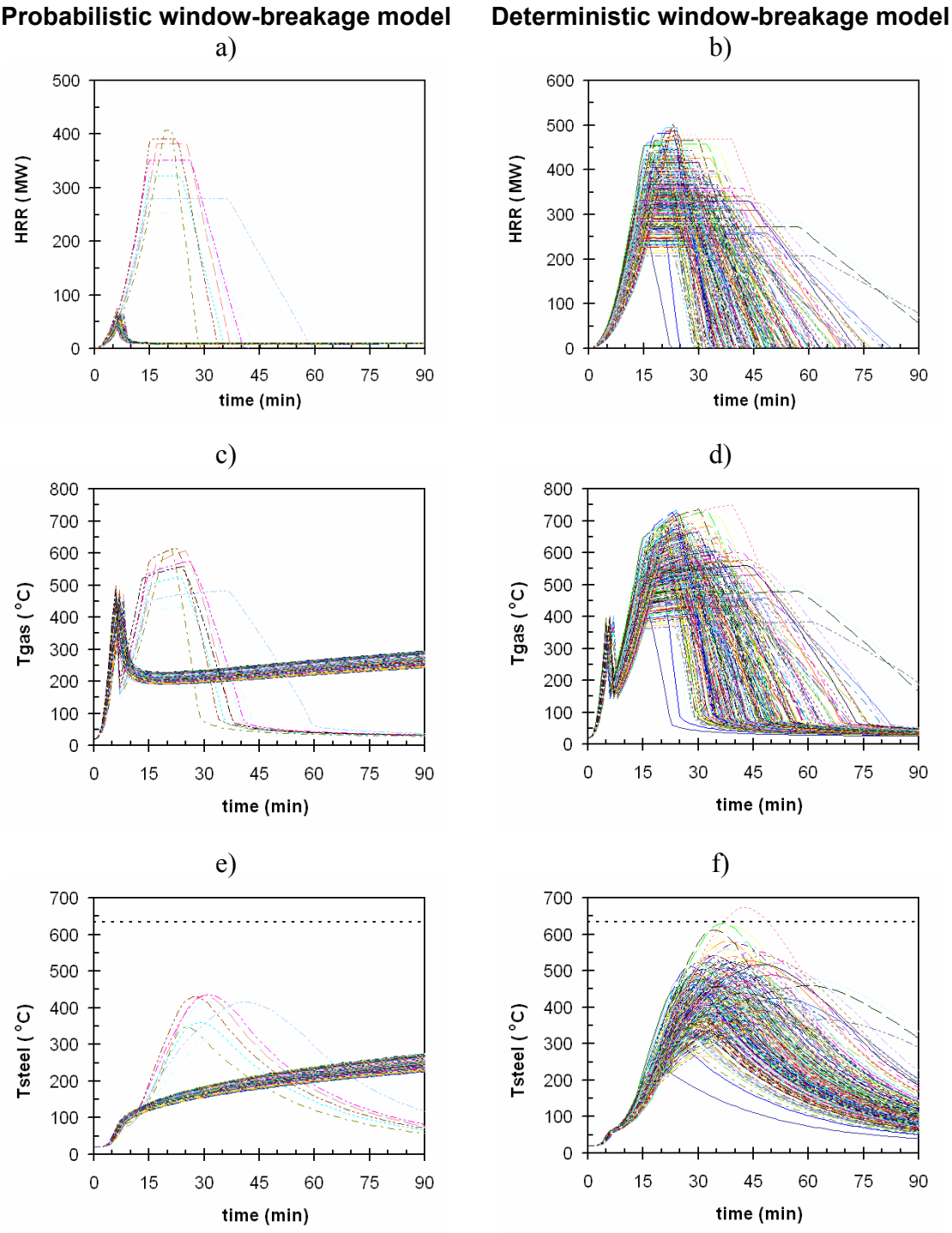

Figure 74. Comparison of the two window-breakage and fallout modelling approaches: Figs. a, c and e show the HRR, hot-gas layer temperature and the temperature of the HE 400 B beams for the probabilistic window-breakage model developed in this report and figs. b, d and f show the same quantities for a deterministic window-breakage model assuming window breakage and fallout at 400 ˚C. A Monte Carlo sample of size 250.

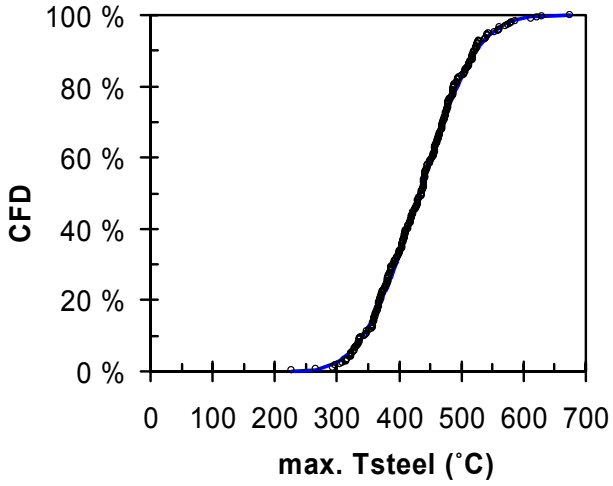

Figure 75. Distribution of maximum steel temperatures for the case of the deterministic window-breakage and fallout model.

Acknowledgements

We thank Mr. Henri Biström for the skilful programming of the MCB program. The deterministic BREAK program was downloaded from the Web site of the National Institute of Standards and Technology (NIST). We gratefully acknowledge and applaud to the NIST policy of rendering fire software freely available for the fire scientist around the world and wish also to express our gratitude for the developers of the BREAK program, A. A. Joshi and P. J. Pagni. It is this same progressive spirit that we have made our software available for any user by listing the MCB FORTRAN code in Appendix C.

The work has been funded by the Finnish National Technology Agency and VTT Building and Transport.

References

Anon. 1999. Fire Spread in Multi-Storey Buildings with Glazed Curtain Wall Facades. Borehamwood, England: Loss Prevention Council. (LPR 11: 1999.)

Babrauskas, V. 2004. Glass breakage in fires [Internet document]. Issaquah, WA, USA: Fire Science and Technology Inc. [Referenced October 20 2004]. Available at: http://www.doctorfire.com/glass.html.

Back, G., Beyler, C. L., DiNenno, P. & Tatem, P. 1994. Wall Incident Heat Flux Distributions Resulting from an Adjacent Fire. In: Kashiwagi, T. (ed.). Fire Safety Science – Proceedings of the Fourth International Symposium. Ottawa, Canada, July 13–17, 1994. Boston, USA: International Association for Fire Safety Science. Pp. 241–252.

Beyler, C. L. 2002. Fire Hazard Calculations for Large, Open Hydrocarbon Fires. SFPE Handbook of Fire Protection Engineering. 3rd Edition. Quincy, Massachusetts: NFPA. Pp. 3-268–3-314. ISBN 087765-451-4.

Cadorin, J.-F. & Franssen, J.-M. 2003. A tool to design steel elements submitted to compartment fires – OZone V2. Part 1: pre- and post-flashover compartment fire model. Fire Safety Journal, Vol. 38, pp. 395–427.

CEN. 2002. Eurocode 1: Actions on Structures – Part 1–2: General Actions – Actions on structures exposed to fire. Brussels: CEN. 59 p. (EN 1991-1-2:2002 E.)

Cuzzillo, B. R. & Pagni, P. J. 1998. Thermal Breakage of Double-Pane Glazing by Fire. Journal of Fire Protection Engineering, Vol. 9, No. 1, pp. 1–11.

Dayan, A. & Tien, C. L. 1974. Radiant Heating from a Cylindrical Fire Column. Combustion Science and Technology, Vol. 9, p. 14.

Dembsey, N. A., Pagni, P. J. & Williamson, R. B. 1996. Compartment Fire Experiments: Comparison to Models. Fire Safety Journal, Vol. 25, No. 3, pp. 187–227.

Drysdale, D. 1999. An Introduction to Fire Dynamics. Second Edition. Chicester, John Wiley & Sons, Ltd. 470 p. ISBN: 0-471-97291-6.

Emmons, H. W. 1986. The Needed Fire Science. In: Grant, C. E. & Pagni, P. J. (eds.). Fire Safety Science – Proceedings of the First International Symposium. NIST, USA, October 7–11.1986. Washington D.C., USA: Hemisphere. Pp. 33–53.

Gardon, R. 1958. Calculation of Temperature Distributions in Glass Plates Undergoing Heat Treatment. Journal of the American Ceramic Society, Vol. 41, pp. 200–208.

Harada, K., Enomoto, A., Uede, K. & Wakamatsu, T. 2000. An Experimental Study on Glass Cracking and Fallout by Radiant Heat Exposure. In: Curtat, M. (ed.). Fire Safety Science – Proceedings of the Sixth International Symposium. July, 5–9, 1999, Poitiers, France. International Association for Fire Safety Science. Pp. 1063–1074.

Hassani, S. K., Shields, T. J. & Silcock, G. W. 1994/1995. An Experimental Investigation into the Behaviour of Glazing in Enclosure Fire. Journal of Applied Fire Science, Vol. 4, pp. 303–323.

Hassani, S. K., Shields, T. J. & Silcock, G. W. 1995/1996. In Situ Experimental Thermal Stress Measurement in Glass Subjected to Enclosure Fire. Journal of Applied Fire Science, Vol. 5, pp. 123–134.

Hietaniemi, J., Hakkarainen, T., Huhta, J., Korhonen, T., Siiskonen, J. & Vaari, J. 2002. Ontelotilojen paloturvallisuus: Ontelopalojen tutkimus kokeellisesti ja mallintamalla. (Fire safety of cavity spaces: Experimental and simulation study of fires in cavities.) VTT Tiedotteita – Research Notes 2128. Espoo: VTT. 125 p. + app. 63 p. Available at: http://www.vtt.fi/inf/pdf/tiedotteet/2002/T2128.pdf.

Hietaniemi, J., Hostikka, S. & Korhonen, T. 2004. Probabilistic Fire Simulation. In: Almand, K. H. (ed.). Proceedings of the 5th International Conference on Performance-Based Codes and Fire Safety Design Methods. October 6–8, 2004. Luxembourg. Bethesda, MD. USA. Society of Fire Protection Engineers. Pp. 280–291.

Holborn, P., Nolan, P., Golt, J. & Townsend, N. 2002. Fires in workplace premises: risk data. Fire Safety Journal, Vol. 37, pp. 303–327.

Hostikka, S. 2004. Private communication.

Hostikka, S. & Keski-Rahkonen, O. 2003. Probabilistic simulation of fire scenarios. Nuclear Engineering and Design, Vol. 224, pp. 301–311.

Hostikka, S., Keski-Rahkonen, O. & Korhonen, T. 2003. Probabilistic Fire Simulator. Theory and User's Manual for Version 1.2. VTT Publications 503. Espoo: VTT. 72 p. + app. 1 p. Available at: http://www.vtt.fi/inf/pdf/publications/2003/P503.pdf.

Hostikka, S., Korhonen, T. & Keski-Rahkonen, O. 2005. Two-Model Monte Carlo Simulation of Fire Scenarios. In Fire Safety Science. Proceedings of the 8th

International Symposium on Fire Safety Science. Tsinghua University, Beijing, China: September 18–23 2005. International Association for Fire Safety Science. 12 p.

Joshi, A. & Pagni, P. J. 1990. Thermal Analysis of a Compartment Fire on Window Glass. Berkeley, CA: University of California Department of Mechanical Engineering. (NIST-GCR-90-579.)

Joshi, A. & Pagni, P. J. 1991. Users' Guide to BREAK1, The Berkeley Algorithm for Breaking Window Glass in a Compartment Fire. Berkeley, CA: University of California Department of Mechanical Engineering. (NIST-GCR-91-596.)

Joshi, A. A. & Pagni, P. J. 1994a. Fire-Induced Thermal Fields in Window Glass: II-Theory. Fire Safety Journal, Vol. 22, No. 1, pp. 25–43.

Joshi, A. A. & Pagni, P. J. 1994b. Fire-Induced Thermal Fields in Window Glass: II-Experiments. Fire Safety Journal, Vol. 22, No. 1, pp. 45–65.

Karlsson, B. & Quintiere, J. G. 2000. Enclosure Fire Dynamics. Boca Raton: CRC Press LLC. 315 p. ISBN 0.8493-1300-7.

Keski-Rahkonen, O. 1988. Breaking of Window Glass Close to Fire. Fire and Materials, Vol. 12, pp. 61–69.

Keski-Rahkonen, O. 1991. Breaking of Window Glass Close to Fire, II: Circular Panes Fire and Materials, Vol. 15, pp. 11–16.

Larsson, R. 1999. Fönsterglas under värmepåverkan – samt beskrivning och utvärdering av datorprogrammet BREAK1. Lund: Lund University, Department of Fire Safety Engineering. 87 p. (Report 5033.) In Swedish.

Lattimer, B. Y. 2002. Heat Fluxes from Fires to Surfaces. SFPE Handbook of Fire Protection Engineering. 3rd Edition. Quincy, Massachusetts: NFPA. Pp. 2-269–2-296. ISBN 087765-451-4.

MeHaffey, J. R., Craft, S. T., Richardson, L. R. & Batista, M. 2004. Fire Experiments in Furnished Houses. In: Bradley, D., Drysdale, D. & Molkov, V. (eds.). Fire and Explosion Hazards – Proceedings of the Fourth International Seminar. Londonderry, Northern Ireland, UK, September 8–12, 2003. Belfast, Northern Ireland, UK: University of Ulster. Pp. 163–174.

Mitler, H. E. & Rockett, J. A. 1987. User's Guide to FIRST, a Comprehensive Single-Room Fire Model. Gaithersburg, MD, USA: National Institute of Standards and Technology. (Report No. 87-3595.)

Mowrer, F. W. 1998. Window Breakage Induced by Exterior Fires Gaithersburg, MD, USA: National Institute for Standards and Technology. (NIST-GCR-98-751.)

Mudan, K. S. 1984. Thermal Radiation Hazards from Hydrocarbon Pool Fires. Progress Energy Combustion Science, Vol. 10, pp.59–80.

Pagni, P. J. 2003. Thermal Glass Breakage. In: Evans, D. (ed.). Fire Safety Science – Proceedings of the Seventh International Symposium. Worcester, MA, USA, June 16–21, 2003. International Association for Fire Safety Science. Pp. 3–22.

Pagni, P. J. & Joshi, A. A. 1991. Glass Breaking in Fires. In: Cox, G. & Langford, B. (eds.). Fire Safety Science – Proceedings of the Third International Symposium. Edinburgh, Scotland, July 8–12, 1991. Essex, England: Elsevier Science Publishers Ltd. Pp. 791–802.

Parry, R., Wade, C. A. & Spearpoint, M. 2003. Implementing a Glass Fracture Module in the BRANZFIRE Zone Model. Journal of Fire Protection Engineering, Vol. 13, pp. 157–183.

Richardson, J. K. & Oleszkiewicz, I. 1987. Fire Tests on Window Assemblies Protected by Automatic Sprinklers. Fire Technology, Vol. 23, pp. 115–132.

Shields, T. J., Silcock, G. W. H. & Hassani, S. K. S. 1997/1998a. The Behavior of Double Glazing in an Enclosure Fire. Journal of Applied Fire Science, Vol. 7, pp. 267–286.

Shields, T. J., Silcock, G. W. H. & Hassani, S. K. S. 1997/1998b. The Behavior of Glazing in a Large Simulated Office Block in a Multi-Story Building. Journal of Applied Fire Science, Vol. 7, pp. 333–352.

Shields, T. J., Silcock, G. W. H. & Flood, M. F. 2001. Performance of Single Glazing Elements Exposed to Enclosure Corner Fires of Increasing Severity. Fire and Materials, Vol. 25, pp. 123–152.

Shields, T. J., Silcock, G. W. H. & Flood, M. F. 2002. Performance of a Single Glazing Assembly Exposed to a Fire in the Centre of an Enclosure. Fire and Materials, Vol. 26, pp. 51–75.

Shokri, M. & Beyler, C. L. 1989. Radiation from Larger Pool Fires. SFPE Journal of Fire Protection Engineering, Vol. 4, No. 1, pp. 141–150.

Sincaglia, P. E. & Barnett, J. R. 1997. Development of a Glass Window Fracture Model for Zone Type Computer Fire Codes. Journal of Fire protection Engineering, Vol 8, No. 3, pp. 1–18.

Skelly, M. J., Roby, R. J. & Beyler, C. L. 1991. An Experimental Investigation of Glass Breakage in Compartment Fires. Journal of Fire Protection Engineering, Vol. 3, pp. 25–34.

Tanaka, T. et al. 1998. Performance-Based Fire Safety Design of a High-rise Office Building, to be published (1998). Referred to by Babrauskas, V. 2004. Glass Breakage in Fires. Available at: http://www.doctorfire.com/glass.html.

Tien, C. L, Lee, K. Y. & Stretton, A. J. 2002. Radiation Heat Transfer. SFPE Handbook of Fire Protection Engineering. 3rd Edition. Quincy, Massachusetts: NFPA. Pp. 1-73–1-89. ISBN 087765-451-4.

Appendix A: On the impact of the glass fallout on fire safety

Windows from inside to outside consitute the most important application of use of glass materials in buildings. Besides this application, glass is used as internal walls or parts of internal walls. During the last years, the trends in acrhitecture have been directed to increased use of glass in buildings and the amount of glazing can be substantial, e.g., in modern office and other commercial buildings.

In a fire, windows on the building interface to the outside act as barriers preventing free flow of air in to the fire and flow of smoke and hot fire gases from the to the outside of the building. In an enclosure fire, there are two opposed processes: on one hand, the windows act to strengthen the fire as obstruction of flow of the smoke and hot gases away from the fire room gives rise to heating up of the enclosure which via the heat feedback accelerates the burning but on the other hand, the restriction posed by the windows to the flow of oxygen to the fire eventually leads to vitiation of the the atmosphere and decelerates the fire. The resultant effects of these processes are illustrated in Figure A1, which shows results of the Ozone zone-model (Cadorin & Franssen 2003) applied to a simple enclosure fire with varying window sizes and varying hot gas temperatures associated with complete window fallout. The input design fire in the room with dimensions of 10 m × 10 m × 3 m is determined according to the fire part of the Eurocode 1 (CEN 2002) to have the heat-release-rate (HRR) rise time of 300 s, HRR per unit area of 250 kW/m^2 (giving maximum HRR of 25 MW) and fire load density of 511 MJ/m^2 (these typical characteristics of an office fire). The HRR curves show that if the windows endure the fire exposure up to hot-layer gas temperature of higher than 370 °C (T_b > 370 °C), the fire growth is cut by the depletion of oxygen in the enclosure and the HRR remains relative low, below 5 MW. If, however, the windows break T_b < 370 °C lower temperatures, the HRR can grow much higher, up to the maximum possible HRR in the most well-ventilated case. If the windows endure the fire exposure up to hot-layer gas temperature of higher than 370 °C, the hot gas-layer temperatures remain relatively low, below 400 °C, which could be tolerated throughout the fire duration by typical steel or steel-concrete as well as wooden structural elements. Thus, usually a high breaking temperature of windows is favourable with respect to structural fire resistance in the room-of-fire-origin. The smoke-layer height curves reveal that with respect to the safety of occupants in the room-of-fire-origin, the situation is reverse: when windows break at low temperatures, the smoke and hot gases are vented out and the smoke layer decends slower than in the case of high window breaking temperature and hence, a high breaking temperature of windows is unfavourable with respect to safety of life in the room-of-fire-origin. However, in the case studied here, the windows should break at very low temperatures (< 100 °C) for the smoke venting to be efficient.

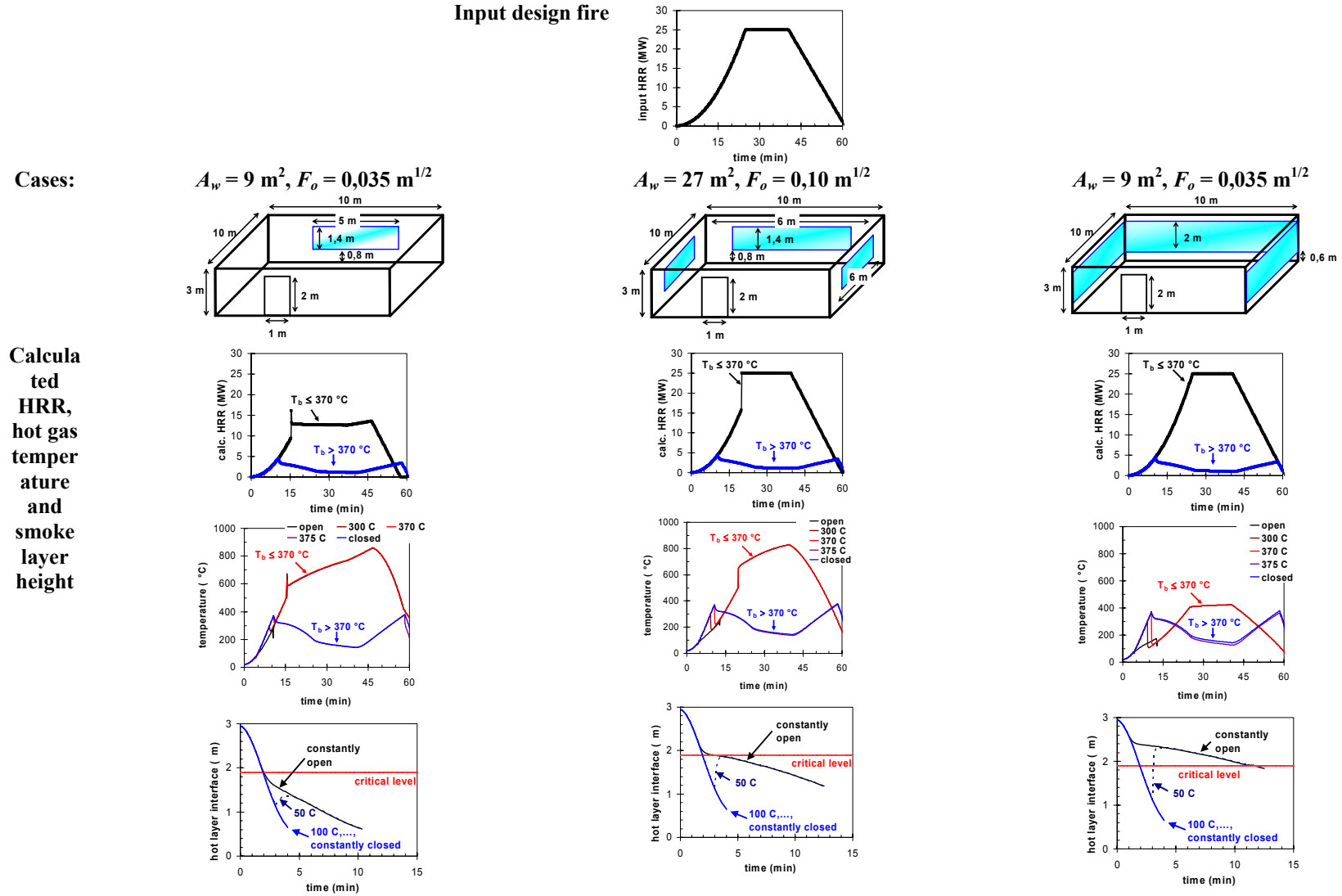

Figure A1. Example of the influence of the window breaking temperature to the fire.

High breaking temperature of windows is advantageous to fire safety also when one considers fire spread beyond the room-of-fire-origin. In most buildings there are two cases to be considered here, fire spread inside the building and external fire spread via the facade. The longer the internal glazing systems endure fire exposure, the more limited internal fire spread is. The same applies to the external fire spread route: if the windows in the room-of-fire-origin do not break, external fire spread is prevented[8].

References to Appendix A

Cadorin, J.-F. & Franssen, J.-M. 2003. A tool to design steel elements submitted to compartment fires – OZone V2. Part 1: pre- and post-flashover compartment fire model. Fire Safety Journal, Vol. 38, pp. 395–427.

CEN. 2002. Eurocode 1: Actions on Structures – Part 1–2: General Actions – Actions on structures exposed to fire. Brussels: CEN. (EN1991-1-2.)

[8] Provided that the external fire spread within the facade is prevented with appropriate fire stopping measures.

Appendix B: Analysis of the influence of different parameters to the first fracture of glass: a deterministic parametric study using the BREAK1 program

The fracture of a glass pane exposed to heating depends on the thermal and mechanical properties of the glass as well as the heat transfer to and from the glass. Important factors are also the thickness and area of the glass pane and the shading thickness, i.e., the dimension of the portion of the glass pane protected from direct heat exposure by the window frame. This Appendix presents a parametric study using the BREAK1 program of the influence of some of these parameter, namely the following:

- glass pane size expressed as the half height of a square-shaped pane
- glass thickness
- glass thermal conductivity
- glass thermal diffusivity
- glass absorption length
- glass breaking stress
- glass Youngs modulus
- glass linear coefficient of expansion
- the shading thickness.

The following parameters are used for the glass thermal and mechanical response parameters unless the particular parameter is the variable of the study:

- pane size = 1 m × 1 m
- pane thickness = 3 mm or 6 mm (mentioned in the relevant Figure caption)
- thermal conductivity = 0,76 W/(mK)
- thermal diffusivity = $3{,}6 \cdot 10^{-7}$ m^2/s
- absorption length = 1 mm
- breaking stress 47 MPa
- Youngs modulus = 70 GPa
- linear coefficient of expansion = $9{,}5 \cdot 10^{-7}$ $°C^{-1}$
- shading thickness 15 mm.

The thermal action of this parametric study has been taken to characterise that generated by the hot gas layer in a smallish room (area 12 m^2, height 2,6 m) with normal-weight concrete floor and ceiling and lightweight-construction walls (gypsum board). The fire connditions are calculated using the Ozone zone model (Cadorin & Franssen 2003). The heat release rate (HRR) rise time is 300 s and the fuel-limited maximum HRR is 3 MW. The ventilation is assumed take place via a 0,8 m wide and 2 m high door (thus, the fire at some stage of its development, the fire size becomes ventilation limited with maximum HRR of 2,1 MW). Figure B1 shows the computed hot gas layer temperature.

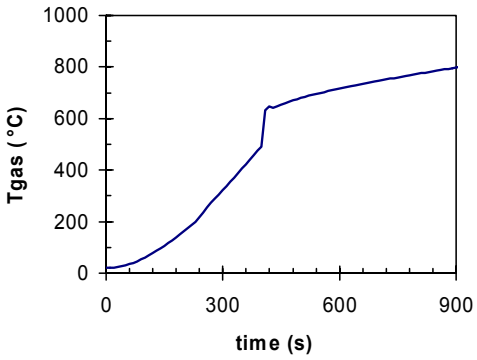

Figure B1. Heat exposure of this parametric study: the hot gas layer temperature.

The results are presented in terms of two temperature values:

- the hot gas layer temperature at the occurrence of the first cracking of the window pane (avg. T_{gas})
- the average glass temperature at the occurrence of the first cracking of the window pane (avg. T_{glass}).

Influence of glass pane size (half height of the square pane)

The study reveals that for small panes with half height less than ~ 20 cm decreasing the glass pane size increases strongly its endurance in thermal exposure (Figure B2). For larger panes with with half height more than ~ 50 cm, however, the influence of the pane size to the occurrence of the first crack is small. These findings apply both to the hot gas layer temperature and the average glass temperature at the occurrence of the first cracking of the window pane.

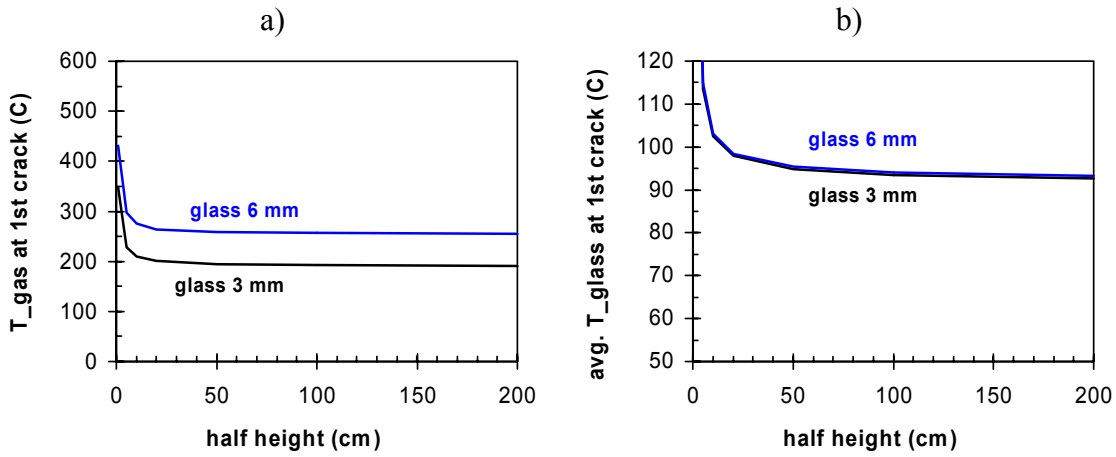

Figure B2. Influence of the glass pane size to the occurrence of the first cracking of the glass pane: a) the hot gas layer temperature and b) the average glass temperature at the occurrence of the first cracking.

Influence of glass thickness

The hot gas layer temperature needed to create a crack in a window pane increases approximately linearly with the glass thickness (Figure B3a). The average glass temperature at the occurrence of the first cracking of the window pane is a non-monotonous function of the glass thickness (Figure B3b): for very thin panes, avg. T_{glass} increases with decreasing glass thickness which is due to rapid heat up of veru thin glass layers. Between glass thickness of 2–6 mm, avg. T_{glass} is roughly constant and starts increase for thicker glass panes.

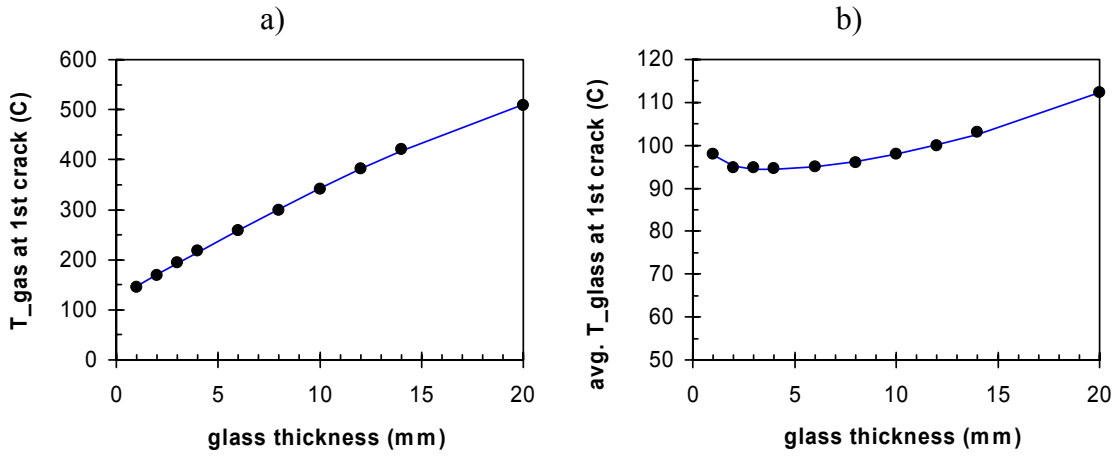

Figure B3. Influence of the glass thickness to the occurrence of the first cracking of the glass pane: a) the hot gas layer temperature and b) the average glass temperature at the occurrence of the first cracking.

Influence of glass thermal conductivity

The hot gas layer temperature needed to create the first fracture in a window pane increases approximately linearly as the thermal conductivity rises (Figure B4a). The average glass temperature at the occurrence of the first cracking of the window pane is approximately constant for different thermal conductivities with the exception of the glass-thickness-dependent peak at around 0,6–0,8 W/(m·K)for the glass thicknesses of 3 mm and 6 (Figure B4b).

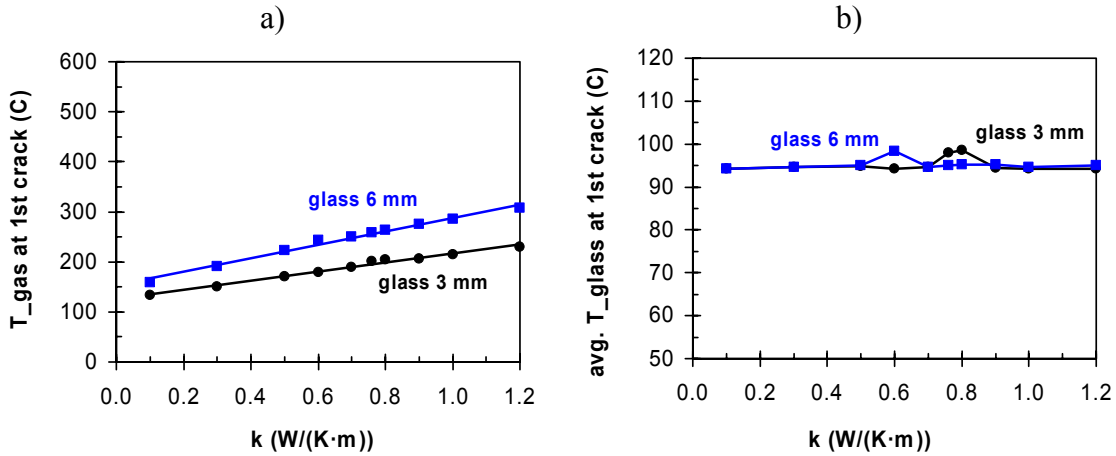

Figure B4. Influence of the glass thermal conductivity to the occurrence of the first cracking of the glass pane: a) the hot gas layer temperature and b) the average glass temperature at the occurrence of the first cracking.

Influence of glass thermal diffusivity

Changes in the thermal diffusity $\alpha = k/(\rho c)$ (ρ = density and c = specific heat) have a more pronounsed influence on the glass cracking than those of the thermal conductivity: the hot gas layer temperature at the first fracture decreases in a non-linear manner as the thermal diffusity increases (Figure B5a). The average glass temperature at the occurrence of the first cracking of the window pane is approximately constant for different thermal diffusivity values (Figure B5b).

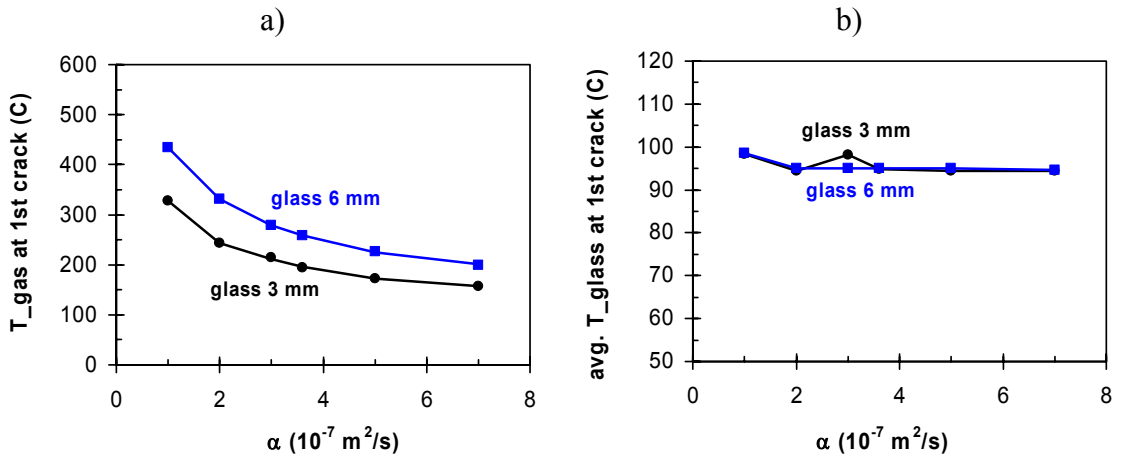

Figure B5. Influence of the glass thermal diffusivity to the occurrence of the first cracking of the glass pane: a) the hot gas layer temperature and b) the average glass temperature at the occurrence of the first cracking.

Influence of glass absorption length

Glass absorption length has only small influence on the hot gas layer temperature and the average glass temperature at the first fracture in a window pane (Figures B6a and b).

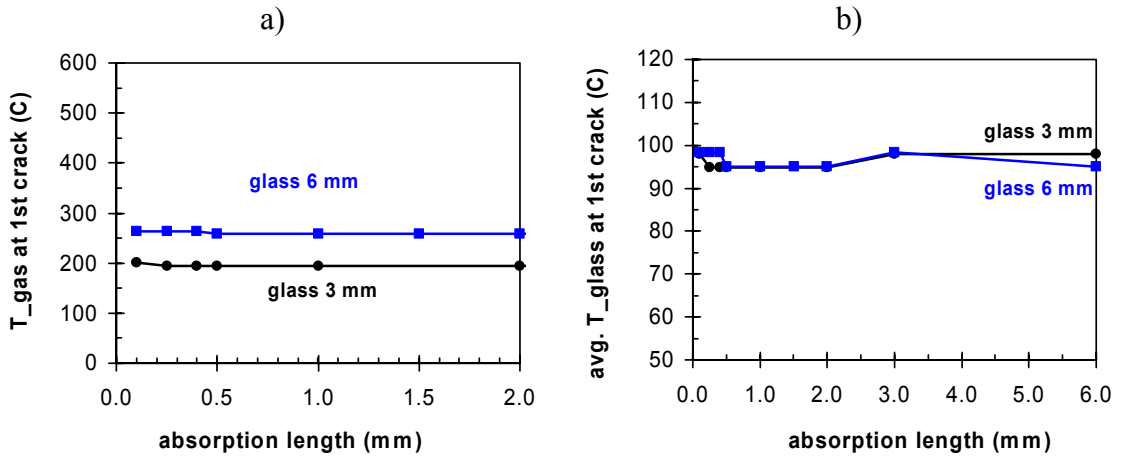

Figure B6. Influence of the glass absorption length to the occurrence of the first cracking of the glass pane: a) the hot gas layer temperature and b) the average glass temperature at the occurrence of the first cracking.

Influence of glass breaking stress

The hot gas layer temperature at the first fracture increases linearly as the glass breaking stress increases (Figure B7a). This applies also to the average glass temperature at the occurrence of the first cracking of the window pane, but here the influence is strong as compared to the influence of several other factors considered above (Figure B7b).

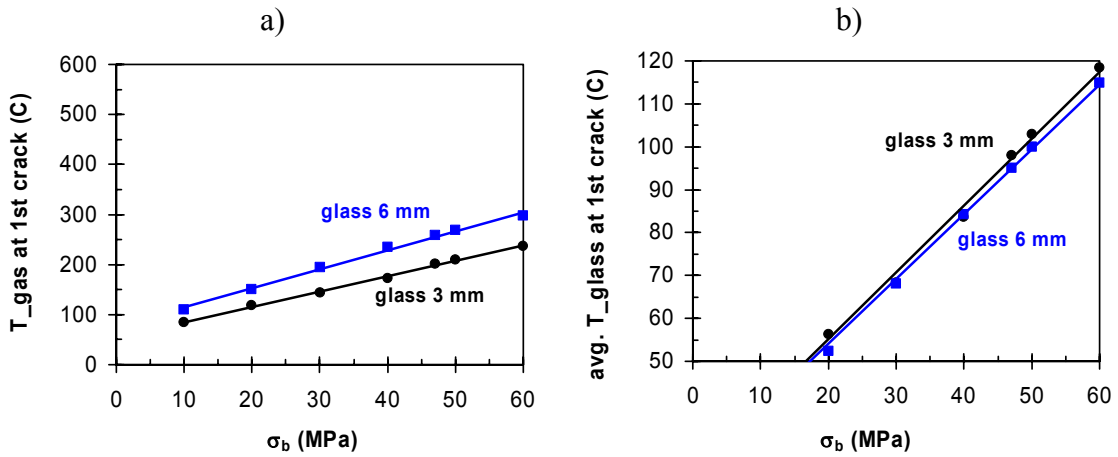

Figure B7. Influence of the glass breaking stress to the occurrence of the first cracking of the glass pane: a) the hot gas layer temperature and b) the average glass temperature at the occurrence of the first cracking.

Influence of glass Young's Modulus

The hot gas layer temperature at the first fracture decreases as the glass Young's modulus increases (Figure B8a). This applies also to the average glass temperature at the occurrence of the first cracking of the window pane, but the influence is relatively strong as compared to the influence of several other factors considered above (Figure B8b).

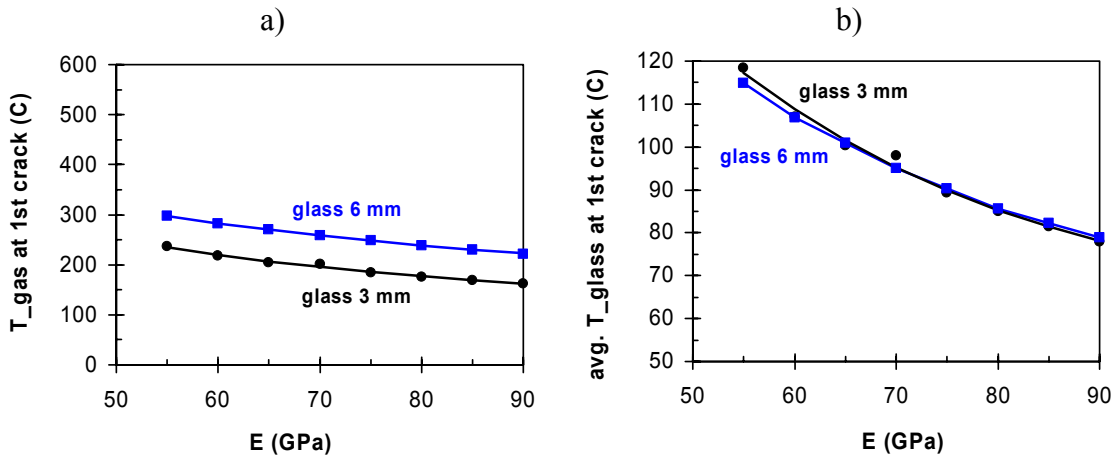

Figure B8. Influence of the glass breaking stress to the occurrence of the first cracking of the glass pane: a) the hot gas layer temperature and b) the average glass temperature at the occurrence of the first cracking.

Influence of glass linear coefficient of expansion

The linear coefficient of expansion (β) is the key factor affecting the generation of the heat-induced stress field in the glass (Figure B9). Consequently its influenece on both the hot gas layer temperature and the average glass temperature at the first fracture: the lower the β value is, the lower the induced stress field is and consequently, the higher the temperatures required for glass breakage.

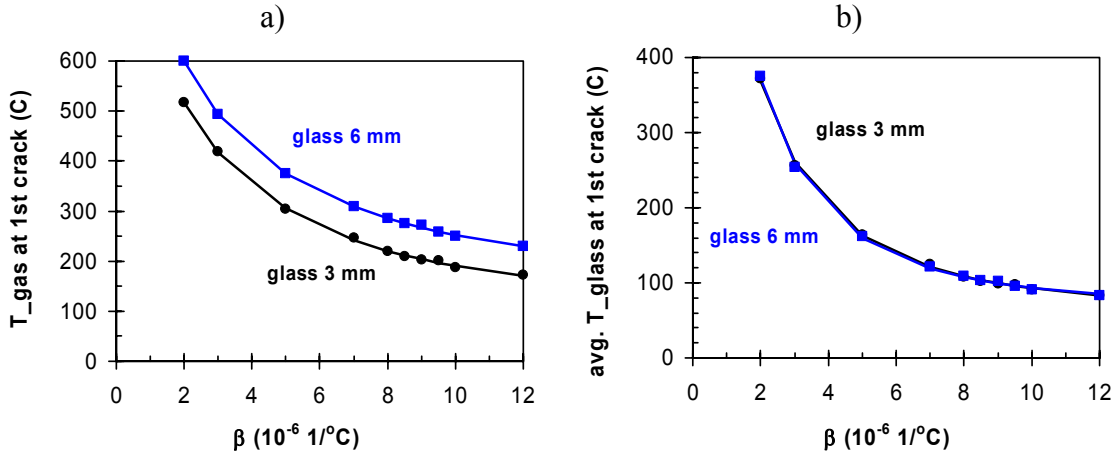

Figure B9. Influence of the glass linear coefficient of expansion to the occurrence of the first cracking of the glass pane: a) the hot gas layer temperature and b) the average glass temperature at the occurrence of the first cracking. Note that the vertical scale in Figfure B8b differs from the other Figures shown in this Appendix.

Influence of shading thickness

Staff of fire testing laboratories carrying out fire resistance tests of glazing systems is well aware of the fact that the shading thickness may have a very significant effect on the performance of the system in a fire resistance test. This phenomenon is seen clearly Figure B10: both the hot gas layer temperature and the average glass temperature at the occurrence of the first cracking of the window pane exhibit a sharp increase for small shading thicknesses (below ca. 5–15 mm depending on the glass thickness). However, comparison of Figures B9b and B10c reveals that the influence of the shading thickness – although notable – is much weaker than the influence of the the linear coefficient of expansion.

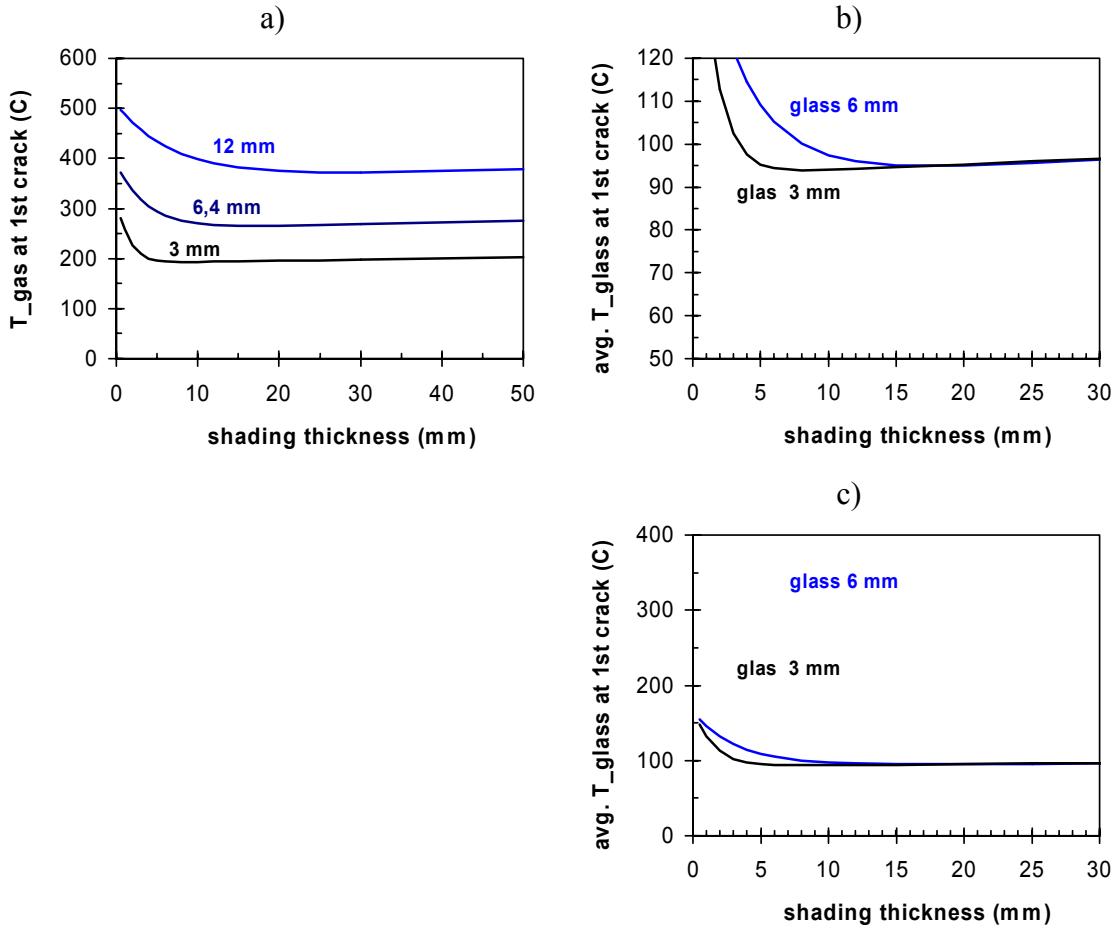

Figure B10. Influence of the shading thickness to the occurrence of the first cracking of the glass panea) the hot gas layer temperature and b) the average glass temperature at the occurrence of the first cracking. c) The influence of shading thickness on the average glass temperature at the occurrence of the first cracking shown on the same scale as the influence of the linear coefficient of expansion in Figure B9b.

References to Appendix B

Cadorin, J.-F. & Franssen, J.-M. 2003. A tool to design steel elements submitted to compartment fires – OZone V2. Part 1: pre- and post-flashover compartment fire model. Fire Safety Journal, Vol. 38, pp. 395–427.

Appendix C: MCB.for program listing

The main program

```
program MCB

use timeStepType

integer*4 nmc, iSeed, maxTime, idx, sidx
integer*2 iRanNum2, iMaxPar2, iSamp2, iNptsMax, iUserGiven, iOutNum2,percent,oldPercent
parameter(iSeed = 0, iRanNum2 = 10, iMaxPar2 = 3, iSamp2 = 1, iNptsMax = 0, iUserGiven = 0, iOutNum2 = 1)

integer*2 RandomType(iRanNum2), RandomNpts(iRanNum2), iMode2(iUserGiven), iNpts2(2)
real*8 RandomPara(iRanNum2,iMaxPar2), xi(iNptsMax,iUserGiven), fuser(iNptsMax,iUserGiven), time_ran
real*8 glassThickness, shadingThickness, halfWidth, m, sigma_u, lambda, ambientTemp
real*8 ambientEmissivity, timeStep, maxRunTime, outputInterval, youngsModulus, bigA
real*8 RankRs(iRanNum2,iOutNum2), RankProbrs(iRanNum2,iOutNum2), width, height, flameDist
real*8, dimension(:,:), allocatable :: RandomVector, buffer, gasTemperature, flameRadiationFlux
real*8, dimension(:,:), allocatable :: heatTransferCoeffHot, hotLayerEmissivity
real*8, dimension(:), allocatable :: thermalDiffusivity, breakingStress, RHR, fireArea, fireDiam, breakTimes
type(resultseries), dimension(:), allocatable :: results
character*1 csvSeparator
character*9 form
character*260 lineBuffer, datafile
character*40 parNames(iRanNum2)
logical ex, datafileGiven, nmcGiven, widthGiven, heightGiven, flameDistGiven, verbose, verboseGiven
logical csvSeparatorGiven, useSemicolon, pauseAtEnd, pauseAtEndGiven, glassThicknessGiven, missing
logical datafileExtra, nmcExtra, widthExtra, heightExtra, flameDistExtra, verboseExtra
logical csvSeparatorExtra, pauseAtEndExtra, glassThicknessExtra, extra

!external randomnumbers, dothestats

interface
   function breakf(thermalConductivity,alpha,beta,sigmab,youngs, &
                   betal,glassThickness,sl,h,h1,tinf,eps,epsi1, &
                   flameRadiationFlux,iendp,gasTemperature,iendt, &
                   heatTransferCoeffHot,iendh,hotLayerEmissivity, &
                   iende,dtime,runmax,toutput)
                         use timeStepType
      implicit double precision(a-h,o-z)
      real*8 gasTemperature(:,:), flameRadiationFlux(:,:)
      real*8 heatTransferCoeffHot(:,:), hotLayerEmissivity(:,:)
      dimension w(1005),uf1(1005),uf2(1005),uf3(1005)
      dimension t1(1005),t2(1005),q1(1005),q2(1005),aj(1005),ug3(1005)
      dimension u(1005),t1g(1005),t2g(1005)
      dimension temp2(1005),temp1(1005)
      dimension tfirex(1005),avgt(1005),xy(10),ivar(10)
                      type(resultseries) breakf
   end function breakf
end interface

write(*,'(a)') 'mcb version 1.0'

missing = .false.
extra = .false.

datafileGiven = .false.
nmcGiven = .false.
widthGiven = .false.
heightGiven = .false.
flameDistGiven = .false.
verboseGiven = .false.
csvSeparatorGiven = .false.
pauseAtEndGiven = .false.
glassThicknessGiven = .false.

datafileExtra = .false.
```

```
nmcExtra = .false.
widthExtra = .false.
heightExtra = .false.
flameDistExtra = .false.
verboseExtra = .false.
csvSeparatorExtra = .false.
pauseAtEndExtra = .false.
glassThicknessExtra = .false.

verbose = .false.
useSemicolon = .false.
pauseAtEnd = .true.

! Read some config data from a file.
inquire(file='mcb.config',exist=ex)
if (.not. ex) then
                write(*,'(a)') 'Error: mcb.config not found.'
                goto 99999
end if
open(20,file='mcb.config',status='old',action='read')
lne = 0
103 continue
                lne = lne + 1
                read(20,'(a)',end=111,err=104) lineBuffer
                idx = index(lineBuffer,':')
                sidx = index(lineBuffer,'#')
                if (sidx .eq. 0) sidx = len(lineBuffer)
                if (len(trim(lineBuffer(1:sidx - 1))) .eq. 0) goto 103
                if (idx .eq. 0) idx = len(lineBuffer)
                select case (lineBuffer(1:idx))
                case ('Datafile:')
                                if (datafileGiven) then
                                                datafileExtra = .true.
                                                extra = .true.
                                end if
                                read(lineBuffer(idx + 1:sidx),'(a)',err=110) datafile
                                datafileGiven = .true.
                case ('Number of Monte Carlo rounds to run:')
                                if (nmcGiven) then
                                                nmcExtra = .true.
                                                extra = .true.
                                end if
                                read(lineBuffer(idx + 1:sidx),'(i)',err=110) nmc
                                nmcGiven = .true.
                case ('Window width (m):')
                                if (widthGiven) then
                                                widthExtra = .true.
                                                extra = .true.
                                end if
                                read(lineBuffer(idx + 1:sidx),'(f)',err=110) width
                                widthGiven = .true.
                case ('Window height (m):')
                                if (heightGiven) then
                                                heightExtra = .true.
                                                extra = .true.
                                end if
                                read(lineBuffer(idx + 1:sidx),'(f)',err=110) height
                                heightGiven = .true.
                case ('Flame distance (m):')
                                if (flameDistGiven) then
                                                flameDistExtra = .true.
                                                extra = .true.
                                end if
                                read(lineBuffer(idx + 1:sidx),'(f)',err=110) flameDist
                                flameDistGiven = .true.
                case ('Glass thickness (m):')
                                if (glassThicknessGiven) then
                                                glassThicknessExtra = .true.
                                                extra = .true.
                                end if
                                read(lineBuffer(idx + 1:sidx),'(f)',err=110) glassThickness
                                glassThicknessGiven = .true.
                case ('Include all input data in output:')
```

```
                                        if (verboseGiven) then
                                                verboseExtra = .true.
                                                extra = .true.
                                        end if
                                        write(form,'(i3)') sidx - idx
                                        read(lineBuffer(idx + 1:sidx),'(l' // form // ')',err=110) verbose
                                        verboseGiven = .true.
                        case ('Use semicolon as field separator in .csv files:')
                                        if (csvSeparatorGiven) then
                                                csvSeparatorExtra = .true.
                                                extra = .true.
                                        end if
                                        write(form,'(i3)') sidx - idx
                                        read(lineBuffer(idx + 1:sidx),'(l' // form // ')',err=110) useSemicolon
                                        csvSeparatorGiven = .true.
                        case ('Pause at end:')
                                        if (pauseAtEndGiven) then
                                                extra = .true.
                                                pauseAtEndExtra = .true.
                                        end if
                                        write(form,'(i3)') sidx - idx
                                        read(lineBuffer(idx + 1:sidx),'(l' // form // ')',err=110) pauseAtEnd
                                        pauseAtEndGivenGiven = .true.
                        case ('')
                                        goto 103
                        case default
                                        goto 110
                        end select
goto 103
111 continue
close(20)

if (.not. datafileGiven) then
                        write(*,'(a)') 'Error: Datafile not given in mcb.config.'
                        missing = .true.
end if
if (datafileExtra) then
                        write(*,'(a)') 'Error: Datafile given more than once in mcb.config.'
end if

if (.not. nmcGiven) then
                        write(*,'(a)') 'Error: Number of rounds not given in mcb.config.'
                        missing = .true.
end if
if (nmcExtra) then
                        write(*,'(a)') 'Error: Number of rounds given more than once in mcb.config.'
end if

if (.not. widthGiven) then
                        write(*,'(a)') 'Error: Window width not given in mcb.config.'
                        missing = .true.
end if
if (widthExtra) then
                        write(*,'(a)') 'Error: Window width given more than once in mcb.config.'
end if

if (.not. heightGiven) then
                        write(*,'(a)') 'Error: Window height not given in mcb.config.'
                        missing = .true.
end if
if (heightExtra) then
                        write(*,'(a)') 'Error: Window height given more than once in mcb.config.'
end if

if (.not. glassThicknessGiven) then
                        write(*,'(a)') 'Error: Glass thickness not given in mcb.config.'
                        missing = .true.
end if
if (glassThicknessExtra) then
                        write(*,'(a)') 'Error: Glass thickness given more than once in mcb.config.'
end if

if (.not. flameDistGiven) then
```

```
                write(*,'(a)') 'Error: Flame distance not given in mcb.config.'
                missing = .true.
end if
if (flameDistExtra) then
                write(*,'(a)') 'Error: Flame distance given more than once in mcb.config.'
end if

if (verboseExtra) then
                write(*,'(a)') 'Error: "Include all input data" given more than once in mcb.config.'
end if

if (csvSeparatorExtra) then
                write(*,'(a)') 'Error: "Use semicolon as field separator" given more than once in mcb.config.'
end if

if (pauseAtEndExtra) then
                write(*,'(a)') 'Error: "Pause at end" given more than once in mcb.config.'
end if

if (.not. useSemicolon) then
                csvSeparator = ','
else
                csvSeparator = ';'
end if

if (missing .or. extra) goto 99999

allocate(RandomVector(nmc,iRanNum2),thermalDiffusivity(nmc), breakingStress(nmc),results(nmc),breakTimes(nmc))
goto 200
110 continue
write(form,'(i9)') ceiling(log10(real(lne)))
write(form,'(i' // form // ')') lne
write(*,'(a,i3,a)') 'Error: Found garbage in the file mcb.config on line ' // trim(form) // ':'
write(*,'(a)') trim(lineBuffer)
goto 99999
104 continue
write(*,'(a,i3,a)') 'Error: Found garbage in the file mcb.config.'
goto 99999
200 continue

write(*,*)' Enter the shading thickness in millimeters, please'
read(*,*, ERR=200) shadingThickness


!write(*,*)
!write(*,*) trim(datafile)
!write(*,*) nmc
!write(*,*) width
!write(*,*) height
!write(*,*) flameDist
!write(*,*) verbose
!goto 99999


! Initialize some values
youngsModulus = 72.0d9
shadingThickness = shadingThickness/1000.0
halfWidth = sqrt(height*width)/2.0
a = 3.86d-2
m = 0.000815*(1000*glassThickness)**2-0.000985*(1000*glassThickness)+1.205
sigma_u = (0.5016*(1000*glassThickness)+34.59)*1d6
lambda = 1/((-0.2919*(1000*glassThickness)**2+2.9309*(1000*glassThickness)+27.497)*1d6)
ambientTemp = 293.15
ambientEmissivity = 1.00
timeStep = 1.0
maxRunTime = 1000.0
outputInterval = 10.0

maxTime = 0.0

allocate(hotLayerEmissivity(2,2))
hotLayerEmissivity(1,1) = 0.0
hotLayerEmissivity(1,2) = 1.0
```

```
hotLayerEmissivity(2,1) = 1000.0
hotLayerEmissivity(2,2) = 1.0
numHotLayerEmissivity = 2

! Initialize variables for the creation of the Monte Carlo data

! 1: thermal conductvity (k), triangular
parNames(1) = 'Thermal conductivity'
RandomType(1) = 7
RandomNpts(1) = 3
RandomPara(1,1) = 0.95
RandomPara(1,2) = 0.7
RandomPara(1,3) = 1.4

! 2: density (rho), triangular
parNames(2) = 'Density'
RandomType(2) = 7
RandomNpts(2) = 3
RandomPara(2,1) = 2500.0
RandomPara(2,2) = 2400.0
RandomPara(2,3) = 2600.0

! 3: specific heat (C), triangular
parNames(3) = 'Specific heat'
RandomType(3) = 7
RandomNpts(3) = 3
RandomPara(3,1) = 820
RandomPara(3,2) = 750
RandomPara(3,3) = 950

! 4: absorption length (l), uniform
parNames(4) = 'Absorption length'
RandomType(4) = 1
RandomNpts(4) = 3
RandomPara(4,1) = 0.0 ! not used
RandomPara(4,2) = 9.0E-4
RandomPara(4,3) = 1.5E-3

! 5: rvec, weibull
parNames(5) = 'rvec'
RandomType(5) = 8
RandomNpts(5) = 3
RandomPara(5,1) = 0.0 ! not used
RandomPara(5,2) = m
RandomPara(5,3) = lambda

! 6: linear coefficient of expansion (beta), triangular
parNames(6) = 'Linear coefficient of expansion'
RandomType(6) = 7
RandomNpts(6) = 3
RandomPara(6,1) = 9.0E-6
RandomPara(6,2) = 8.5E-6
RandomPara(6,3) = 9.5E-6

! 7: unexposed side heat transfer coefficient (h_out), triangular
parNames(7) = 'Unexposed side heat transfer coefficient'
RandomType(7) = 7
RandomNpts(7) = 3
RandomPara(7,1) = 7.41
RandomPara(7,2) = 2.82
RandomPara(7,3) = 7.48

! 8: emissivity of glass (epsilon), uniform
parNames(8) = 'Emissivity of glass'
RandomType(8) = 1
RandomNpts(8) = 3
RandomPara(8,1) = 0.0 ! not used
RandomPara(8,2) = 0.85
RandomPara(8,3) = 0.95

! 9: the parameter a of the modified Back & al model (a), triangular
parNames(9) = 'a'
RandomType(9) = 7
```

```
RandomNpts(9) = 3
RandomPara(9,1) = 1.0
RandomPara(9,2) = 0.8
RandomPara(9,3) = 1.1

! 10: the value eta for heat transfer coeff. on hot layer side (eta), gamma
parNames(10) = 'eta'
RandomType(10) = 3
RandomNpts(10) = 3
RandomPara(10,1) = 0.0 ! not used
RandomPara(10,2) = 4.18243
RandomPara(10,3) = 2.63311

! Create the Monte Carlo data
call RandomNumbers(nmc,iSeed,iRanNum2,iMaxPar2,iSamp2,RandomPara, RandomType, &
        RandomNpts, iNptsMax, iUserGiven,iMode2,iNpts2,xi,fuser, &
                                                                RandomVector,time_ran)

thermalDiffusivity = RandomVector(:,1)/(RandomVector(:,2)*RandomVector(:,3))
breakingStress = sigma_u + RandomVector(:,5)*(a/(2*width+2*height))**(1/m)

if (verbose) then
        open(15,file='Monte Carlo data.csv',status='replace',action='write')
        open(16,file='Flame radiation flux.csv',status='replace',action='write')
        open(17,file='Heat transfer coefficient on hot layer side.csv',status='replace',action='write')
        write(16,'(a)') 'Time' // csvSeparator // 'Flame radiation flux'
        write(17,'(a)') 'Time' // csvSeparator // 'Heat transfer coefficient on hot layer side'
        write(form,'(i2)') iRanNum2 + 1
        write(15,'(' // form // '(a,:"' // csvSeparator // '"))') (trim(parNames(i)),i=1,iRanNum2),'Breaking stress'
        do i = 1,nmc
                write(15,'(' // form // '(e12.5e3,:"' // csvSeparator // '"))')
(RandomVector(i,j),j=1,iRanNum2),breakingStress(i)
        end do
        close(15)
end if

if ((RandomVector(1,9) .ge. 0.8) .and. (RandomVector(1,9) .le. 1.0)) then
        bigA = -(1.4 - 1.0)/(1.0 - 0.8)*(RandomVector(1,9) - 0.8) + 1.4
else
        if ((RandomVector(1,9) .gt. 1.0) .and. (RandomVector(1,9) .le. 1.1)) then
                bigA = -(1.0 - 0.7)/(1.1 - 1.0)*(RandomVector(1,9) - 1.0) + 1.0
        end if
end if

inquire(file=datafile,exist=ex)
if (.not. ex) then
        write(*,'(a)') 'Error: Datafile specified in mcb.config not found.'
        goto 99999
end if
open(30,file=datafile,status='old',action='read')

allocate(buffer(10000,5))
read(30,*)
read(30,*)
numTmp = 1
101 continue
        read(30,'(f10.0,10x,f10.0,40x,f10.0,30x,f10.0)',end=100,err=102)
buffer(numTmp,1),buffer(numTmp,2), &
                buffer(numTmp,3),buffer(numTmp,4)
        buffer(numTmp,2) = buffer(numTmp,2) + 273.15
        numTmp = numTmp + 1
goto 101
102 continue
write(*,'(a)') 'Error: Found garbage in the datafile.'
goto 99999
100 numTmp = numTmp - 1
allocate(gasTemperature(numTmp,2),RHR(numTmp),FireArea(numTmp),FireDiam(numTmp),flameRadiationFlux(numT
mp,2), &
        heatTransferCoeffHot(numTmp,2))
gasTemperature = buffer(1:numTmp,1:2)
RHR = buffer(1:numTmp,3)
flameRadiationFlux(:,1) = gasTemperature(:,1)
numFlameRadiationFlux = numTmp
```

```
heatTransferCoeffHot(:,1) = gasTemperature(:,1)
numHeatTransferCoeffHot = numTmp
fireDiam = buffer(1:numTmp,4)
close(30)
deallocate(buffer)

! Main Monte Carlo loop
percent = 0
oldPercent = 0
do i = 1,nmc

                percent = int(real(i)/real(nmc)*100.0)
                if (percent .ne. oldPercent) then
                                write(*,'(i3,a)') percent,'% ready'
                                oldPercent = percent
                end if

!               where(FireDiam .ge. 2*flameDist) flameRadiationFlux(:,2) = RHR*RandomVector(i,9)*exp(-(bigA*flameDist/(fireDiam/2)**2))
!               where(FireDiam .lt. 2*flameDist) flameRadiationFlux(:,2) = &
!                               200*(1 - exp(-0.09*(RHR**(1/3))))*RandomVector(i,9)*exp(-(bigA)**2)*(flameDist/(fireDiam/2))**(-1.7)

                where(FireDiam .ge. 2*flameDist) flameRadiationFlux(:,2) = (200*(1 -exp(-0.09*((RHR/1000.)**(1/3))))*RandomVector(i,9) &
                                *exp(-(bigA*flameDist/(fireDiam/2)**2)))*1000
   where(FireDiam .lt. 2*flameDist) flameRadiationFlux(:,2) = (0.38*200*(1 - exp(-0.09*(((-(bigA*flameDist/(fireDiam/2)**2)) &
                                *RHR/1000.)**(1/3))))*RandomVector(i,9)*exp(-(bigA)**2)*(flameDist/(fireDiam/2))**(-1.7))*1000
! old version of h_hot:         heatTransferCoeffHot(:,2) = min((0.051*RHR/1000 + RandomVector(i,10)),100.0)*1000
! new version of h_hot, see GlassPropertyDistributions.xls sheet "h_hot_side_v3"
   heatTransferCoeffHot(:,2) = (60*( (RHR/1000)**2.1927/((RHR/1000)**2.1927 + 995.506**2)) + RandomVector(i,10))

open(50,file='JH_check.dat',status='replace',action='write')


                if (verbose) then
                                do j = 1,numFlameRadiationFlux
                                                write(16,'(2(e12.5e3,:"' // csvSeparator // '"))') (flameRadiationFlux(j,k),k = 1,2)
                                end do
                                write(16,*)
                                do j = 1,numHeatTransferCoeffHot
                                                write(17,'(2(e12.5e3,:"' // csvSeparator // '"))') (heatTransferCoeffHot(j,k),k = 1,2)
                                end do
                                write(17,*)
                end if

   write(50,1011)RandomVector(i,1),thermalDiffusivity(i),RandomVector(i,4),breakingStress(i),youngsModulus, &

                RandomVector(i,6),glassThickness,shadingThickness,halfWidth,RandomVector(i,7),ambientTemp, &

                RandomVector(1,8),ambientEmissivity,numFlameRadiationFlux, &

                numTmp,numHeatTransferCoeffHot,numHotLayerEmissivity, &

                timeStep,maxRunTime,outputInterval

                results(i) = breakf(RandomVector(i,1),thermalDiffusivity(i),RandomVector(i,4),breakingStress(i),youngsModulus, &

                RandomVector(i,6),glassThickness,shadingThickness,halfWidth,RandomVector(i,7),ambientTemp, &

                RandomVector(1,8),ambientEmissivity,flameRadiationFlux,numFlameRadiationFlux,gasTemperature, &

                numTmp,heatTransferCoeffHot,numHeatTransferCoeffHot,hotLayerEmissivity,numHotLayerEmissivity, &

                timeStep,maxRunTime,outputInterval)
```

```
                length = size(results(i)%points)
                if (length .gt. maxTime) maxTime = length
end do

close(50)
1011 format(20(D20.10,1x))

! Write the results to files
open(10,file='All series.csv',status='replace',action='write')
open(11,file='Exposed glass temperature.csv',status='replace',action='write')
open(12,file='Unexposed glass temperature.csv',status='replace',action='write')
open(13,file='Breaking conditions.csv',status='replace',action='write')


write(form,'(i9)') maxTime
write(10,'(a)') 'Time' // csvSeparator // 'Gas temperature' // csvSeparator // 'Exposed' // csvSeparator // 'Unexposed' &
                                                                                // csvSeparator // 'Theta' // csvSeparator // 'Tau'
write(10,'(a)') '(s)' // csvSeparator // 'T(°C)' // csvSeparator // 'T(°C)' // csvSeparator // 'T(°C)' // csvSeparator &
                                                                                // '(Average)' // csvSeparator // ''
write(11,'(' // form // '(e12.5e3,:"' // csvSeparator // '"))') (outputInterval*i,i=1,maxTime - 1)
write(12,'(' // form // '(e12.5e3,:"' // csvSeparator // '"))') (outputInterval*i,i=1,maxTime - 1)
write(13,'(''n' // csvSeparator // 'Window breaks at time (s)' // csvSeparator // &
                                                                                'Gas temperature at window breaking time (°C)' // csvSeparator // 'tc (s)' // csvSeparator // 'Tc (°C)' &
                                                                                // csvSeparator // 'Avg. delta T (K)' // csvSeparator // 'Avg. T break (°C)'')')

form = ''

do i = 1,nmc
                length = size(results(i)%points)
                do j = 1,length
                                write(10,'(6(e12.5e3,:"' // csvSeparator // '"))') results(i)%points(j)%time,gasTemperature(j,2) - 273.15, &
                                                                results(i)%points(j)%exposed - 273.15,results(i)%points(j)%unexposed-273.15, &


                results(i)%points(j)%theta,results(i)%points(j)%tau
                end do

                if (results(i)%broken) then
                                write(form,'(i9)') length

                                write(11,'(' // form // '(e12.5e3,:"' // csvSeparator // '"))') (results(i)%points(j)%exposed - 275.15,j = 1,length - 1)
                                write(12,'(' // form // '(e12.5e3,:"' // csvSeparator // '"))') (results(i)%points(j)%unexposed - 275.15,j = 1,length - 1)
                                write(13,'(i4,"' // csvSeparator // '",6(e12.5e3,:"' // csvSeparator // '"))') i,results(i)%points(length)%time, &

                gasTemperature(length,2),results(i)%tcs,results(i)%tck,results(i)%avgDeltaT,results(i)%avgTBreak - 273.15
                else
                                write(10,'(a)') trim(results(i)%message)
                                write(11,'(a)') trim(results(i)%message)
                                write(12,'(a)') trim(results(i)%message)
                                write(13,'(i4,"' // csvSeparator // '",a)') i,trim(results(i)%message)
                end if
                write(10,*)

                breakTimes(i) = results(i)%points(length)%time
end do

close(10)
close(11)
close(12)
close(13)

if (verbose) then
                close(16)
```

```
                close(17)
end if

call DoTheStats(nmc,iRanNum2,iOutNum2,RandomVector,breakTimes,RankRs,RankProbrs,time_ran)

open(14,file='Statistics.csv',status='replace',action='write')
write(14,'("Parameter' // csvSeparator // 'RankRs' // csvSeparator // 'RankProbrs")')
do i = 1,iRanNum2
                write(14,'(a,"' // csvSeparator // '",e12.5e3,"' // csvSeparator // '",e12.5e3)') &
                                                parNames(i),RankRs(i,1),RankProbrs(i,1)
end do
close(14)

write(*,'(a)') 'mcb finished successfully.'
99999 continue
if (pauseAtEnd) then
                write(*,*)
                write(*,'(a)') 'Press return to end program.'
                read(*,*)
end if
end
```

The BREAK1 code used as a Fortan function

```
                function breakf(thermalConductivity,alpha,beta,sigmab,youngs,
                1               betal,glassThickness,sl,h,h1,tinf,eps,epsi1,
    2           flameRadiationFlux,iendp,gasTemperature,iendt,
    3           heatTransferCoeffHot,iendh,hotLayerEmissivity,
    4           iende,dtime,runmax,toutput)
                use kern
                use lin
                use newt
                use timeStepType
                implicit double precision(a-h,o-z)

                real*8 gasTemperature(:,:),flameRadiationFlux(:,:)
                real*8 heatTransferCoeffHot(:,:),hotLayerEmissivity(:,:)
                real*8, dimension(1005) :: aj,q1,q2,t1,t2,t1g,t2g,temp2,temp1,u,w
                dimension tfirex(1005),avgt(1005),xy(10),ivar(10)
                real*8, dimension(:), allocatable :: dimtime,p,dambt,tamb,th2,dh2
                real*8, dimension(:), allocatable :: teps2,deps2
                integer numResults
                type(timepoint) results(1005)
                type(resultseries) breakf
c
c
c aio = Io
c beta = reciprocal of absorption coefficient
c ak                = thermal conductivity
c alpha= thermal diffusivity
c al                = thickness of the glass
c h1                = heat transfer coeff on un-exposed side
c h2                = heat transfer coeff on exposed side
c tfirex= ambient temp on exposed side
c tinf = ambient temp on unexposed side
c t2i  = ambient temp on exposed side (initially)
c eps  = emissivity of glass
c epsi = emissivity of surroundings ( un-exposed side)
c nk                = no of terms for series in kernels
c nt                = no of time steps
c dt                = size of the time step
c error= error allowed in the soln of eqn using newton's method
c errmax = error allowed between solns of time step sizes
c p                 = dimensional flame radiation flux
c tamb = dimensional ambient temp of exposed side

                 nk=3
```

```
c**********************************************************************
c                          TITLE OF THE PROGRAM
c**********************************************************************

c                       write(*,301)
c301                    format(20x,'BREAK1- VERSION 1.0')
c                       write(*,302)
c302                    format(15x,'A. A. Joshi and P. J. Pagni')
c                      write(*,303)
c303                    format(10x,'Department of Mechanical Engineering')
c                      write(*,304)
c304                    format(10x,'University of California at Berkeley')
c                      write(*,305)
c305                    format(20x,'Berkeley, CA 94720')
c
c                       write(*,15453)
c                       write(*,1545)
c1545                   format(1x,'This program calculates the temperature history of th
c     1e surfaces')
c                      write(*,15451)
c15451   format(1x,'of a glass window for given fire parameters.')
c                      write(*,15452)
c15452   format(1x,'The calculations are stopped when the glass breaks.')
c                       write(*,15453)
c15453   format(1x,'')
c                       write(*,15453)
c                      write(*,16793)
c16793   format(1x,'Hit RETURN to continue')
c                      write(*,15453)
c                      read(*,*)

c**********************************************************************
c                          DISCLAIMER
c**********************************************************************

c                      write(*,401)
c401                    format(1x,'*****************************************************
c     1*******')
c                      write(*,402)
c402                    format(1x,'*       Warning: Read the disclaimer before using this pro
c     1gram  *')
c                      write(*,403)
c403                    format(1x,'*       ------------------------------------------------
c     1----  *')
c                       write(*,404)
c404                    format(1x,'*       This program was developed under grants from the
c     1                 *')
c                      write(*,4041)
c4041                   format(1x,'*       National Institute of Standards and Technology, ho
c     1wever *')
c                      write(*,4042)
c4042                   format(1x,'*       no certification or applicability is implied.  Man
c     1y                *')
c                      write(*,405)
c405                    format(1x,'*       assumptions are made concerning the physical prope
c     1rties *')
c                      write(*,4051)
c4051                   format(1x,'*       of glass and the phenomenology of breakage. Only y
c     1ou are*')
c                      write(*,406)
c406                    format(1x,'*       responsible for your calculations with this progra
c     1m. Use*')
c                      write(*,408)
c408                    format(1x,'*       should be restricted to predicting when ordinary
c     1glass *')
c                      write(*,409)
c409                    format(1x,'*       in ordinary windows may break under the assumption
c     1s in  *')
c                      write(*,410)
c410                    format(1x,'*       your choice of input parameters.  Do not use the
c     1                 *')
c                      write(*,411)
```

```
c411                  format(1x,'*       program to calculate conditions under which glass
c     1 will *')
c                     write(*,412)
c412                  format(1x,'*       not break.          The properties of a particular piece o
c     1f              *')
c                     write(*,413)
c413                  format(1x,'*       glass and the accuracy of each set of input are bo
c     1th             *')
c                     write(*,414)
c414                  format(1x,'*       sufficiently uncertain that no confidence can be p
c     1laced *')
c                     write(*,415)
c415                  format(1x,'*       in any calculation which predicts that a window wi
c     1ll             *')
c                     write(*,420)
c420                  format(1x,'*       not break.

c     1               *')
c                     write(*,401)
c                     write(*,16793)

c*******************************************************************************
c
c                                          SET UP THE [DEFAULT] VALUES
c
c*******************************************************************************

                      ak=thermalConductivity
                      al=glassThickness
                      t2i=300.d0
                      dt=.00893
                      t=0.d0
                      allocate(dimtime(iendp+1),p(iendp+1))
                      dimtime(1:iendp)=flameRadiationFlux(1:iendp,1)
                      p(1:iendp)=flameRadiationFlux(1:iendp,2)
                      allocate(dambt(iendt+1),tamb(iendt+1))
                      dambt(1:iendt)=gasTemperature(1:iendt,1)
                      tamb(1:iendt)=gasTemperature(1:iendt,2)
                      allocate(th2(iendh+1),dh2(iendh+1))
                      th2(1:iendh)=heatTransferCoeffHot(1:iendh,1)
                      dh2(1:iendh)=heatTransferCoeffHot(1:iendh,2)
                      allocate(teps2(iende+1),deps2(iende+1))
                      teps2(1:iende)=hotLayerEmissivity(1:iende,1)
                      deps2(1:iende)=hotLayerEmissivity(1:iende,2)
                      ibr=0

                      numResults = 0

9926  error=1.d-6
                      dt=dtime*alpha/al**2.d0
                      nk=3
     sig=5.67d-8
c initial temperature distribution
       t2i=tamb(1)
       call init(ak,sig,eps,al,h1,h2(1),tinf,t2i,r,ti)
       sig=5.67d-8

c constants in this problem

       pi=4.d0*datan(1.d0)
                      g=beta/al
                      g11=1.d0/g
                      tc=sigmab/(betal*youngs)
                      comm=eps*sig*al/ak
                      ca=(h2(1)*al*(tfirex(1)-ti)+sig*al*(epsi(1)*tfirex(1)**4.d0
    1     -eps*sig*al*ti**4.d0))/(ak*tc)
                      cb=-(h2(1)*al+4.d0*eps*sig*(ti**3.d0)*al)/ak
                      cc=-6.d0*comm*tc*(ti**2.d0)
                      cd=-4.d0*comm*(tc**2.d0)*ti
                      ce=-comm*tc**3.d0
                      cf=(h1*al*(ti-tinf)-epsi1*sig*al*tinf**4.d0
    1     +eps*sig*al*ti**4.d0)/(ak*tc)
                      cg=(h1*al+4.d0*eps*sig*ti**3.d0*al)/ak
```

```
                    tcrit=60.d0/tc
      nt=runmax/dtime+1



      tf=(nt-1)*dt
                    tf1=tf+dt
                    time=0.d0
                    iendpa=iendp+1
                    dimtime(iendpa)=tf1*al**2.d0/alpha
                    p(iendpa)=p(iendp)
                    do 1001 k=1,nt
                     do 2001 i=2,iendpa
2001     if(time.le.dimtime(i).and.time.ge.dimtime(i-1))
    1call linear(dimtime(i-1),dimtime(i),p(i-1),p(i),time,aaj)
                     aj(k)=aaj/(ak*tc/al)
1001     time=time+dtime

                     time=0.d0

      iendta=iendt+1
                    dambt(iendta)=tf1*al**2.d0/alpha
                    tamb(iendta)=tamb(iendt)
                    do 6001 k=1,nt
                     do 7001 i=2,iendta
7001     if(time.le.dambt(i).and.time.ge.dambt(i-1))
    1call linear(dambt(i-1),dambt(i),tamb(i-1),tamb(i),time
    1    ,tfirex(k))
6001     time=time+dtime

                    time=0.d0

                    iendha=iendh+1
                    th2(iendha)=tf1*al**2.d0/alpha
                    dh2(iendha)=dh2(iendh)
                    do 6002 k=1,nt
                     do 7009 i=2,iendha
7009     if(time.le.th2(i).and.time.ge.th2(i-1))
    1call linear(th2(i-1),th2(i),dh2(i-1),dh2(i),time,h2(k))
6002     time=time+dtime

      time=0.d0

                    iendea=iende+1
                    teps2(iendea)=tf1*al**2.d0/alpha
                    deps2(iendea)=deps2(iende)
                    do 6003 k=1,nt
                     do 7003 i=2,iendea
7003     if(time.le.teps2(i).and.time.ge.teps2(i-1))call
    1linear(teps2(i-1),teps2(i),deps2(i-1),deps2(i),time,epsi(k))
6003     time=time+dtime

                    ca=(h2(1)*al*(tfirex(1)-ti)+sig*al*(epsi(1)*tfirex(1)**4.d0
    1    -eps*ti**4.d0))/(ak*tc)
                    cb=-(h2(1)*al+4.d0*eps*sig*(ti**3.d0)*al)/ak


      iflag=0
                    t2(1)=0
                    t1(1)=r*al/tc
                    time=al**2.d0*t/alpha
                    temp2(1)=t2(1)*tc+ti
                    temp1(1)=t1(1)*tc+ti
c initialize comparison values to 0
                    do 1333 i=1,nt
                    t1g(i)=0.d0
1333    t2g(i)=0.d0

c call subroutine for kernels
1228    u(1)=0.d0
                    do 4221 k=2,nt,1+1*iflag
4221    u(k)=(float(k-1)*dt)**.5d0
```

```
      call kernel(u,nt,iflag)
333     format(1x,5(d12.6,2x))
                  go to 2345



c  start calculation of temp


2345              taumax=runmax*alpha/al**2.d0
      nto=runmax/toutput+1

      t=0

c   evaluate the multiplication factor

                  if(h/al.le.10.d0)then
                  ff=1.d0/(.5d0*dtanh(sl/al)+.5d0*al/(sl+h)*(dlog(dcosh(
    1h/al))-dlog(dcosh(sl/al))))
                  else
                  ff=1.d0/(.5d0*dtanh(sl/al)+.5d0*al/(sl+h)*(dlog(.5d0)
    1+h/al-dlog(dcosh(sl/al))))
                  endif

      du=dt**.5d0

c    evaluate weights for numerical integration

      do 10 k=2,nt
                  i=k-1
      w(1)=1.d0
      w(k)=(float(k-1))**.5d0-(float(k-2))**.5d0
       do 2 j=2,k-1
2       w(j)=(float(j))**.5d0-(float(j-2))**.5d0

                  q2(i)=ca+cb*t2(i)+cc*t2(i)**2.d0+cd*t2(i)**3.d0+ce*t2(i)**4.d0
                  q1(i)=cf+cg*t1(i)-cc*t1(i)**2.d0-cd*t1(i)**3.d0-ce*t1(i)**4.d0

c defining the function of time change of incoming radiative flux

                  t=t+dt


c defining the change in ambient temp on exposed side

                  ca=(h2(k)*al*(tfirex(k)-ti)+sig*al*(epsi(k)*tfirex(k)**4.d0
    1   -eps*ti**4.d0))/(ak*tc)
                  cb=-(h2(k)*al+4.d0*eps*sig*(ti**3.d0)*al)/ak
                   a=0.d0
                   b=0.d0
                   do 20 j=2,k
                   a=a+w(j)*(uf1(j)*q1(k+1-j)+uf2(j)*q2(k+1-j))
20       b=b+w(j)*(-uf2(j)*q1(k+1-j)-uf1(j)*q2(k+1-j))

                   do 1421 j=1,k
                   a=a+w(j)*((uf2(j)+uf1(j))*r*al/tc
    1     +g11*uf3(j)*aj(k+1-j))
1421     b=b+w(j)*((-uf1(j)-uf2(j))*r*al/tc
    1     +g11*ug3(j)*aj(k+1-j))



       ak1=du*a
                   ak2=du*b+r*al/tc
                   y=du*uf2(1)*w(1)
                   z=-du*uf2(1)*w(1)
                   x1=y*ca
                   x2=(cb-1.d0/y)*y
                   x3=cc*y
                   x4=cd*y
                   x5=ce*y
                   y1=z*cf
                   y2=(cg-1.d0/z)*z
```

```
      y3=-cc*z
                  y4=-cd*z
                  y5=-ce*z

                  t2guess=t2(k-1)
                  t1guess=t2(k-1)
                  call newton(ak1,x1,x2,x3,x4,x5,t2guess)
                  call newton(ak2,y1,y2,y3,y4,y5,t1guess)

      if(t2guess.lt.0.d0)t2guess=0
      t2(k)=t2guess
                  if(t1guess.lt.t1(1))t1guess=t1(1)
                  t1(k)=t1guess
                  chi=(1.d0-derfc(t**.5d0))/2.d0
                  avgt(k)=(t1(k)+t2(k))*chi
                  time=t*al**2.d0/alpha


                  temp2(k)=t2(k)*tc+ti
                  temp1(k)=t1(k)*tc+ti

      do 6543 i=1,nto
                  diff=time-i*toutput
                  if(diff.lt.0)diff=-diff
                  if(diff.le..001d0) then
                              numResults = numResults + 1
                              results(numResults)%time=time
                              results(numResults)%exposed=temp2(k)
                              results(numResults)%unexposed=temp1(k)
                              results(numResults)%theta=avgt(k)
                              results(numResults)%tau=t
                  end if
6543              continue
                  if(avgt(k).ge.ff)then
                  ibr=1
                              numResults = numResults + 1
                              results(numResults)%time=time
                              results(numResults)%exposed=temp2(k)
                              results(numResults)%unexposed=temp1(k)
                              results(numResults)%theta=avgt(k)
                              results(numResults)%tau=t
                  go to 1330
                  endif
                  q2(k)=ca+cb*t2(k)+cc*t2(k)**2.d0+cd*t2(k)**3.d0+ce*t2(k)**4.d0
      q1(k)=cf+cg*t1(k)-cc*t1(k)**2.d0-cd*t1(k)**3.d0-ce*t1(k)**4.d0

10     continue

      go to 1330

1330              if(ibr.eq.1)then
                              avgtinit=(temp2(1)+temp1(1))/2.d0
                              breakf%avgTBreak=(temp2(k)+temp1(k))*chi+ti*(1.d0-2.d0*chi)
                              breakf%avgDeltaT=breakf%avgTBreak-avgtinit
                              breakf%tcs=al**2.d0/alpha
                              breakf%tck=sigmab/(betal*youngs)
                              breakf%broken=.true.
                  else
                              tfdim=tf*al**2.d0/alpha
                              write(breakf%message,8123) tfdim
c                             if(ioutput.eq.'y')write(21,8123)tfdim
8123                          format(1x,'Window did not break in run time of',f8.2,' [s]')
c                             if(ioutput.eq.'y')write(21,15453)
c                             if(ioutput.eq.'y')write(21,1667)timec,tempc
c                             if(ioutput.eq.'y')write(21,1668)g
                              breakf%broken=.false.
     endif
                  allocate(breakf%points(numResults))
                  breakf%points=results(1:numResults)

                  end function breakf
```

```
c*********************************************************************
c
c             FUNCTION DERFC
c
c*********************************************************************

      FUNCTION DERFC(D)
      implicit double precision(a-h,o-z)
      IF(D.LT.0.)THEN
        DERFC=1.d0+GAMMP(.5d0,D**2)
      ELSE
        DERFC=1.d0-GAMMP(.5d0,D**2)
      ENDIF
      RETURN
      END

c*********************************************************************
c
c       FUNCTION GAMMLN
c
c*********************************************************************

      FUNCTION GAMMLN(XX)
      implicit double precision(a-h,o-z)
      dimension cof(6)
      DATA COF,STP/76.18009173D0,-86.50532033D0,24.01409822D0,
     *    -1.231739516D0,.120858003D-2,-.536382D-5,2.50662827465D0/
      DATA HALF,ONE,FPF/0.5D0,1.0D0,5.5D0/
      X=XX-ONE
      TMP=X+FPF
      TMP=(X+HALF)*DLOG(TMP)-TMP
      SER=ONE
      DO 11 J=1,6
        X=X+ONE
        SER=SER+COF(J)/X
11    CONTINUE
      GAMMLN=TMP+DLOG(STP*SER)
      RETURN
      END

c*********************************************************************
c
c       FUNCTION GAMMP
c
c*********************************************************************

      FUNCTION GAMMP(A,X)
      implicit double precision(a-h,o-z)
      IF(X.LT.0..OR.A.LE.0.)PAUSE
      IF(X.LT.A+1.)THEN
        CALL GSER(GAMSER,A,X,GLN)
        GAMMP=GAMSER
      ELSE
        CALL GCF(GAMMCF,A,X,GLN)
        GAMMP=1.-GAMMCF
      ENDIF
      RETURN
      END

c*********************************************************************
c
c             SUBROUTINE GCF
c
c*********************************************************************

      SUBROUTINE GCF(GAMMCF,A,X,GLN)
      implicit double precision(a-h,o-z)
      PARAMETER (ITMAX=100,EPS=3.d-7)
      GLN=GAMMLN(A)
      GOLD=0.
      A0=1.
      A1=X
      B0=0.
```

```
      B1=1.
      FAC=1.
      DO 11 N=1,ITMAX
        AN=FLOAT(N)
        ANA=AN-A
        A0=(A1+A0*ANA)*FAC
        B0=(B1+B0*ANA)*FAC
        ANF=AN*FAC
        A1=X*A0+ANF*A1
        B1=X*B0+ANF*B1
        IF(A1.NE.0.)THEN
          FAC=1./A1
          G=B1*FAC
          IF(ABS((G-GOLD)/G).LT.EPS)GO TO 1
          GOLD=G
        ENDIF
11    CONTINUE
      PAUSE 'A too large, ITMAX too small'
1     GAMMCF=dEXP(-X+A*dLOG(X)-GLN)*G
      RETURN
      END

c**********************************************************************
c
c         SUBROUTINE GSER
c
c**********************************************************************

      SUBROUTINE GSER(GAMSER,A,X,GLN)
      implicit double precision (a-h,o-z)
      PARAMETER (ITMAX=1000,EPS=3.d-7)
      GLN=GAMMLN(A)
      IF(X.LE.0.)THEN
        IF(X.LT.0.)PAUSE
        GAMSER=0.
        RETURN
      ENDIF
      AP=A
      SUM=1./A
      DEL=SUM
      DO 11 N=1,ITMAX
        AP=AP+1.
        DEL=DEL*X/AP
        SUM=SUM+DEL
        IF(ABS(DEL).LT.ABS(SUM)*EPS)GO TO 1
11    CONTINUE
      PAUSE 'A too large, ITMAX too small'
1     GAMSER=SUM*DEXP(-X+A*DLOG(X)-GLN)
      RETURN
      END

c**********************************************************************
c
c subroutine to calculate initial temperature
c
c**********************************************************************

                        subroutine init(ak,sig,eps,al,h1,h2,tinf,t2i,r,ti)
                        implicit double precision(a-h,o-z)
        dimension tti(2)

        tti(1)=(tinf+t2i)/2.d0
1        r=(h2*(t2i-tti(1))+sig*eps*(t2i**4.d0-tti(1)**4.d0))/(-ak)
                        tti(2)=(-r*(ak+h1*al)+h1*tinf-sig*eps*((tti(1)+r*al)
     1          **4.d0-tinf**4.d0))/h1
                        res=(tti(2)-tti(1))/tti(2)
                        if(res.le.0)res=-res
                        if(res.ge.0.001d0)then
                        tti(1)=tti(2)*.1d0+tti(1)*.9d0
                        go to 1
                        endif
                        ti=tti(2)
                        return
```

```
                        end

c*****************************************************************
c
c subroutine for linear interpolation
c
c*****************************************************************

                        subroutine linear(a,b,c,d,e,f)
                        use lin

                        implicit double precision(a-h,o-z)
c                       common /lin/ ak,tc,al

                        f=c+(e-a)*(d-c)/
     1          (b-a)

          return
                        end

c*****************************************************************
c
c         SUBROUTINE FOR EVALUATING KERNELS
c
c*****************************************************************

                      subroutine kernel(u,nn,iflag)
                      use kern

                      implicit double precision(a-h,o-z)
      dimension ug1(1005),ug2(1005),u(1005)

       uf1(1)=0.d0
                      uf2(1)=1.d0/pi**.5d0
                      ug1(1)=-uf2(1)
                      ug2(1)=-uf1(1)
                      uf3(1)=0.d0
                      ug3(1)=0.d0



                      bbb=-g*(dexp(-g11)-1.d0)

                      do 1001 k=2,nn,1+1*iflag



c    long time solution

       rtu=.05d0
       if(u(k).le.rtu) go to 1000


       aa=0
                      do 1 i=1,nk
1       aa=aa+dexp(-(i*pi*u(k))**2.d0)*(-1.d0)**i

                      uf1(k)=-u(k)*(1.d0+2.d0*aa)
                      ug2(k)=-uf1(k)

                      bb=0
                      do 2 i=1,nk
2       bb=bb+dexp(-(i*pi*u(k))**2.d0)

                      uf2(k)=u(k)*(1.d0+2.d0*bb)
                      ug1(k)=-uf2(k)



        d=0
                       e=0
                       do 3 i=1,nk
                       d=((-1.d0)**i*dexp(-g11)-1.d0)*2.d0
```

```
     1     /((-(i*pi)**2.d0-g11**2.)*g)
 3       e=e+d*dexp(-(i*pi*u(k))**2.d0)

                       uf3(k)=u(k)*(bbb+e)

         d=0
                        e=0
                        do 4 i=1,nk
                        d=(dexp(-g11)-(-1.d0)**i)*2.d0
     1     /((-(i*pi)**2.d0-g11**2.)*g)
 4       e=e+d*dexp(-(i*pi*u(k))**2.d0)

                       ug3(k)=u(k)*(bbb+e)

                       go to 2000

c    short time solution

1000     aa=0
                       do 7 i=0,nk
7       aa=aa+dexp(-(2.d0*i+1.d0)**2.d0/(4.d0*u(k)**2.d0))

                       uf1(k)=-2.d0*aa/(pi**.5d0)
                       ug2(k)=-uf1(k)

        bb=0
                       do 8 i=1,nk
8       bb=bb+dexp(-(2.d0*i)**2.d0/(4.d0*u(k)**2.d0))

        uf2(k)=(1.d0+2.d0*bb)/(pi)**0.5d0
                       ug1(k)=-uf2(k)


                       a=dexp((u(k)/g)**2.d0)
        bb=u(k)/g
                       b=-dexp(bb**2.d0)/2.d0*
     1    (derfc(-bb)-derfc(bb))

          c=0
                        d=0
                        e=0
                        f=0
                        do 9 i=0,nk
                        cc=(2.d0*i+1)/(2.d0*u(k))

                        d=d+dexp(-(2.d0*i+1.d0)/g)*derfc(cc-bb)-
     1     dexp((2.d0*i+1.d0)/g)*derfc(cc+bb)

 9        continue
          do 10 i=1,nk
                        dd=i/u(k)

                        f=f+dexp(-2.d0*i/g)*derfc(dd-bb)-
     1     dexp(2.d0*i/g)*derfc(dd+bb)
10        continue

          uf3(k)=u(k)*(a+b+dexp(-g11)*d*a-a*f)

          ug3(k)=u(k)*(dexp(-g11)*(a-b+a*f)-a*d)
2000      continue

1001      continue
          return
                        end

c*************************************************************************
c
c            SUBROUTINE FOR FINDING ROOTS OF THE EQUATION
c
c*************************************************************************


          subroutine newton(ak,c1,c2,c3,c4,c5,guess)
```

```
                    use newt
                    implicit double precision(a-h,o-z)
c                   common /newt/ error
                    dimension x(2)

      x(1)=guess
                    it=0
1      it=it+1
                    f=ak+c1+c2*x(1)+c3*x(1)**2.d0
     1    +c4*x(1)**3.d0+c5*x(1)**4.d0

                    dfdx=c2+2.d0*c3*x(1)+3.d0*c4*x(1)**2.d0
     1       +4.d0*c5*x(1)**3.d0

                    x(2)=x(1)-f/dfdx

      if(x(2).le.1d-8)then
                    check=x(2)-x(1)
                    else
                    check=(x(2)-x(1))/x(2)
                    endif
                    if(check.lt.0)check=-check

                     if(check.ge.error)then
                      x(1)=x(2)
                       if(it.ge.100)go to 2
                       go to 1
       endif

                     go to 4
2       write(6,100)
100      format(1x,'iteration limit exceeded')
4       guess=x(2)
                     return
                     end
```

Other Subroutines

The MCB program needs subroutines to create random numbers from certain statistical distributions, namely the

- uniform distribution
- triangular distribution
- Weibull distribution
- gamma distribution.

There is freely available software to create a random number in the interval [0,1] (Press et al. 1989, Chapter 7) and the gamma distribution, e.g., the *Library of Routines for Cumulative Distribution Functions Inverses, and Other Parameters* (DCDFLIB) at the Internet address http://odin.mdacc.tmc.edu/anonftp/#DCDFLIB. The random numbers from the triangular distribution y_T and the Weibull distribution y_W can be generated from

the random number x generated from the uniform distribution in the interval [0,1] using the analytical expression for the inverse triangular and inverse Weibull distribution:

$$y_T = \begin{cases} a + \sqrt{x \cdot (b-a) \cdot (c-a)}, & x \in \left[0, \dfrac{c-a}{b-a}\right] \\ b - \sqrt{(1-x) \cdot (b-a) \cdot (b-c)}, & x \in \left[\dfrac{c-a}{b-a}, 1\right] \end{cases}, \text{ and} \qquad \text{(C1)}$$

$$y_W = x_{\min} + \beta \cdot \left\{ \ln\left[\frac{1}{1-x}\right] \right\}^{1/\alpha}, \qquad \text{(C2)}$$

where a, b and c are the minimum, maximum and peak positions of the triangular distribution, respectively, and $x_{\min}$, β and α are the parameters of the Weibull distribution with cumulative frequency function given by $F(x) = 1 - \exp\left(-\left(\dfrac{x - x_{\min}}{\beta}\right)^{\alpha}\right)$.

Program code for calculting the Spearman Rank-Order Correlation Coefficients can be found in Press et al. (1989), p. 489.

The first input file: contents and format

Program *MCB.for* reads its instructions from a file *MCB.config*. The contents and format of this file is as follows:

```
# Sample mcb configuration file
#


# Obligatory parameters

Datafile: pieni_huone.pri
Number of Monte Carlo rounds to run: 500
Window width (m): 1.000
Window height (m): 1.200
Glass thickness (m): 0.003
Flame distance (m): 100.0

# Optional parametrs

Include all input data in output: true     # 'true' causes mcb to output LOTS of mostly useless data

Use semicolon as field separator in .csv files: true     # 'true' causes mcb to generate broken csv.
                                         # This way the csv files will, howewer,
                                         # work better with Microsoft Excel

Pause at end: false     # 'true' gives time to see the possible error messages
                        # if the program was not run from the command line
```

The fire conditions are provided in the input file specified after the promt Datafile: in the file MCB.config (e.g. in the example above, this inoput file in *pieni_huone.pri*). The format of this file is similar to the output file format of the Ozone model (Cadorin & Franssen 2003), i.e., the input contents and format are as follows:

time	p_floor	TU	TL	Zs	mOx	RHRdata	RHR	mfdata	mf	FireArea	FireDiam	zVirtOrig	Lflame
[s]	[Pa]	[°C]	[°C]	[m]	[kg]	[W]	[W]	[kg/s]	[kg/s]	[m²]	[m]	[m]	[m]
0.0	0.000	20.000	20.000	2.550	8.532	0.	0.	0.000	0.000	0.000	0.000	0.000	0.000
5.0	-0.043	20.155	19.985	2.509	8.533	278.	278.	0.000	0.000	0.001	0.038	0.011	0.102
....													

Actually, *MCB.for* uses only the time, the upper layer temperature TU and the calculated RHR.

References to Appendix C

Cadorin, J.-F. & Franssen, J.-M. 2003. A tool to design steel elements submitted to compartment fires – OZone V2. Part 1: pre- and post-flashover compartment fire model. Fire Safety Journal, Vol. 38, pp. 395–427.

Press, W. H., Flannery, B. P., Teukolsky, S. A. & Vetterling, W. P. 1989. Numerical Recipes – The Art of Scientific Computing (Fortran Version). Cambridge, England: Cambridge University Press. ISBN 0 521 38330 7.

VTT WORKING PAPERS

VTT RAKENNUS- JA YHDYSKUNTATEKNIIKKA –
VTT BYGG OCH TRANSPORT – VTT BUILDING AND TRANSPORT

11 Lakka, Antti. Rakennustyömaan tuottavuus. 2004. 26 s. + liitt. 15 s.

14 Koivu, Tapio, Tukiainen, Sampo, Nummelin, Johanna, Atkin, Brian & Tainio, Risto. Institutional complexity affecting the outcomes of global projects. 2004. 59 p. + app. 2 p.

15 Rönty, Vesa, Keski-Rahkonen, Olavi & Hassinen, Jukka-Pekka. Reliability of sprinkler systems. Exploration and analysis of data from nuclear and non-nuclear installations. 2004. 89 p. + app. 9 p.

18 Nyyssönen, Teemu, Rajakko, Jaana & Keski-Rahkonen, Olavi. On the reliability of fire detection and alarm systems. Exploration and analysis of data from nuclear and non-nuclear installations. 2005. 62 p. + app. 6 p.

19 Tillander, Kati, Korhonen, Timo & Keski-Rahkonen, Olavi. Pelastustoimen määräiset seurantamittarit. 2005. 123 s. + liitt. 5 s.

20 Simo Hostikka & Johan Mangs. MASIFIRE – Map Based Simulation of Fires in Forest-Urban Interface. Reference and user's guide for version 1.0. 2005. 52 p. + app. 2 p.

21 Kortesmaa, Markku & Kevarinmäki, Ari. Massiivipuu maatilarakentamisessa. Suunnitteluohje. 2005. 76 s. + liitt. 6 s.

22 Ojanen, Tuomo & Ahonen, Jarkko. Moisture performance properties of exterior sheathing products made of spruce plywood or OSB. 2005. 52 p. + app. 12 p.

27 Kevarinmäki, Ari. Konenaulojen ulosvetolujuus. 2005. 24 s. + liitt. 12 s.

29 Oksanen, Tuuli, Kevarinmäki, Ari, Yli-Koski, Rainer & Kaitila, Olli. Ruostumattomasta teräksestä valmistettujen puurakenteiden liitosten palonkestävyys. 2005. 104 s. + liitt. 108 s.

31 Hietaniemi, Jukka. A Probabilistic Approach to Wood Charring Rate. 2005. 53 p.

32 Korhonen, Timo & Hietaniemi, Jukka. Fire Safety of Wooden Façades in Residential Suburb Multi-Storey Buildings. 2005. 66 p. + app. 40 p.

37 Hietaniemi, Jukka & Rinne, Tuomo. Tulipalojen yksittäispäästöt ilmaan: laskennallinen lähestymistapa. 2005. 78 s.

38 Kevarinmäki, Ari, Oksanen, Tuuli & Yli-Koski, Rainer. Ruostumattomasta teräksestä valmistettujen puurakenteiden liitosten suunnittelu. Yleiset ohjeet ja palomitoitus. 2005. 51 s. + liitt. 12 s.

39 Mroz, Arkadiusz & Kärnä, Tuomo. Mitigation of ice loading. Feasibility study of semi-active solution. 2005. 34 p.

40 Paloposki, Tuomas, Tillander, Kati, Virolainen, Kimmo, Nissilä, Minna & Survo, Kyösti. Sammutusjätevedet ja ympäristö. 2005. 75 s. + liitt. 10 s.

41 Hietaniemi, Jukka. Probabilistic simulation of glass fracture and fallout in fire. 2005. 88 p. + app. 33 p.

ISBN 951–38–6593–2 (URL: http://www.vtt.fi/inf/pdf/)
ISSN 1459–7683 (URL: http://www.vtt.fi/inf/pdf/)